

DESIGN AND DEVELOPMENT OF A HYBRID DRONE

by

Reeghan Osmond

Eleazar Pestano

A report presented to the
British Columbia Institute of Technology
in partial fulfillment of the requirement for the degree of
Bachelor of Engineering (Mechanical)

Faculty Advisor: Cyrus Raoufi, Ph.D., P.Eng.

Program Head: Mehrzad Tabatabaian, Ph.D., P.Eng.

Burnaby, British Columbia, Canada, 2019

© Reeghan Osmond, Eleazar Pestano, 2019

Author's Declaration

We hereby declare that we are the sole authors of this report.



Reeghan Osmond



Eleazar Pestano

We further authorize the British Columbia Institute of Technology to distribute digitally, or printed paper, copies of this report, in total or in part, at the request of other institutions or individuals for the purpose of scholarly activity.



Reeghan Osmond



Eleazar Pestano

Abstract

In response to request for proposal (RFP) document by Buzz Drone Inc., the design team at Falcon drone Inc. was contracted to design and develop a hybrid drone as a proof-of-concept. The objective of the project was to build a fully functional prototype of a drone that had the ability to both fly and drive on land. By adding the driving feature, the goal was to save energy and reduce power consumption due to the limited power supply that a drone would typically have from just its battery. This project was divided into two phases: Phase 1 which focused on the drone portion of the project, and Phase 2 which incorporate the addition of the driving aspect to the drone. The design was targeted towards the hobbyist drone market, including consumers, enthusiast, educators and new users. They require the drone to be unique, enjoyable to use, lightweight, portable, compact, robust, easy to user, safe and reliable. Moreover, some technical requirements include a maximum weight of 3.5 kg and maximum size of 2.5 ft³.

The deliverables of this project include a 3D model, fabrication drawings and stress analysis of the final concept using SolidWorks, a wiring diagram, a LabVIEW code for the drone and drive controls and a physical prototype.

In terms of documentation, a proposal presentation, a design review package and presentation, and a final report and presentations were required as well.

The scope of the project consists of current status research, concept generation, concept selection, design refinement, theoretical background research, and prototyping and testing.

The current status research included research on drones that were currently in the market and patented. Through this, concepts were generated through sketches, then selected and further refined to ensure requirements were met. Significant changes to the design were made throughout this process. The chosen concept was modelled in SolidWorks, where a brief stress analysis was conducted for verification.

Further research was conducted regarding the design and operation of drones, which included aspects about the sizing of their propellers, motors, electronic speed controllers (ESC) and battery. Research was also conducted regarding the drive mode motors. Control of the motors for both the drone and driving aspects were investigated as well. This included rolling, pitching and yawing in drones and various speed differentials that would allow the drone to maneuver on land.

The design incorporated both off-the-shelf components and customized parts. The entire manufacturing and assembly process was documented. This involved

various process such as hand lay-up for the composite baseplates, drilling, band sawing, milling, punching and sanding. As well, a wiring diagram was provided to illustrate the connection between the electrical components. Lastly, details regarding the LabVIEW program was explained in detail to demonstrate how the drone was controlled.

Multiple tests were conducted in order to refine the controls, which incorporated a complementary filter, low-pass filter, average calculator and PID control. Despite facing various mechanical, electrical and programming challenges, Falcon Drone Inc. was able to successfully build a physical prototype for Buzz Drone Inc. by May 3rd, 2019 which met the technical requirements and needs of the customer.

Acknowledgements

Without the help and guidance from the following individuals, this project would not have been possible. Their broad levels of expertise were invaluable throughout this process.

- Cyrus Raoufi, Ph.D., P.Eng. – Faculty Advisor
- Johan Fourie, Ph.D., P.Eng. – Project Supervisor
- Christopher Townsend – Manufacturing Advisor
- Greg King, M.B.A., P.Eng. – Composites Manufacturing Advisor
- Vahid Askari, Ph.D., P.Eng. – Mechanical Design Advisor
- Eric Saczuk, Ph.D. – Geomatics Instructor

As the faculty advisor of this project, Dr. Raoufi helped guide the design team throughout the course of the project. His knowledge about SolidWorks, electric motors, and many other important aspects of the design process were paramount to the success of the project.

Dr. Fourie helped the team develop management skills that ensured the timely and successful completion of the project. His knowledge in the field of manufacturing and mechanical design was also extremely important to the team.

Both Christopher Townsend and Greg King have an incredible amount of expertise in the field of manufacturing. They gave the team insight into different manufacturing processes including how to safely work with composites.

Dr. Askari's expertise in mechanics and stress analyses helped the team complete many important calculations throughout the course of the project.

The design team would also like to thank Dr. Saczuk for sharing his knowledge and expertise about drones. By looking at and examining some of his drones, the team was able to generate more design ideas.

Table of Contents

| | |
|----------------------------------|------|
| Author’s Declaration..... | iii |
| Abstract..... | v |
| Acknowledgements..... | ix |
| Table of Contents..... | xi |
| List of Tables..... | xvii |
| List of Illustrations..... | xix |
| 1. Introduction..... | 1 |
| 1.1. Problem Statement..... | 1 |
| 1.2. Objectives..... | 2 |
| 1.3. Scope..... | 3 |
| 1.4. Technical Requirements..... | 4 |
| 2. Current Status Research..... | 5 |
| 2.1. Market Research..... | 5 |
| 2.2. Patent Research..... | 9 |
| 2.3. Target Market..... | 11 |
| 2.3.1. Customer Needs..... | 11 |
| 3. Preliminary Design..... | 13 |
| 3.1. Concept Generation..... | 13 |
| 3.2. Concept Selection..... | 17 |
| 3.2.1. Chosen Concept..... | 20 |
| 3.2.2. Design Refinements..... | 21 |
| 4. Theoretical Background..... | 23 |

| | |
|--|----|
| 4.1. Phase 1 Theory..... | 23 |
| 4.1.1. Secondary Research | 25 |
| 4.1.1.1 Number of Propellers | 25 |
| 4.1.1.2 Required Thrust Force..... | 27 |
| 4.1.1.3 Propeller Sizing..... | 29 |
| 4.1.1.4 Motor and ESC Sizing..... | 31 |
| 4.1.1.5 Battery Sizing..... | 33 |
| 4.1.2. Equation Derivations..... | 34 |
| 4.1.2.1 Thrust Force Equation..... | 34 |
| 4.1.2.2 Propeller Torque Equation | 38 |
| 4.1.2.3 Motor Torque Equation..... | 39 |
| 4.1.3. Calculations..... | 42 |
| 4.1.3.1 Sample Calculation | 42 |
| 4.1.3.2 Final Iteration | 48 |
| 4.1.4. Motor Control..... | 49 |
| 4.1.4.1 Feedback Control: Accelerometer and Gyroscope..... | 49 |
| 4.1.4.2 Complementary Filter | 52 |
| 4.1.4.3 Drone Maneuvering: Roll, Pitch and Yaw | 53 |
| 4.1.4.4 PID Controls and its Role..... | 56 |
| 4.2. Phase 2 Theory..... | 58 |
| 4.2.1. Secondary Research | 60 |

| | |
|---|----|
| 4.2.1.1 Motor and Driver Sizing | 60 |
| 4.2.2. Motor Control | 61 |
| 4.2.2.1 Reversing Motor Direction and Braking: H-Bridge | 62 |
| 4.3. Stress Analysis | 63 |
| 5. Prototyping and Testing | 65 |
| 5.1. Phase 1 Manufacturing | 65 |
| 5.1.1. Top and Bottom Plates | 65 |
| 5.1.2. Carbon Fibre Tubes | 71 |
| 5.1.3. Expansion Clamps | 74 |
| 5.1.4. Propeller Motor Mounts..... | 74 |
| 5.1.5. Tube Clamps | 76 |
| 5.2. Phase 2 Manufacturing | 79 |
| 5.2.1. Rear Motor Mounts..... | 79 |
| 5.3. Drone Assembly | 80 |
| 5.4. Phase 1 Electrical Wiring | 82 |
| 5.5. Phase 2 Electrical Wiring | 84 |
| 5.6. Phase 1 Programming | 85 |
| 5.6.1. LabVIEW Front Panel | 85 |
| 5.6.2. LabVIEW VI..... | 90 |
| 5.6.2.1 Accelerometer Code | 90 |
| 5.6.2.2 Gyroscope Code..... | 92 |

| | |
|--|-----|
| 5.6.2.3 Complementary Filter | 93 |
| 5.6.2.4 Filtering and Averaging | 95 |
| 5.6.2.5 PID Controls..... | 97 |
| 5.6.2.6 PWM Motor Controls..... | 98 |
| 5.7. Phase 2 Programming..... | 100 |
| 5.7.1. LabVIEW Front Panel..... | 100 |
| 5.7.2. LabVIEW VI..... | 100 |
| 5.7.2.1 Drive Controls | 101 |
| 5.8. Phase 1 Testing..... | 102 |
| 5.9. Phase 2 Testing..... | 102 |
| 6. Discussion of Results and Conclusion | 103 |
| 6.1. Final Concept and Results..... | 103 |
| 6.2. Conclusion..... | 107 |
| 6.3. Project Challenges..... | 108 |
| 6.3.1. Manufacturing Challenges | 108 |
| 6.3.2. Electrical Challenges..... | 108 |
| 6.3.3. Programming Challenges | 109 |
| 6.4. Future Work | 110 |
| Bibliography..... | 111 |
| Appendix A. Request for Proposal..... | 119 |
| Appendix B. Project Management Items | 123 |
| B.1. Work Breakdown Structure | 124 |
| B.2. Simplified Responsibility Assignment Matrix | 125 |

| | |
|--|-----|
| B.3. Simplified Gantt Chart | 126 |
| B.4. Milestone Chart | 127 |
| Appendix C. Design Review Package | 129 |
| Appendix D. Manufacturing Drawings | 145 |

List of Tables

| | |
|--|-----|
| Table 1.1. Hybrid Drone Technical Requirements | 4 |
| Table 4.1: DJI Inspire 2 Specifications [9] | 27 |
| Table 4.2: LiPo Battery Sizes and Voltages | 33 |
| Table C.1: Technical Requirements..... | 131 |

List of Illustrations

| | |
|---|----|
| Figure 2.1. B-Unstoppable Tank Drone [4]..... | 5 |
| Figure 2.2. Syma X9 Flying Car [7] | 6 |
| Figure 2.3. PowerVision PowerEgg Drone [8]..... | 7 |
| Figure 2.4. DJI Inspire 2 Drone [10] | 8 |
| Figure 2.5. Vehicle with Aerial and Ground Mobility (CA 2787279) [11]..... | 9 |
| Figure 2.6. Flying Device with Improved Movement on the Ground (US007959104) [12] | 10 |
| Figure 3.1. Concept 1: Two Folding Wheel/Propellers | 13 |
| Figure 3.2. Concept 2: Landing Wheels/Propellers | 14 |
| Figure 3.3. Concept 3: Independent Wheels/Propellers | 15 |
| Figure 3.4. Concept 4: Folding Wheels/Propellers | 16 |
| Figure 3.5. Concept 4: Flying Mode Isometric View | 17 |
| Figure 3.6. Concept 4: Driving Mode Isometric View | 17 |
| Figure 3.7. Concept 4: Top, Front, and Side Views of the Landing Mechanism | 18 |
| Figure 3.8. Concept 4: SolidWorks Model | 19 |
| Figure 3.9. Concept 3: SolidWorks Model of Detailed Isometric View | 20 |
| Figure 3.10. Updated SolidWorks Model of Concept Three | 21 |
| Figure 4.1: Brushless DC Motor Circuit [13] | 23 |
| Figure 4.2: Brushless DC Motor Components [14]..... | 24 |
| Figure 4.3: Different Drone Propeller Configurations [21]..... | 26 |

| | |
|---|----|
| Figure 4.4: DJI Inspire 2 Drone [22]..... | 27 |
| Figure 4.5: Difference Between Propeller Pitch Sizes [26] | 29 |
| Figure 4.6: Propeller Thrust Force Diagram | 34 |
| Figure 4.7: Propeller Wing Velocity Diagram [37] | 36 |
| Figure 4.8: Typical DC Motor Circuit [39]..... | 39 |
| Figure 4.9: Torque-Speed Curve [39] | 41 |
| Figure 4.10: Actuator Sizing Flow Chart | 42 |
| Figure 4.11: Minimum Speed Required vs. Propeller Size for a 1 kg Thrust Force..... | 43 |
| Figure 4.12: Six Degrees of Freedom of a Quadcopter [43]..... | 49 |
| Figure 4.13: Coriolis Effect in a MEMS Gyroscope [44]..... | 50 |
| Figure 4.14: Tuning Fork Configuration in a MEMS Gyroscope [45] | 51 |
| Figure 4.15: Complimentary Filter Block Diagram [46] | 52 |
| Figure 4.16: Reversing BLDC Motor Polarity [47] | 53 |
| Figure 4.17: Roll, Pitch and Yaw of a Quadcopter [48] | 54 |
| Figure 4.18: Roll, Pitch and Yaw Summary [49]..... | 54 |
| Figure 4.19: Basic Quadcopter Configuration [50]..... | 55 |
| Figure 4.20: Brushed DC Motor Circuit [13]..... | 58 |
| Figure 4.21: Commutator and Brushes [53]..... | 59 |
| Figure 4.22: Basic Drive Configurations [54]..... | 61 |
| Figure 4.23: H-Bridge Circuit [55] | 62 |
| Figure 4.24. SolidWorks Stress Analysis Results..... | 63 |

| | |
|---|----|
| Figure 4.25. Highest Stress Location for Drone Design..... | 63 |
| Figure 5.1. Smooth Plastic Sheet..... | 66 |
| Figure 5.2. Carbon Fibre Squares | 67 |
| Figure 5.3. Balsa Wood Stock | 67 |
| Figure 5.4. Mixing Epoxy Resin..... | 68 |
| Figure 5.5. Adding Epoxy Resin to Carbon Fibre Sheet | 68 |
| Figure 5.6. Sandwich Composite before the Epoxy Set | 69 |
| Figure 5.7. Sandwich Composite during the Drilling Process..... | 70 |
| Figure 5.8. Cutting of the Carbon Fibre Tubes..... | 71 |
| Figure 5.9. Milling Machine with Edgefinder | 72 |
| Figure 5.10. Adding Holes to Carbon Fibre Tubes..... | 72 |
| Figure 5.11. Deburring the Carbon Fibre Tubes..... | 73 |
| Figure 5.12. Completed Carbon Fibre Tube | 73 |
| Figure 5.13. Scribed Sheet Metal for Propeller Motor Mounts..... | 74 |
| Figure 5.14. Punching Holes into the Propeller Motor Mount Parts | 75 |
| Figure 5.15. Adding Holes to the Square Tubing with the Milling Machine | 77 |
| Figure 5.16. Removing Material from the Tube Clamps..... | 77 |
| Figure 5.17. Finished Tube Clamps..... | 78 |
| Figure 5.18. Removing Excess Material Using a Sanding Machine | 79 |
| Figure 5.19. Exploded View of the Final Drone SolidWorks Model | 80 |

| | |
|---|-----|
| Figure 5.20: Drone Hardware Wiring Diagram | 82 |
| Figure 5.21: MyRIO MXP Connector Details | 83 |
| Figure 5.22: Drive Hardware Wiring Diagram | 84 |
| Figure 5.23: Drone Controls Front Panel | 85 |
| Figure 5.24: Drone Graphical Data Front Panel | 86 |
| Figure 5.25: PID Controls Front Panel..... | 87 |
| Figure 5.26: Filter Controls Front Panel | 88 |
| Figure 5.27: Drone Troubleshooting Graphical Data Front Panel | 89 |
| Figure 5.28: FGPA MyRIO Onboard Accelerometer VI..... | 90 |
| Figure 5.29: L3G4200D Three-Axis Gyroscope VI | 92 |
| Figure 5.30: Complementary Filter VI..... | 93 |
| Figure 5.31: Filtering and Averaging VI..... | 95 |
| Figure 5.32: Filtering and Averaging SubVI | 96 |
| Figure 5.33: PID Controls VI..... | 97 |
| Figure 5.34: Drone Motor Configuration..... | 98 |
| Figure 5.35: PWM Motor Controls VI..... | 99 |
| Figure 5.36: Drive Controls Front Panel | 100 |
| Figure 5.37: Drive Controls | 101 |
| Figure 6.1: Final Hybrid Drone Concept | 103 |
| Figure 6.2. Front View of Final Drone SolidWorks Model | 104 |
| Figure 6.3. Side View of Final Drone SolidWorks Model..... | 104 |

| | |
|--|-----|
| Figure 6.4. Top View of Final Drone SolidWorks Model..... | 105 |
| Figure C.1: Desired Motion Profile of the Rear Motors..... | 132 |
| Figure C.2: Free Body Diagram of Drone Assembly | 134 |
| Figure C.3: DC Motor Control Code with LabVIEW | 136 |
| Figure C.4: Servo Motor Control Code with LabVIEW | 136 |
| Figure C.5: Model of Overall Drone Design | 138 |
| Figure C.6: Model of Front Wheel Assembly | 138 |
| Figure C.7: Exploded View of the Front Wheel Assembly..... | 139 |
| Figure C.8: Model of Rear Wheel Assembly | 140 |
| Figure C.9: Exploded View of the Rear Wheel Assembly..... | 141 |
| Figure C.10: Gantt and Milestone Chart..... | 142 |

1. Introduction

In this chapter, background information about the project is outlined. The information was generated in response to the Request for Proposal (RFP) presented by Buzz Drone Inc. in October 2018. The RFP can be seen in Appendix A. It was reformatted to the style of this report.

1.1. Problem Statement

Originally, drones or unmanned aerial vehicles were invented for use in military applications because they could be controlled remotely—removing pilots from the dangers of war [1]. Now, drones are also used in many other diverse industries because they are customizable, portable, lightweight, and cost much less than other aircrafts.

Drones are invaluable in many industries, ranging from mapping and photography to farming and mining [2]. Hobbyists and enthusiasts are also always looking for new and interesting drone designs and concepts. They use drones for racing, for taking photos, and for simply enjoying the flying experience. With their large variety and customizability, drones are extremely enticing to consumers.

The design, development and prototyping of a flying and driving drone was requested by Buzz Drone Inc. in their October 2018 RFP document (Appendix A). The purpose of this project is thus, to create a unique drone which has the ability to fly and drive so that it can be commercialized by Buzz Drone Inc.

This concept has not yet been popularized and adds flexibility and uniqueness to the drone experience. The addition of a drive mode for maneuvering will greatly reduce power consumption, making the drone's battery last longer (driving requires less power than flying). It will also allow for easier navigation in places where flying is prohibited or challenging.

The novelty and power efficiency of this new hybrid drone concept will allow it to be extremely successful when competing in the diverse drone market.

1.2. Objectives

The objective of this project was to design and prototype a unique hybrid drone that has the ability to fly in the air and drive on land. The overall power consumption of the drone was required to be reduced with the addition of the drive mode. Although the drone should be able to fly and drive, it was not required to do so autonomously. It is also not required to perform any complex movements; the ability to lift-off and drive on the ground was sufficient for a proof of concept. The following was delivered in accordance with Buzz Drone Inc.'s RFP document (Appendix A).

- the SolidWorks model of the drone assembly
- the fabrication drawings created with SolidWorks
- the wiring diagram of the drone
- the LabVIEW code used to control the drone
- a SolidWorks stress analysis
- a proposal presentation
- a design review package and presentation
- the physical prototype of the drone
- the final report and presentation

Through discussions with Buzz Drone Inc. it was decided that LabVIEW and myRIO be used to program the drone's controls rather than MATLAB Simulink and BeagleBone or Raspberry Pi (personal communications, C. Raoufi, January 10th, 2019).

Some other key objectives included using mainly off-the-shelf components and lightweight materials in the design and manufacturing of the drone.

The design was also required to be compact (desktop-sized) and portable. Originally, the drone was also meant to be foldable with propellers that could function as wheels, however, it was later decided that the wheels and propellers can also be separate (personal communications, C. Raoufi, January 10th, 2019).

1.3. Scope

The design and development of a hybrid drone includes a fully functional physical prototype which can fly and drive. The following was completed for this project, in accordance with Buzz Drone Inc.'s RFP (Appendix A).

- drone market research
- theoretical background research about drones
- concept generation and sketching
- designing a drone that can fly and drive
- creating a SolidWorks model of the drone
- creating the fabrication drawings
- manufacturing and purchasing components
- programming the drone to drive with LabVIEW and myRIO
- programming the drone to lift-off the ground with LabVIEW and myRIO
- assembly of the electrical and mechanical components
- testing the drone controls

The following are some activities that were not considered to be a part of the scope for this project.

- power efficiency calculations
- controlling the drone autonomously
- control optimization (limited to simple motion)
- destructive testing
- manufacturing of motors, propellers and other off-the-shelf components

1.4. Technical Requirements

The technical requirements for this project are summarized below in Table 1.1. They were determined to be reasonable standards based on market research (see section 2.1 Market Research).

| Requirement Criterion | Requirement Value |
|--|--------------------------|
| Maximum Mass (kg) | 3.5 |
| Maximum Height (m) | 90 |
| Maximum Overall Size (ft ³) | 2.5 |
| Maximum Air Speed (m/s) | 15 |
| Maximum Ground Speed (m/s) | 3 |
| Note: Max. height comes from Transport Canada Drone Regulations [3]. | |

Table 1.1. Hybrid Drone Technical Requirements

It is important to note that the hybrid drone's maximum weight of 3.5 kg is well below the Transport Canada Drone Regulation of 35 kg [3].

2. Current Status Research

Research into the current status of drones was completed before generating concepts for the hybrid drone. The current status research outlined in this section includes market and patent research as well as target market identification. This was completed to gain insight and ideas from available designs on the market, and to ensure that customer requirements were met.

2.1. Market Research

Firstly, different types of drones with the ability to fly and drive were researched.

The “B-Unstoppable” tank drone can be seen below in Figure 2.1.. It features four propellers and neoprene treads [4]. The treads are meant to allow the drone to emulate a tank while driving on land and the propellers allow the drone to fly. This drone is small and portable with a length, width and height of 23.5 cm, 12.5 cm, and 5.5 cm respectively [5]. It is also lightweight at only 84 g [5]. This concept is quite unique as there does not appear to be many other drones like this on the market.



Figure 2.1. B-Unstoppable Tank Drone [4]

The “Syma X9 Flying Car” drone can be seen below in Figure 2.2.. It includes four wheels and four propellers so that it can fly and drive on land. This drone is also small and portable with a length, width and height of 17.5 cm, 16.5 cm, and 6 cm respectively [6]. It is also quite lightweight at 85 g [6]. This concept is unique as well since there are not many drones on the market that can fly and drive. However, out of the drones that have this dual functionality, this style—with four propellers and four wheels—is more popular. Its popularity is likely due to the simplicity of adding four wheels to the drone without drastically changing its shape.



Figure 2.2. Syma X9 Flying Car [7]

To include both wheels and propellers into the design of the hybrid drone, a folding mechanism was considered. With a folding mechanism, the drone’s wheels could rotate up to form propellers.

Below, in Figure 2.3., is the “PowerVision PowerEgg drone”. This drone has a folding mechanism which allows its propellers to be stored when not in use. However, this product does not have wheels for a drive mode. It is larger with a size of 27.2 cm in height and 47.6 cm in diameter, when unfolded, and it weighs 2.1 kg [8]. The egg shape of this drone is extremely unique and so is its ability to fold-in its propellers.



Figure 2.3. PowerVision PowerEgg Drone [8]

The “DJI Inspire 2” drone is one of the most popular drones on the market. An image of this drone can be seen below, in Figure 2.4.. Although it does not have the ability to drive or fold, it does have some moving parts. When the drone is flying, it moves its propellers and landing gear up so that they will not restrict the view of the camera (personal communications, E. Saczuk, November, 6th, 2018). This is done with a leadscrew located at the centre of the drone, where its arms attach to the body (personal communications, E. Saczuk, November, 6th, 2018). The “DJI Inspire 2” is a much larger drone with a mass of 3.44 kg and an overall length, width and height of 42.7 cm, 31.7 cm, and 42.5 cm respectively [9]. This drone also has an attractive look with its carbon fibre arms and smooth plastic body (personal communications, E. Saczuk, November, 6th, 2018). The “DJI Inspire 2” can also fly extremely fast at a maximum of 94 km/h [9].



Figure 2.4. DJI Inspire 2 Drone [10]

2.2. Patent Research

Two patents for drones with folding mechanism were investigated. Both of these patents allow the drone to fly and drive.

The first patent was found through the Canadian Intellectual Property Office and can be seen below in Figure 2.5.. The 25th item noted in the sketch appears to be a geared motor, which is meshed to a larger gear, on a wheel (item 4). There appears to be another type of motor (item 9) that may be used to spin propellers. These propellers are located directly above the wheels of the vehicle. Item 33 appears to be a hinge or locking mechanism that would allow the vehicle to be folded to transition between flying and driving.

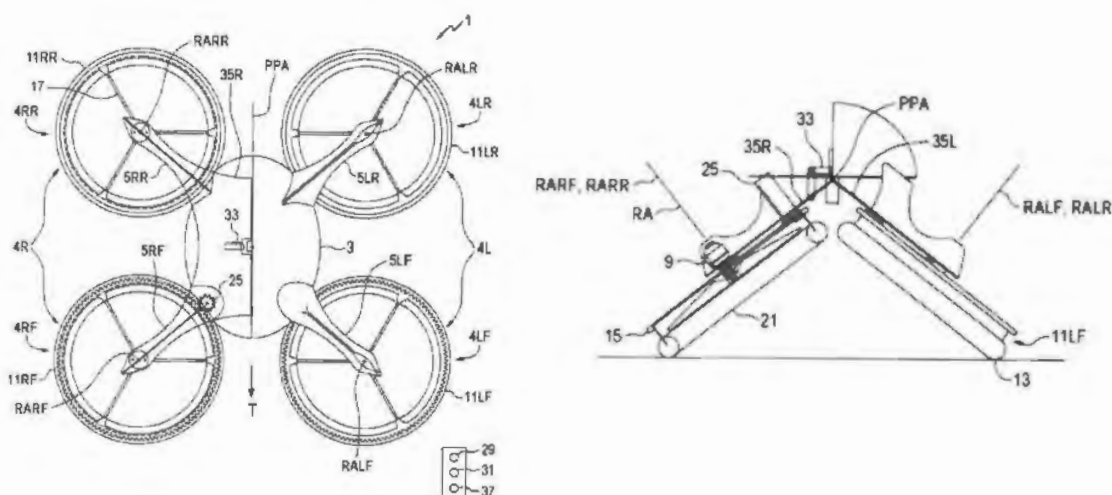


Figure 2.5. Vehicle with Aerial and Ground Mobility (CA 2787279) [11]

The second patent was found through the United States Patent and Trademark Office and can be seen below in Figure 2.6.. The 1st item appears to be propellers that are combined with wheels (item 4). These combined propeller-wheels appear to be powered by the same motor (item 6). The device appears to have a folding mechanism which can retract its landing gear as it transitions into a driving mode and vice versa.

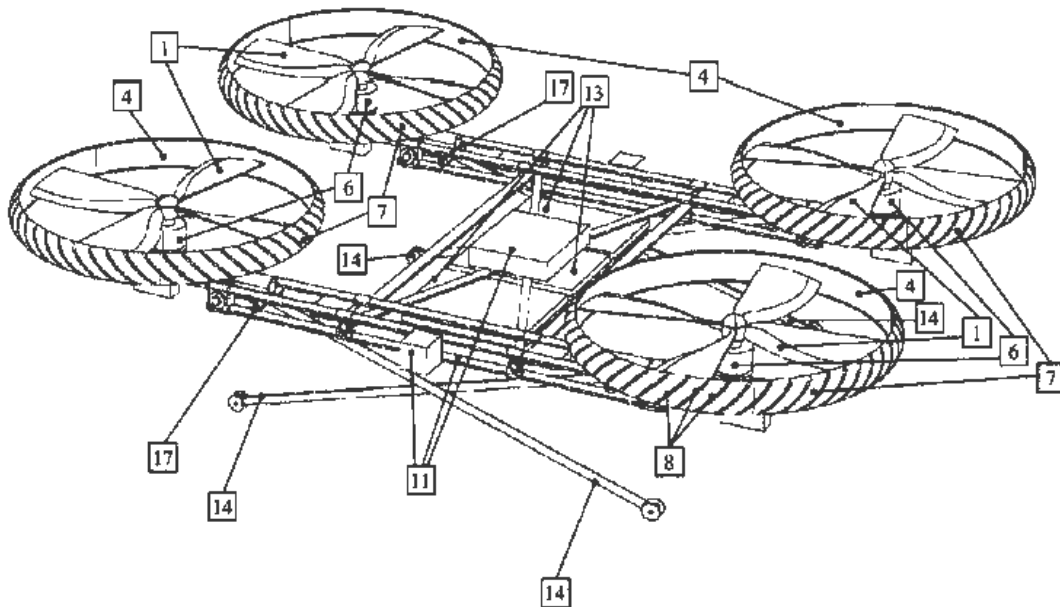


Figure 2.6. Flying Device with Improved Movement on the Ground (US007959104) [12]

In the first patent, the driving and flying modes were powered using separate motors and in the second patent, these modes were powered by the same motor.

2.3. Target Market

The target market for this project was the hobbyist drone market. This included general consumers, enthusiasts, educators, and new users. Because of this, the hybrid drone was designed to be unique, with its separate driving and flying modes. Essentially, the hybrid drone was designed to produce the same enjoyment as other drones but with the bonus functionality of an RC car.

Some other, secondary markets which would benefit from the hybrid drone includes those like the mining and military industries. With these two modes, the hybrid drone can maneuver in tighter spaces. The drone's battery power can also be conserved when it is driving (as this requires less power). However, the hybrid drone was only designed to meet the needs of the hobbyist drone market.

2.3.1. Customer Needs

As mentioned above, the target market for this project was the hobbyist drone market. The main features required by these customers for the hybrid drone's design were determined to be the following (ranked in descending order of importance).

- unique
- enjoyable to use
- lightweight
- portable
- compact
- robust
- easy to use
- safe
- reliable

Throughout the design process, these characteristics were taken into account to ensure customer satisfaction.

3. Preliminary Design

The concept generation and selection processes were outlined in this chapter. The ideas for these concepts were generated after completing market and patent research (seen in chapter 2) to see what is already available commercially. The selected concept was chosen, in the end, based on the needs of the target, hobbyist market and the technical requirements.

3.1. Concept Generation

All of the concepts to follow include a combination of wheels and propellers that would allow the drone to achieve both the flying and driving mode requirements for this project.

The first concept can be seen below in Figure 3.1.. This concept utilized folding mechanisms to change between the flying and driving modes. As shown in the sketch below, while in the driving mode, the two back propellers would fold downward to create wheels. The front propellers would rotate backwards to ensure that the drone was still balanced. In both flying and driving modes, the front wheel would remain in the same position. The front wheel would be used to allow the drone to turn while driving. This concept would require a separate landing mechanism to help it transition between modes.

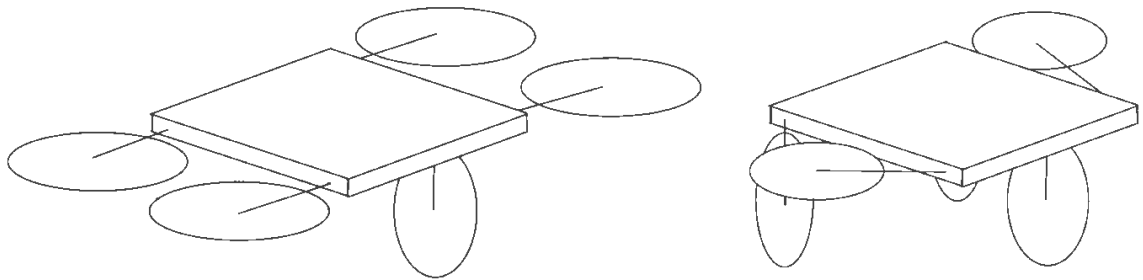


Figure 3.1. Concept 1: Two Folding Wheel/Propellers

The second concept can be seen below in Figure 3.2.. This concept also utilized a folding mechanism to transition between the flying and driving modes. To transition between these modes, a set of motors and four gears would be used to rotate a linkage. This linkage would then enable the drone's propeller/wheels to sit vertically on the ground like wheels. The propellers would have a thin, curved component underneath them which would also help them complete this transition between modes. The curved component would allow the propellers rotate into wheels more easily while already on the ground. This concept would not require a separate landing mechanism because of the curved component.

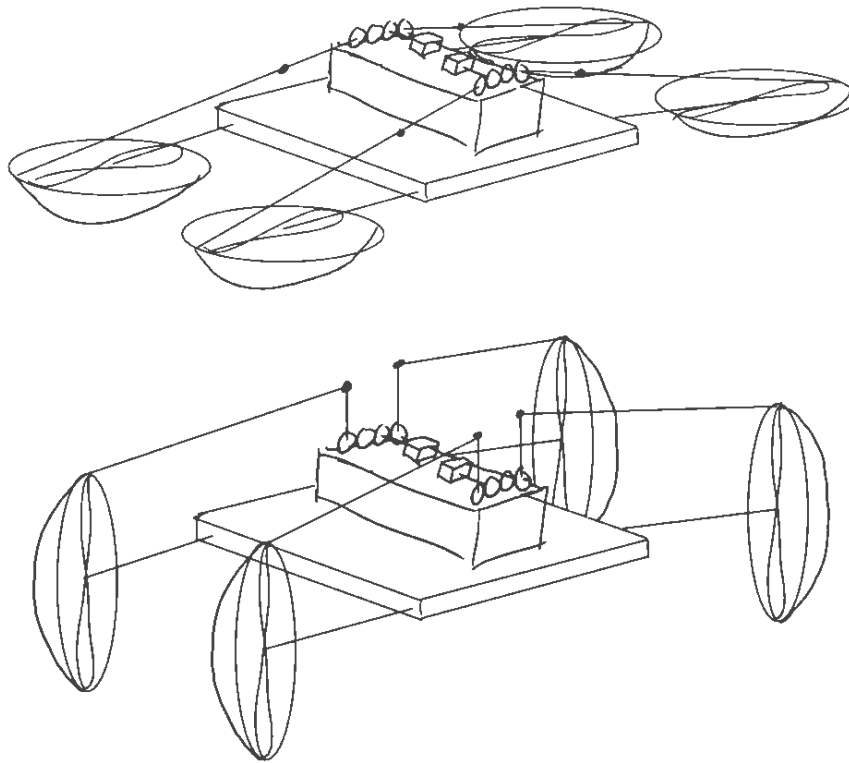


Figure 3.2. Concept 2: Landing Wheels/Propellers

The third concept can be seen below in Figure 3.3.. This concept had independent wheels and propellers. Only two of the wheels would be powered by motors to ensure that the drone had turning capabilities while in the driving mode. The other two wheels would be used for stability and to ensure that the drone was balanced. This concept would not require a separate landing mechanism because the wheels would also be used for landing.

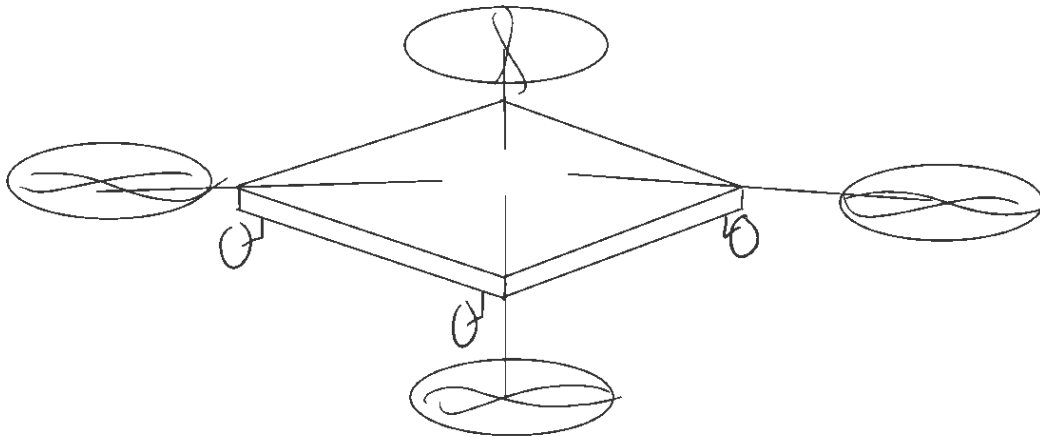


Figure 3.3. Concept 3: Independent Wheels/Propellers

The final concept can be seen below in Figure 3.4.. This concept used a folding mechanism to transition between the flying and driving modes. The dotted lines in the sketch below indicate how the drone would look when folded, and in its driving mode. Thus, the four propellers would also be used as wheels. This concept requires a separate, retractable landing mechanism to help it transition between modes.

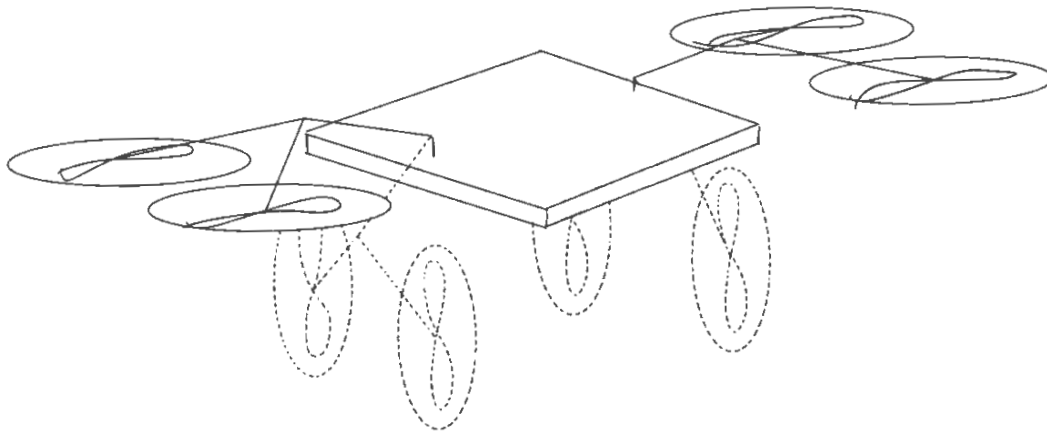


Figure 3.4. Concept 4: Folding Wheels/Propellers

3.2. Concept Selection

Initially, the fourth concept was chosen because of its unique folding mechanism and lower apparent motor requirement. A more detailed sketch of the flying and driving modes for this concept can be seen below in Figure 3.5. and Figure 3.6. respectively.

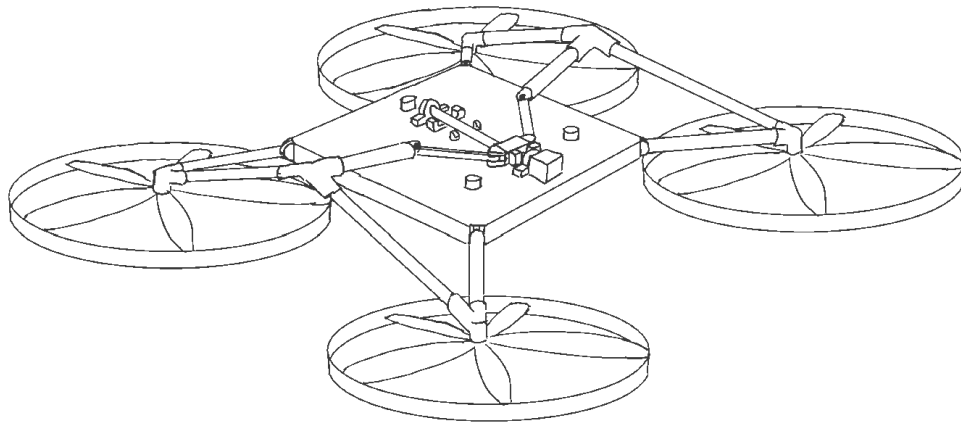


Figure 3.5. Concept 4: Flying Mode Isometric View

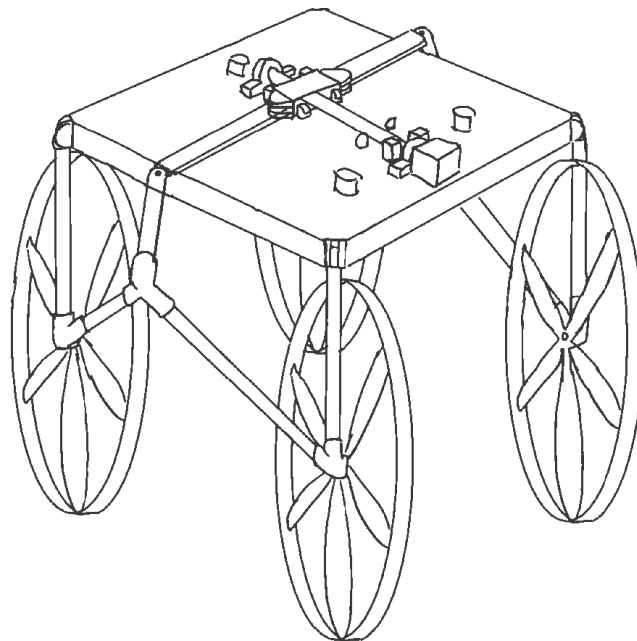


Figure 3.6. Concept 4: Driving Mode Isometric View

In this refined sketch, the folding mechanism can be seen more clearly. The mechanism would include a leadscrew, attached to a motor that would allow linkages to move and transition the drone between its flying and driving modes. While in either mode, small, normally extended solenoids would be used to lock the leadscrew in place—acting as mechanical stops. During a transition between modes, the solenoids would be powered (electrically) to allow the linkages on the leadscrew to move freely.

Although not visible in the sketches on the previous page, this concept also would also include a landing mechanism to ensure that the drone could transition between modes.

Below in Figure 3.7., a more detailed sketch of the top, front, and side views of the landing mechanism and solenoids can be seen.

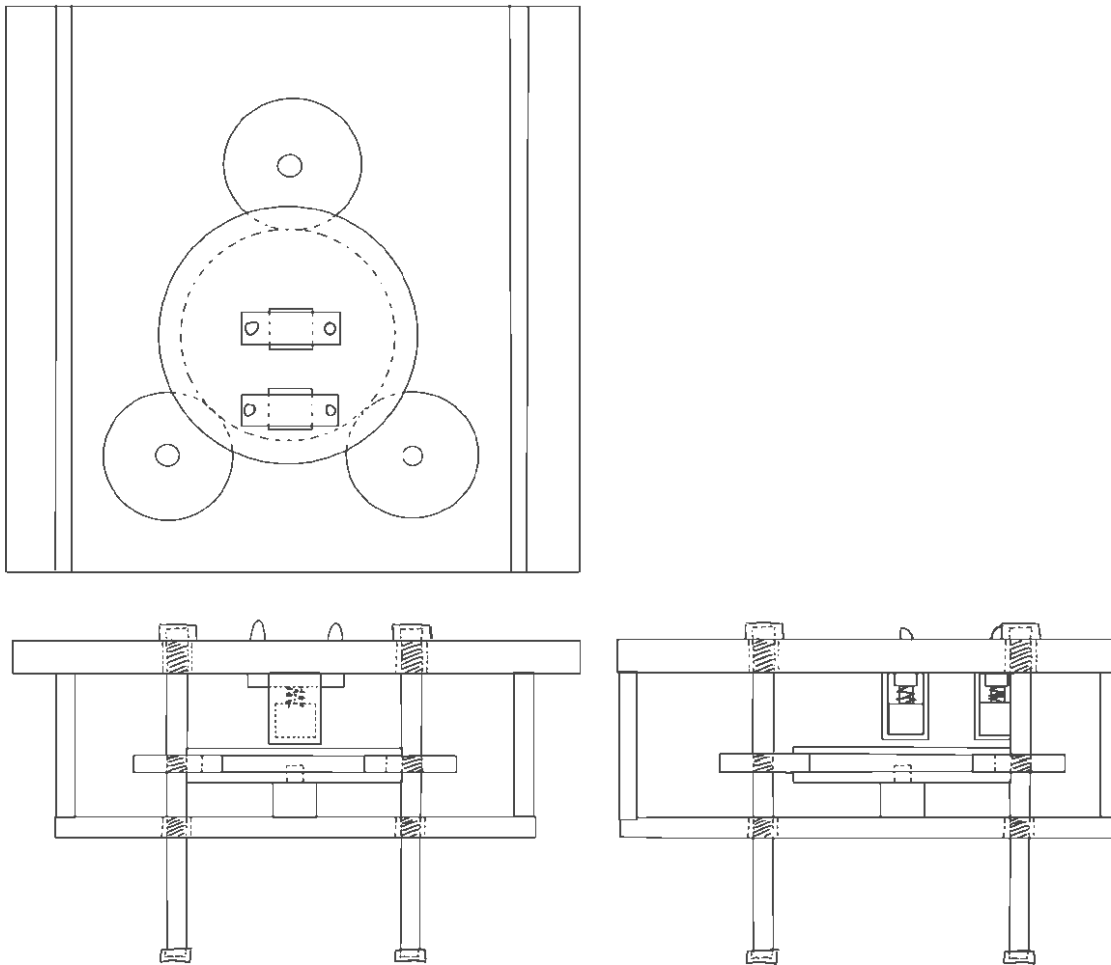


Figure 3.7. Concept 4: Top, Front, and Side Views of the Landing Mechanism

As seen in Figure 3.7., on the previous page, the solenoids needed for the drone's folding mechanism would sit inside the body of the drone. Only the extendible components of the solenoids would be extended through the top plate of the body.

The landing mechanism for this concept (also seen in Figure 3.7.) would include three leadscrews, powered by a motor. The motor would be connected to a large central gear, which when turned, would mesh with three other gears to turn the leadscrews. The smaller gears would have threaded centre holes to ensure that they would be able to move the leadscrews up and down. The larger gear would need an upper and lower lip to ensure that the smaller gears do not move up and down with the leadscrews. Finally, either the top or bottom body plate would also require threading to ensure that the leadscrews moves up and down rather than simply turning with the gears.

With all of these mechanisms taken into account, a preliminary SolidWorks model was created and can be seen below in Figure 3.8..

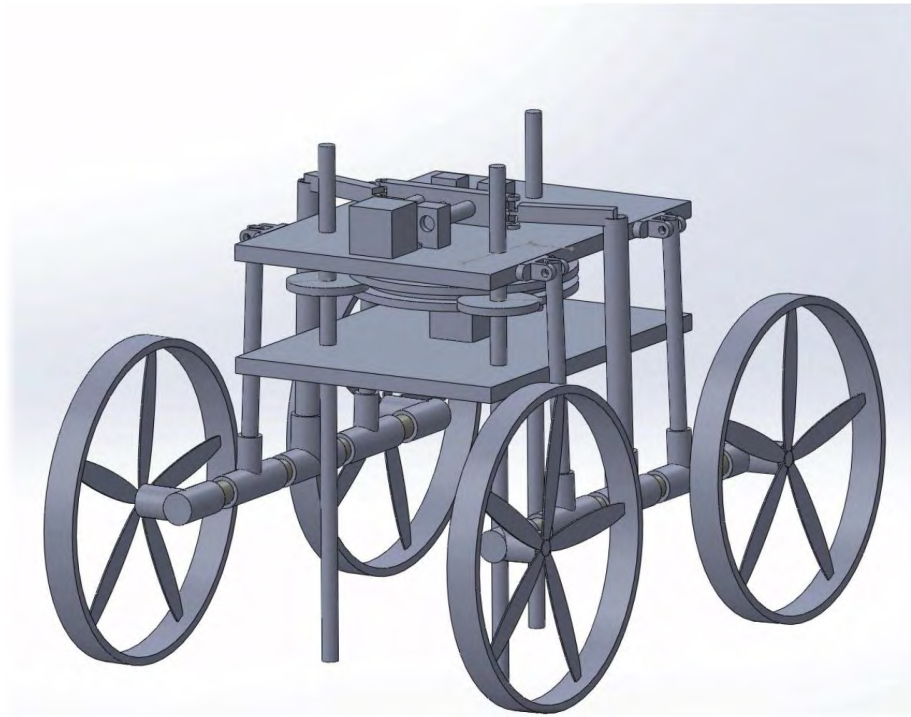


Figure 3.8. Concept 4: SolidWorks Model

After creating the SolidWorks model of this concept, it was determined that with all of these components, the drone would likely be extremely complicated, large, and heavy. It became apparent that using only one style of motor for both the flying and driving aspects of this project was not possible. The flying mode required high rotational speeds and low torque whereas the driving mode required low rotational speeds and high torque. These were competing constraints that were difficult to overcome. Thus, it was determined that a concept with separate motors and propellers should be used instead (personal communications, C. Raoufi, January 10th, 2019).

3.2.1. Chosen Concept

After further research, it was found that the fourth concept would not be suitable for this project because of its complexity and bulkiness. Instead, concept number three was chosen moving forward. Since the third concept involved separate wheels and propellers, no folding mechanism was required—reducing the number of moving parts and complexity.

The first iteration of this concept involved only three wheels: one controlled by a servo motor that would allow the drone to turn, and two controlled by brushless DC motors that would allow the drone to actually drive. The initial SolidWorks model for this concept can be seen below in Figure 3.9..

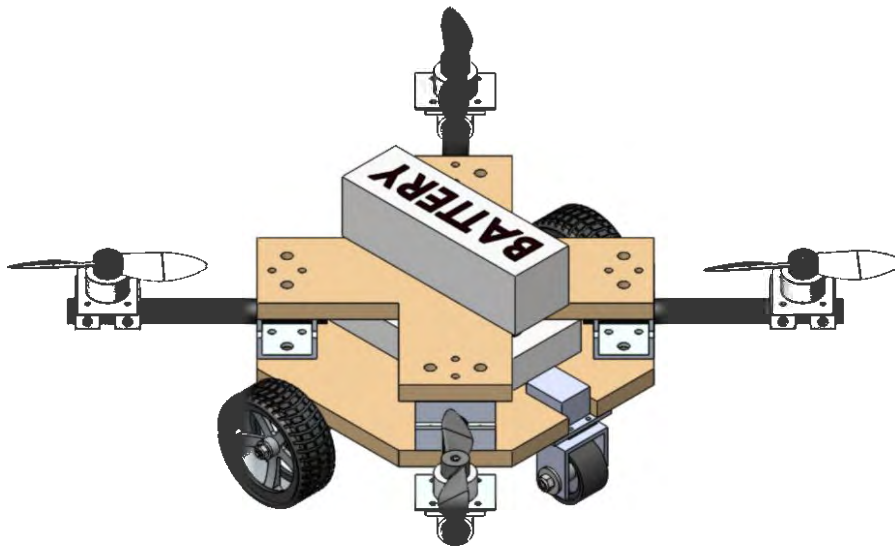


Figure 3.9. Concept 3: SolidWorks Model of Detailed Isometric View

This model was presented during the technical design review in February 2019. During the design review, feedback and changes were suggested, allowing for further design refinements. A better view of the model and a detailed view of the driving mechanisms can be seen starting on the sixth page of the design review package (Appendix C).

3.2.2. Design Refinements

Some of the suggestions received during the design review included:

- replacing the front, servo-controlled wheel with a caster,
- using the rear wheels for turning by slowing down one side to turn,
- moving the rear wheels to the centre of the drone to ensure balance, and
- adding another caster wheel at the back of the drone to balance with the front caster.

These changes were implemented into the drone's design and the updated SolidWorks model can be seen below in Figure 3.10.. It is important to note that the fasteners were omitted from this image. In section 6.1 Final Concept and Results, a more detailed view of the model can be seen.

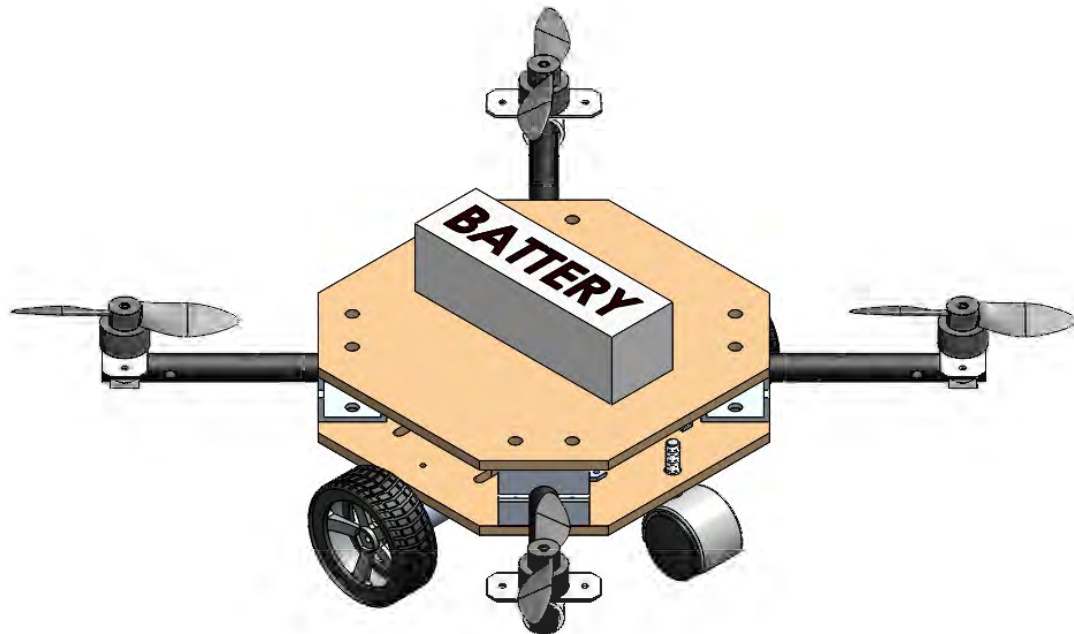


Figure 3.10. Updated SolidWorks Model of Concept Three

4. Theoretical Background

In this section, the secondary research regarding the development of the hybrid drone concept is described. This includes the propeller, motor and ESC selection of Phase 1 and the motor and driver selection of Phase 2. As previously mentioned, Phase 1 incorporated flying aspect of the project while Phase 2 featured the driving aspect.

4.1. Phase 1 Theory

The theoretical background for the flying portion of the project are presented in this section. This included the secondary research, equation derivations, sample calculations and motor control theory which was conducted to ensure the motors, propellers, electronic speed controllers (ESC) and battery were properly selected and could interface with one another.

In Phase 1, the type of motors used were Brushless DC (BLDC) motors, which are different from the conventional motors that utilize brushes to rub against a commutator which energizes armature windings [13]. A typical BLDC motor utilizes three coils as shown below in Figure 4.1.

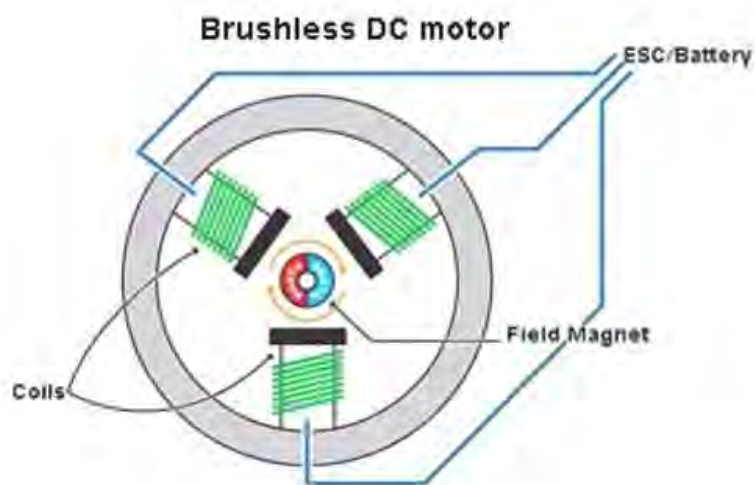


Figure 4.1: Brushless DC Motor Circuit [13]

BLDC motors work with help from permanent magnets located on a rotor and the windings/coils located in the stator. Essentially, when each of the three coils are powered and

unpowered sequentially, they create a rotating magnetic field which attracts the magnets on the rotor—allowing it to spin [13]. The components are broken down and shown in Figure 4.2.

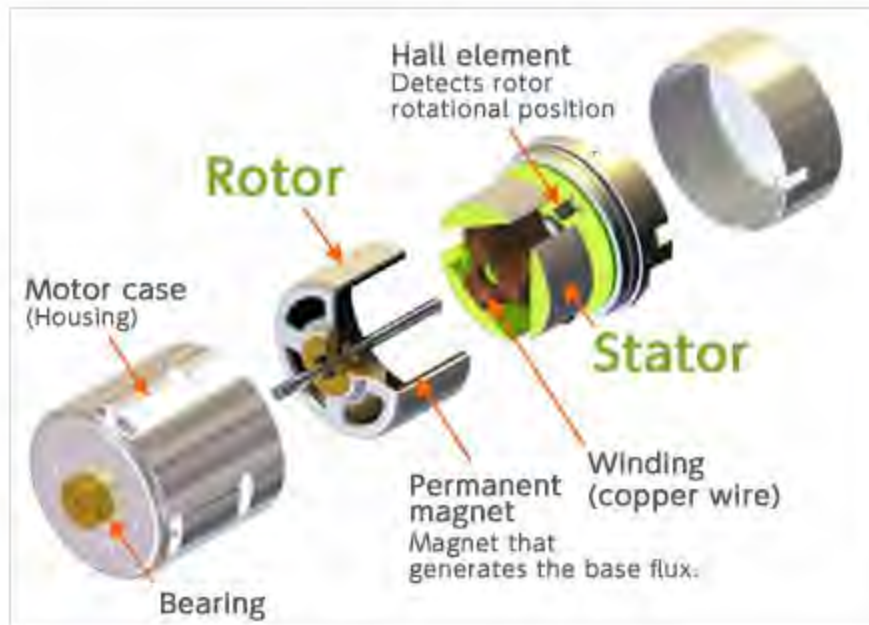


Figure 4.2: Brushless DC Motor Components [14]

4.1.1. Secondary Research

In this section, the secondary research conducted for this project is described. This was necessary in taking the first step in the iterative selection process for the motors, propellers, electronic speed controller (ESC), and battery.

4.1.1.1 Number of Propellers

There are many different drone propeller configurations. A company in Zurich, Switzerland was able to create a drone with a single propeller which uses a motion similar to a “descending maple seed” [15] [16]. This allowed for the drone to have three degrees of freedom with only one mechanical actuator [16]. A drone with two propellers has also been created which varies its propellers’ rotational speed within each revolution [17]. For instance, to move the drone to the left, the right half of the propellers’ rotations will be faster than the left [17]. This creates a higher thrust on one side of the drone, allowing it to move left in response to the unbalanced forces [17]. Three propeller drones are also possible, but the design still requires four motors as an extra servo motor is needed to rotate the rear motor [18] [19]. This ensures that the drone is stable in the yaw direction of rotation [18] [19]. With these three designs, the drone would require complex algorithms and feedback to ensure that the propellers are able to compensate for uneven thrust forces with changing angular accelerations [15] [17] [18].

Drones with four, six, or eight propellers are inherently balanced because of their even number of propellers [18] [20]. They require half of their propellers to rotate in the clockwise direction and the other half to rotate in the counter clockwise direction [18] [20]. This ensures that the drone will only move up and down if all of the propellers rotate at the same speed [18] [20]. To move in other directions and to perform yaw, pitch, and roll rotations, different propellers need to rotate at different speeds [18] [20]. However, to get these variable speeds, less complex feedback is required [18] [20]. Again, this is because of the inherent symmetry of these types of drones which are naturally balanced when hovering [18] [20]. Figure 4.15 on the next page shows some of the different available drone configurations.

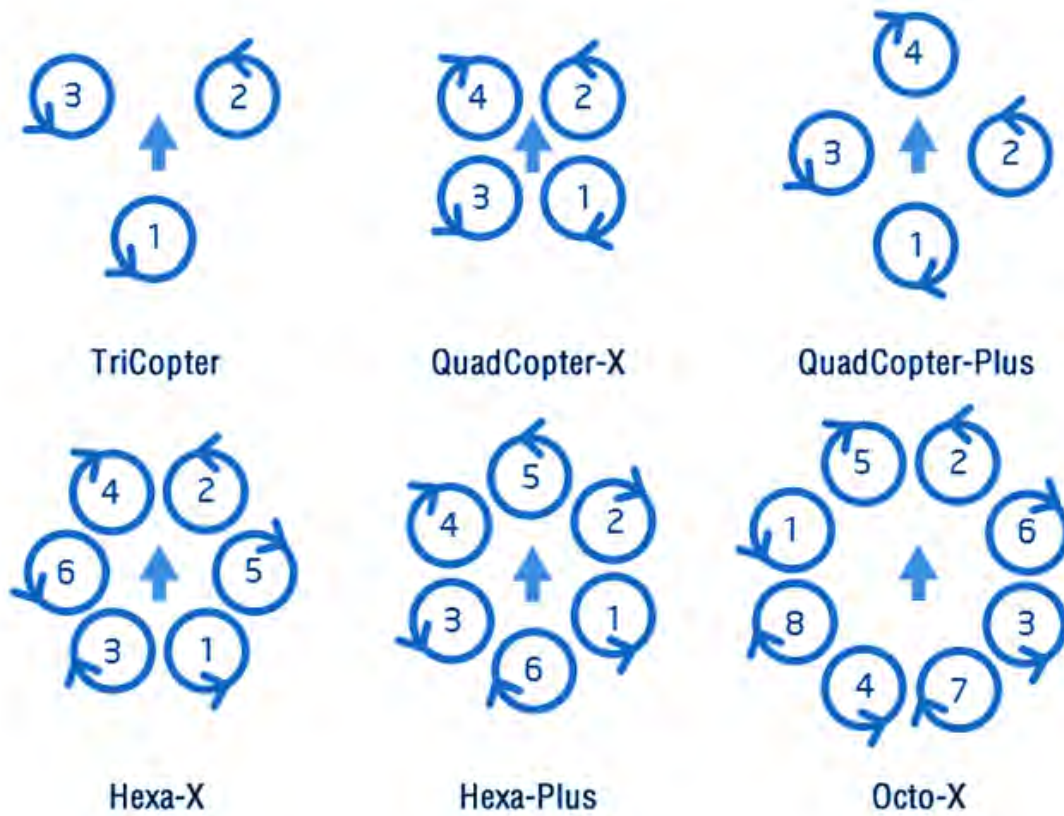


Figure 4.3: Different Drone Propeller Configurations [21]

As four propeller drones (quadcopters) require the least amount of motors and have the simplest motion controls, this was the type of drone chosen for this project. Thus, four motors and propellers were later specified.

4.1.1.2 Required Thrust Force

To estimate the mass of the project's design, the DJI Inspire 2 drone (seen in Figure 4.4) was used as a baseline for comparison. Because the DJI Inspire 2 is very robust, structurally sound, and is aesthetically pleasing it was a good choice for design inspiration.



Figure 4.4: DJI Inspire 2 Drone [22]

Below, in Table 4.1, is a list of DJI Inspire 2 specifications.

| Specification | Specification Value |
|------------------------|---------------------|
| Model | T650A |
| Weight (g) | 3440 |
| Diagonal Distance (mm) | 605 |
| Battery Type | LiPo 6S |
| Battery Capacity (mAh) | 4280 |
| Battery Voltage (V) | 22.8 |

Table 4.1: DJI Inspire 2 Specifications [9]

As seen in Table 4.1 (on the previous page), the DJI Inspire drone is 3.440 kg and has a 605 mm distance between diagonal propellers (not including the propeller sizes). This is a relatively heavy and large drone. Because of this, and as the drone being designed in this project will be approximately desktop sized, a 2 kg mass will be assumed instead. This assumed mass will later be used to specify the motors and propellers.

By assuming that the project's drone design will be approximately 2 kg, the thrust requirement of the design can be determined.

From using Newton's laws ($\sum F = 0$), it can be shown that for the drone to hover in the air, the thrust required needs to be equal to the weight of the drone ($F_{thrust} = F_{weight}$). Therefore, the required thrust produced by the propellers needs to be greater than that of the drone's mass to allow for it to overcome its own weight during liftoff.

Typically, the ratio of thrust to weight used for drone designs is two to one [23]. This allows for moderate maneuverability and can account for some wind [23].

Thus, the desired thrust for this design was determined to be 4 kg ($2 \text{ kg} * 2 = 4 \text{ kg}$). Since the design will use four motors and four propellers, the required thrust can be divided by four. This led to a 1 kg thrust force requirement per motor ($4 \text{ kg} / 4 = 1 \text{ kg}$).

4.1.1.3 Propeller Sizing

After determining that the drone design will incorporate four propellers (and four motors) that will each provide 1 kg of thrust, research was done on the different types of propellers available.

Propellers can have different amounts of blades. Propellers with more blades produce higher torques but are less efficient [24] [25]. Thus, to maximize efficiency, a propeller with only two blades will be specified.

Furthermore, when specifying the propeller blades, the diameter and pitch of the propellers are important characteristics. For propellers with two blades, the diameter indicates the length of both of the blades combined [24] [25]. In other words, the diameter is twice the length of one blade. A propeller with a larger diameter will produce a higher thrust than a smaller propeller rotating at the same speed [24] [25]. However, larger propellers also have larger moments of inertia leading to higher power requirements [24] [25].

The pitch of a propeller represents how far the propellers will travel in a single revolution [24] [25]. The pitch of the propellers is related to the angle at which the blades are rotated about the center hub [24] [25]. A propeller with a higher pitch will be able to more easily produce thrust at higher speeds [24] [25]. Conversely, propellers with lower pitches produce higher thrusts at lower speeds [24] [25]. Figure 4.5 below shows the difference between a high and low pitch.

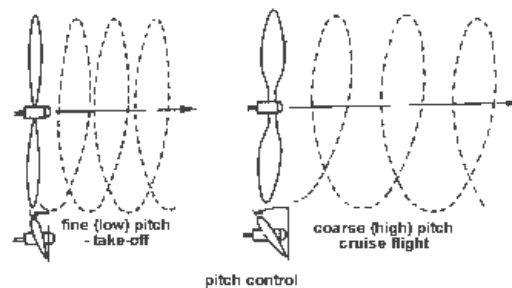


Figure 4.5: Difference Between Propeller Pitch Sizes [26]

Other important factors needed to consider when sizing a propeller includes the C_t (thrust coefficient) and C_p (power coefficient) factors [27]. These factors are determined experimentally by the manufacturer and take into account the shape and pitch of the propellers [27]. With these factors, the diameter of the propeller and the propeller rpm, the desired thrust forces and the required motor torques can be determined. The equations used to determine the thrust and torque can be seen in the sections 4.1.2.1 Thrust Force Equation and 4.1.2.2 Propeller Torque Equation.

Since the thrust of the propellers depend on many factors, this is typically an iterative process. First an approximate propeller size is used based on market research. For instance, the DJI Inspire 2 drone uses a 15-inch propeller blade (Table 4.1). But again, since the drone design for this project will require less thrust, a smaller propeller can be used.

4.1.1.4 Motor and ESC Sizing

After determining the thrust produced by a propeller and the required motor torque, the desired Kv value of a motor is typically calculated. The Kv value indicates the no-load velocity of the motor at a specified voltage [28]. For instance, if the Kv value of a motor is 700 Kv and 1 V is supplied to the motor, then the no-load velocity will be 700 rpm [28]. This constant is inherent for electric motors and is an important attribute for sizing [28].

To get the required Kv value, first an approximate Kv value must be determined from market research. Again, the DJI Inspire 2 drone (Table 4.1) motors have a Kv value of 365 Kv [29]. Because the drone design for this project will be smaller than the DJI Inspire 2, a higher Kv is needed. This is because higher Kv values are used to produce lower thrusts as there is an inverse relationship between thrust and rpm [28].

After finding a motor with the desired Kv value, the winding resistance, and motor supply voltage can be used to determine the motor's torque at different speeds. This resistance is provided by the supplier and the voltage can be chosen based on battery specifications. The equation used to find the motor's torque and subsequent propeller thrust based on the Kv value was derived in the section 4.1.2.3 Motor Torque Equation.

This is also an iterative process. A motor with a specified Kv value can be iteratively checked to see if it can produce the correct thrust with a given propeller running at a specific speed. If the motor can never produce enough torque with the chosen propellers, either a motor with a lower Kv should be chosen or larger propeller should be checked.

A sample calculation of this process can be seen in section 4.1.3 Calculations.

An electronic speed controller, ESC, is similar to a motor driver (explained in section 4.2.1.1 Motor and Driver Sizing) and takes in a digital signal in the form of pulse width modulation (PWM) from the microcontroller to control the brushless DC (BLDC) motor [30]. The ESC is required to meet the voltage and current requirements of the motor to prevent overheating and other issues.

Pulse width modulation is essentially a digital signal that is continuously turned on and off at a rate set by the user [31]. A PWM signal requires a duty cycle and a frequency. The duty cycle is the ratio of how long the signal is turned on to how long it is off, which can be varied and controlled by the user. Essentially, in terms of controlling a BLDC motor, increasing the duty cycle increases the average voltage provided to the motor and thus the motor's speed. The frequency is typically set a constant value that should be compatible to the motor being controlled.

4.1.1.5 Battery Sizing

The typical battery type found for drones were LiPo batteries, which came in various nominal voltages as shown below in Table 4.2. Each cell has a voltage of 3.7 V and the number of cells is denoted by the number in front of the “S” in its sizing. Larger battery sizes exist, but the typical maximum voltage required for drones only goes up to 6S.

| Size of Battery | Supply Voltage (V) |
|-----------------|--------------------|
| 1S | 3.7 |
| 2S | 7.4 |
| 3S | 11.1 |
| 4S | 14.8 |
| 5S | 18.5 |
| 6S | 22.2 |

Table 4.2: LiPo Battery Sizes and Voltages

The capacity of the battery is determined by its milliamp-hour (mAh) rating. A 5000 mAh battery would be able to output a current of 5 A for an hour. However, the maximum continuous and burst discharge rate of a battery is determined by its discharge rate (C). The output current can be calculated with the following equation.

$$\text{Output Current} = \text{Discharge rate} \times \text{Capacity}$$

A battery with a 50C continuous discharge rate and a 5000 mAh capacity would allow for a continuous current output of 250A for a 1/50th of an hour. While the output current is directionally proportional to the discharge rate, the time until the battery drained is inversely proportional.

4.1.2. Equation Derivations

To specify the motors and propellers used to enable the drone to fly, three equations were derived. The derivation of the thrust force and torque produced by the propeller and the torque generated by the motor are described in detail in the following sections.

4.1.2.1 Thrust Force Equation

For the calculations and equations in this section, several sources were used as a reference [32] [33] [34] [35] [36].

To begin determining the relationship between thrust, diameter and speed, the following equation using to relate thrust force to pressure. An illustration of where this force comes from can be seen below in Figure 4.6.

$$F_{thrust} = A * \Delta P \quad \text{Equation 4.1}$$

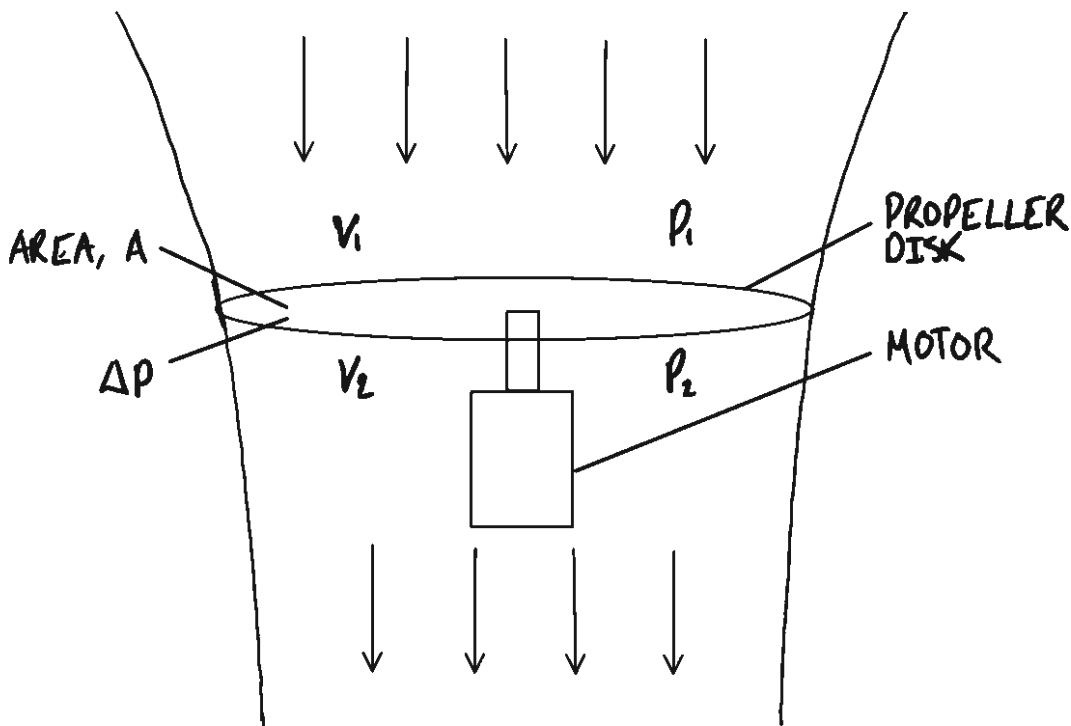


Figure 4.6: Propeller Thrust Force Diagram

Through Bernoulli's equation, an equation for the pressure difference ΔP can be found.

$$P_1 + \frac{1}{2}\rho v_1^2 + \rho g h_1 = P_2 + \frac{1}{2}\rho v_2^2 + \rho g h_2$$

Assuming ideal conditions, such as stagnant air, the vertical component of the initial velocity v_1 (velocity of the air entering the propeller) can be assumed to be zero. The velocity leaving the propeller can be represented by the vertical component of the final velocity v_2 . Also, assuming the height of the air entering and leaving the propeller, h_1 and h_2 , are equal or have negligible differences, we can find the pressure difference to be the following.

$$P_1 - P_2 = \Delta P = \frac{1}{2}\rho v_2^2 \quad \text{Equation 4.2}$$

Plugging equation 4.1 into equation 4.2,

$$F_{thrust} = \frac{1}{2}\rho A v_2^2 \quad \text{Equation 4.3}$$

The area in equation 4.3 would represent the projected area of the propeller, which is proportional to the square of the diameter. The C is a constant that takes into consideration the shape and pitch of the propeller.

$$A \propto D^2$$

$$A = C D^2 \quad \text{Equation 4.4}$$

The relationship of the linear (vertical) velocity produced by the propeller and the angular velocity of the propeller can also be seen below in Figure 4.7. The total velocity of the air is represented by v_{air} , which takes into account both the horizontal and vertical component of the air relative to the propeller. As well, angles that need to be taken into consideration for these derivations include the pitch angle, θ , the attack angle, α , and the difference between these two angles, ϕ . Where ϕ and θ are not constants as they change relative to how much the drone is pitching relative to the ground.

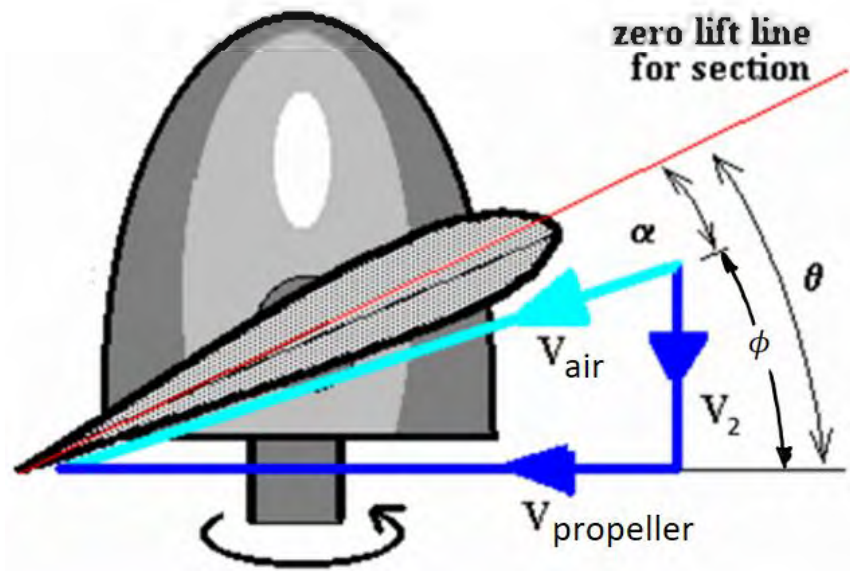


Figure 4.7: Propeller Wing Velocity Diagram [37]

Velocity v_2 can then be rewritten to the following in terms the angular velocity, n , in rev/s.

$$v_2 = \frac{v_{propeller}}{\tan(\theta - \alpha)} = \frac{v_{propeller}}{\tan \phi} = \frac{r\omega}{\tan \phi}$$

$$\rightarrow v_2 = \frac{\left(\frac{D}{Z}\right) (2\pi n)}{\tan \phi}$$

$$\rightarrow v_2 = \frac{D\pi n}{\tan \phi}$$

Equation 4.5

Plugging equation 4.4 and 4.5 back into equation 4.3:

$$F_{thrust} = \frac{1}{2} \rho A v_2^2 \rightarrow F_{thrust} = \frac{1}{2} \rho (CD^2) \left(\frac{D\pi n}{\tan \phi} \right)^2$$

$$\rightarrow F_{thrust} = C \left(\frac{\pi}{\tan \phi} \right)^2 \rho n^2 D^4$$

Some of the terms in the equation can be combined to get the coefficient of thrust, $C_t = C \left(\frac{\pi}{\tan \phi} \right)^2$. The coefficient of thrust must be determined through experimentation like a drag coefficient, as it depends on many changing factors which cannot be calculated. This is typically provided by a supplier. The air density (ρ) is in slug/ft³, n is in rev/s, and D in ft.

$$F_{thrust} = C_t \rho n^2 D^4 \quad \text{Equation 4.6}$$

4.1.2.2 Propeller Torque Equation

For this section, several sources were used for reference [32] [33] [34] [35].

To find the propeller torque, first the power requirement was found using the equation derived for F_{thrust} and v_2 (refer back to Figure 4.7).

$$Power = F_{thrust} v_2$$

$$where F_{thrust} = C_t \rho n^2 D^4, v_2 = \frac{r\omega}{\tan \phi}$$

$$Power = (C_t \rho n^2 D^4) \frac{r\omega}{\tan \phi} = (C_t \rho n^2 D^4) \frac{\left(\frac{D}{2}\right) (2\pi n)}{\tan \phi} = (C_t \rho n^2 D^4) \frac{D\pi n}{\tan \phi}$$

$$\rightarrow Power = \frac{C_t \pi}{\tan \phi} \rho n^3 D^5$$

Some of the terms can be combined again to get the power coefficient. This is a value that is typically provided by a supplier.

$$Power = C_p \rho n^3 D^5 [lb - ft] \quad \text{Equation 4.7}$$

$$Power = \frac{C_p \rho n^3 D^5}{550} [HP]$$

Now, the equation for torque can be found as follows (where n is in rev/s).

$$Power = T\omega$$

$$T = \frac{Power}{\omega} = \frac{12 * Power_{lb-ft}}{2\pi n} \left[\frac{lb - in}{s} \right]$$

$$\rightarrow T_{lb-in} = \frac{6 * Power_{lb-ft}}{\pi n} \quad \text{Equation 4.8}$$

4.1.2.3 Motor Torque Equation

For this section, the “Torque Equation and the Relationship with DC Motors” by Danielle Collins was used as a reference [38].

A typical DC motor circuit can be seen below to help illustrate the operations of a DC motor. A description of how a DC motor functions can be seen in section 4.1 Phase 1 Theory. Essentially, by running a current through its coils, a magnetic force can be produced which results in a torque. The torque created by the motor when spinning is dependent on the power supplied to it.

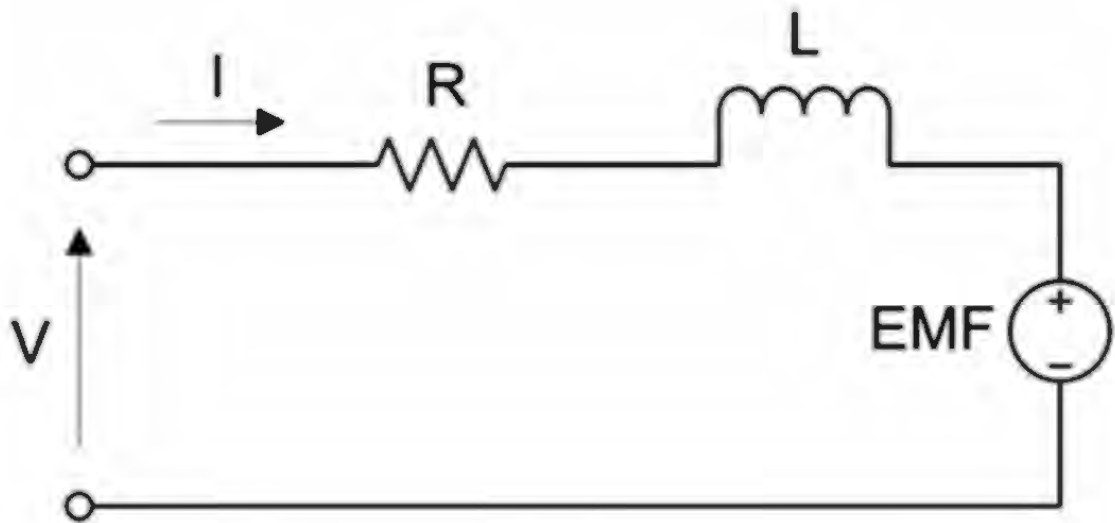


Figure 4.8: Typical DC Motor Circuit [39]

From Figure 4.8 on the previous page, the voltage is equal to the voltage drop across the internal resistance (R) inductor (L) and back-EMF (E). This is summarized by the equation below.

$$V = IR + L \frac{dI}{dt} + E$$

By assuming a constant current, this equation becomes

$$V = IR + E \quad \text{Equation 4.9}$$

For a motor, the back-EMF voltage is generated by the rotation of the coil and can be found by the following, k is the electrical constant from the motor and ω is the angular velocity of the motor.

$$E = k_e \omega \quad \text{Equation 4.10}$$

Similarly, the current through the motor is directly related to the motor's torque, $T = k_t I$, where k_t is a torque constant from the motor. Therefore, the current (I) can be found as the following.

$$I = \frac{T}{k_t} \quad \text{Equation 4.11}$$

Plugging equation 6.0 and 6.1 into equation 5.0, it now becomes,

$$V = \frac{T}{k_t} R + k_e \omega \quad \text{Equation 4.12}$$

However, for DC motors, the electrical and motor constants are equal ($k = k_e = k_t$), changing the equation to be the following.

$$V = \frac{T}{k} R + k \omega \quad \text{Equation 4.13}$$

This equation can be rearranged to determine the torque produced by the motor, based on input voltage.

$$T_{motor} = \frac{V - \omega k}{R} k \quad \text{Equation 4.14}$$

In this equation, the constant k is equal to $\frac{1}{k_v}$, where k_v is the motor constant typically given in $\frac{rpm}{V}$ and would need to be converted to $\frac{rad}{s}$.

The relationship between torque and rotational speed in a typical DC motor is illustrated below in Figure 4.9.

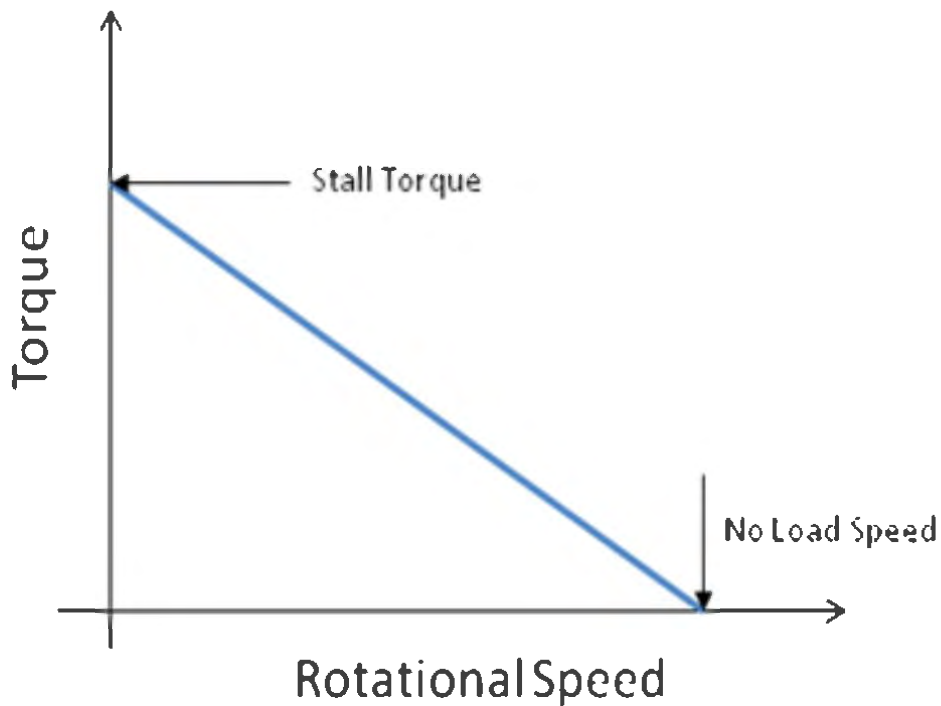


Figure 4.9: Torque-Speed Curve [39]

4.1.3. Calculations

In this section, a sample calculation is provided for one iteration of a motor and propeller selection process. The last iteration conducted to size the motors and propellers chosen for the project was provided to demonstrate the validity of the choices.

4.1.3.1 Sample Calculation

An overview of the actuator sizing procedure can be seen flow chart below seen in Figure 4.10. The details of the main steps (1 to 8) are also demonstrated through a sample calculation in the next few pages. The final selection of the motor and propeller are shown in 4.1.3.1 Sample Calculation.

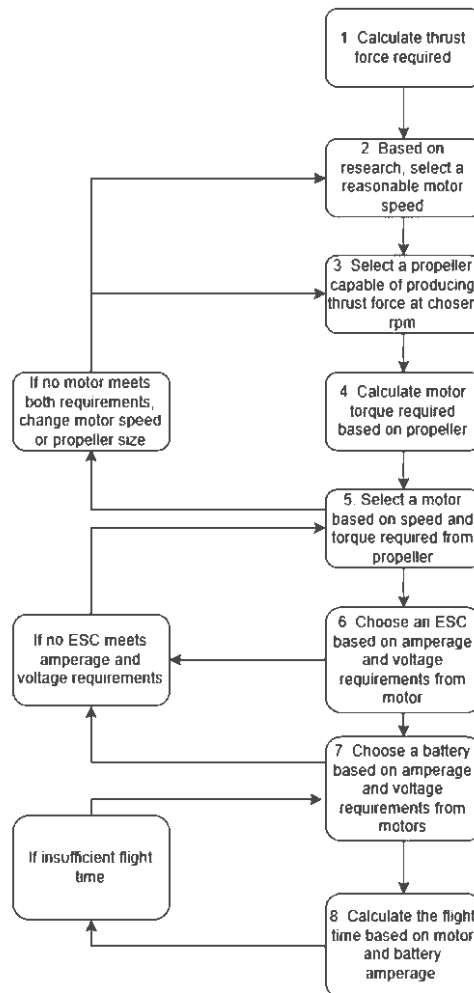


Figure 4.10: Actuator Sizing Flow Chart

Step 1: Calculating thrust force required

The weight requirement of the drone was determined to be about 2 kg (from 4.1.1 Secondary Research). Thus, the thrust force should be at least double the weight.

$$F_{total} = 2m_{drone} = 2(2) = 4 \text{ kg force}$$

Each propeller would have to be able to at least produce a thrust force of 1 kg (2.2 lb).

$$F_{propeller} = \frac{F_{total}}{\text{no. of propellers}} = \frac{4}{4} = 1 \frac{\text{kg force}}{\text{propeller}}$$

Step 2: Based on research, select a reasonable motor speed

Based on research, Figure 4.11 was made to help establish a reasonable motor speed when using propellers greater than six inches in size. The table represents the minimum speed required for a certain propeller size to produce a thrust force of at least 1 kg (2.2 lb).

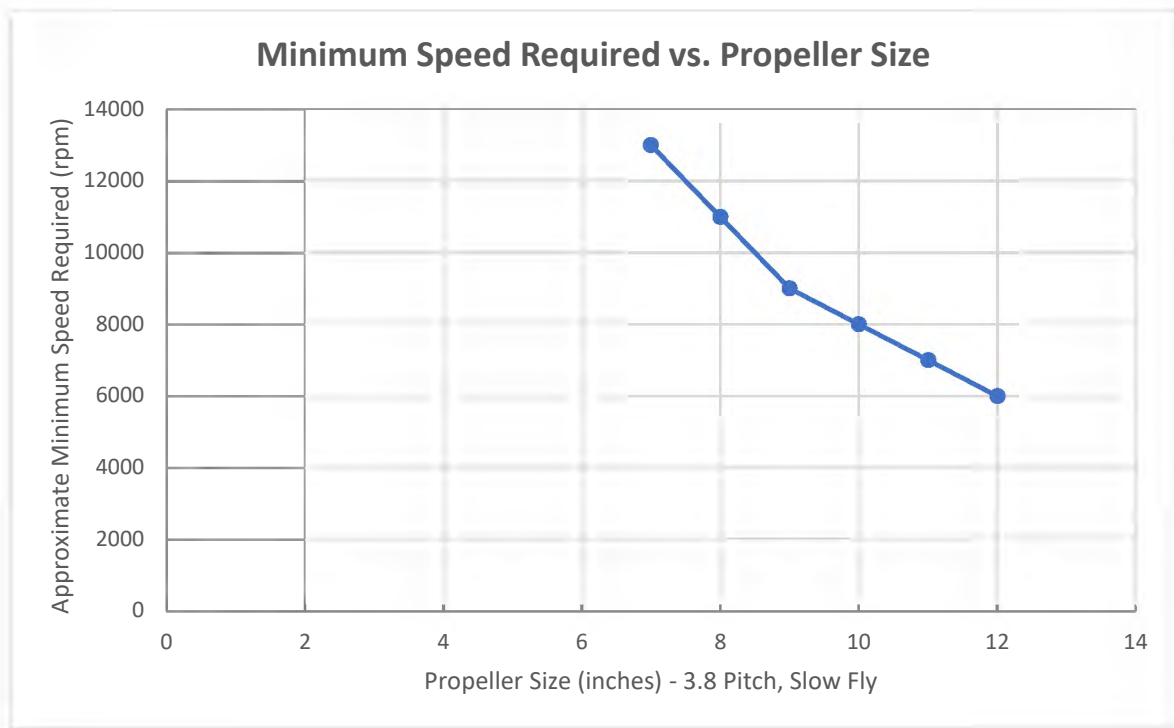


Figure 4.11: Minimum Speed Required vs. Propeller Size for a 1 kg Thrust Force
For this example, a motor speed of 8000 rpm was chosen for the first iteration.

Step 3: Select a propeller capable of producing thrust force at chosen rpm

The minimum thrust force required of each propeller was determined to be 1 kg (2.2 lb) to lift a 2 kg drone with four propellers.

Taking APC propeller 10x3.8SF, the C_t is given to be 0.1280 by the manufacturer.

By running this propeller at 8000 rpm and by assuming air density of 1.225 kg/m^3 ($0.0023769 \text{ slug/ft}^3$), we get the following thrust force.

$$F_{thrust} = 0.1280(0.0023769) \left(\frac{8000}{60}\right)^2 \left(\frac{10}{12}\right)^4$$

$$F_{thrust} = \mathbf{2.6084 \text{ lbf}}$$

Therefore, this propeller was a suitable choice.

Step 4: Determine the torque require to be overcome by the motor due to the propeller.

For the same APC propeller 10x3.8SF from the previous sample calculations, the C_p is given to be 0.0533 by the manufacturer. The torque required to be overcome can then be calculated as follows:

$$P_{lb-ft} = 0.0533(0.0023769) \left(\frac{8000}{60}\right)^3 \left(\frac{10}{12}\right)^5$$

$$P_{lb-ft} = 120.68 \text{ lb} - \text{ft}$$

$$T_{propeller} = \frac{12(120.68)}{\frac{2\pi}{60}(8000)}$$

$$T_{propeller} = \mathbf{1.7286 \text{ lb} - \text{in}}$$

Step 5: Select a motor based on speed and torque required from propeller

To begin actuator sizing, research was conducted to estimate the Kv range desired for the chosen motor, which included using the DJI Inspire 2 drone as a reference point. The DJI Inspire 2 uses a 3512 Brushless DC motor that produced a thrust force of 2kg, ranging from 350 Kv to 750 Kv. Therefore, a higher Kv range was acceptable as the thrust force required for this design is only 1 kg. Research confirmed that the motor constant required for this drone should range from 700 Kv to 1000 Kv.

The UAV Brushless Motor MS2814 from T-Motor for example, has a motor constant of 770 Kv (rpm/V) and an internal resistance of 100 mΩ.

The speed of the motor can be calculated based on the Kv and input voltage. Assuming an input voltage of 14.8 V (3S LiPo, see Step 7), the no load speed achievable can be calculated as follows.

$$n_{no\ load} = Kv * V = 770 * 14.8 = \mathbf{11,396\ rpm}$$

This speed is much greater than the maximum speed required (8000 rpm) and is therefore viable. This speed is however, the no load speed and the actual maximum speed under loading will be slightly lower than 11,396 rpm. Increasing the amount of voltage cells from the assumed battery (3S LiPo, see Step 7) will help meet the speed requirement if a voltage of 14.8 V is not sufficient.

The motor torque is typically either supplied by the manufacturer or can be calculated from the internal resistance and Kv of the motor. For this motor, torque was not supplied, but the internal resistance was given instead.

To determine how much torque the motor can output, equation 5.3 can be used by taking the specifications provided from a chosen motor. The torque produced can be calculated as follows, using a voltage input of 14.8 V again.

$$T = \frac{V - \omega k}{R} k$$

$$\text{where } k = \frac{1}{k_v} = \frac{1}{770 \left(\frac{60}{2\pi}\right)}$$

$$T = \frac{\left(14.8 - \left(8000 * \frac{2\pi}{60}\right) \left(\frac{1}{770 \left(\frac{2\pi}{60}\right)}\right)\right)}{0.1} \left(\frac{1}{770 \left(\frac{2\pi}{60}\right)}\right)$$

$$T = 0.54696 \text{ Nm} \left(\frac{8.8507 \text{ lb} - \text{in}}{1 \text{ Nm}}\right)$$

$$T_{motor} = \mathbf{4.841 \text{ lb} - \text{in}}$$

Because T_{motor} (4.841 lb - in) was greater than $T_{propeller}$ (1.730 lb - in) and $n_{no \text{ load}}$ (11,396 rpm) was found to be greater the minimum speed required (8000 rpm), the combination of this motor and the propeller is deemed valid choice to produce sufficient thrust force for the drone to fly.

Step 6: Choose an ESC based on amperage and voltage requirements from motor

The chosen motor has a voltage requirement of 14.8 V and a current requirement of around 20 A when producing its maximum thrust. Thus, an ESC specified to work under these conditions should be chosen.

Step 7: Choose a battery based on amperage and voltage requirement from motor

Similarly, for the voltage and current requirements of 14.8 V and 20 A (max) respectively, need to be powered by a 4S LiPo battery. This is because a 4S LiPo battery produces a nominal, continuous voltage of 14.8 V.

Step 8: Calculate the flight time based on motor and battery amperage

After choosing a 4S battery, the mAh capacity should be noted in order to estimate the flight time of the drone. Since the drone will be experiencing a maximum of 20 A, the minimum flight time can be calculated as shown below.

$$\text{Flight Time (min)} = \frac{\text{Total Battery Amperage}}{\text{No. of Motors} * \text{Motor Drawn Amperage}}$$

$$\text{Flight Time (min)} = \frac{(5000 \text{ mah}) * \left(\frac{A}{1000\text{ma}}\right) * \left(60 \frac{\text{min}}{h}\right)}{4 * 20 A} = 3.75 \text{ minutes}$$

The maximum flight time can be calculated based on the hovering thrust required (0.5 kg per motor). This equates to 4.7 A.

$$\text{Flight Time (max)} = \frac{(5000 \text{ mah}) * \left(\frac{A}{1000\text{ma}}\right) * \left(60 \frac{\text{min}}{h}\right)}{4 * 4.7 A} = 15.96 \text{ minutes}$$

4.1.3.2 Final Iteration

Due to the small, desktop size requirement, the propeller size was revised and iterated multiple times.

By going through step 1 to 8, the following results were obtained.

- Step 1: $F_{propeller} = 1 \frac{kg\ force}{propeller}$
- Step 2: *Motor Speed* = 25,000 rpm
- Step 3: $F_{thrust} = 2.283\ lbf$
- Step 4:
 - $T_{propeller} = 1.355\ lb - in$
 - $n_{no\ load} = 42,180\ rpm$
- Step 5: $T_{motor} = 4.0222\ lb - in$
- Step 6:
 - Voltage Requirement: 22.2 V
 - Current Requirement: ~30 A
- Step 7: 6S LiPo Battery
- Step 8:
 - *Flight time (min)* = 1.875 minutes
 - *Flight time (max)* = 3.75 minutes

The final propeller size was determined to be APC propeller 5x4.3E [40]. Moreover, the final motor was chosen to be EMAX RSII 2306 1900kv Motor [41] [42].

In case the APC propeller 5x4.3E were not capable of producing enough thrust force, 6045 bull nose propellers were also considered.

4.1.4. Motor Control

In this section, the theory behind motor controls for drones are described in detail. This included theoretical background on accelerometers and gyroscopes, and how they would be combined using a complementary filter. Additionally, drone maneuvering and PID control feedback loops are discussed in the sections to follow.

4.1.4.1 Feedback Control: Accelerometer and Gyroscope

In order to control the movement of a quadcopter, microcontroller feedback was required to maintain stability. When the drone is mid-air, it has six degrees of freedom (DOF) as seen below in Figure 4.12. These included linear translation and angular rotation about the x, y and z axes. The setpoint values for these axes can be chosen arbitrarily by the user.

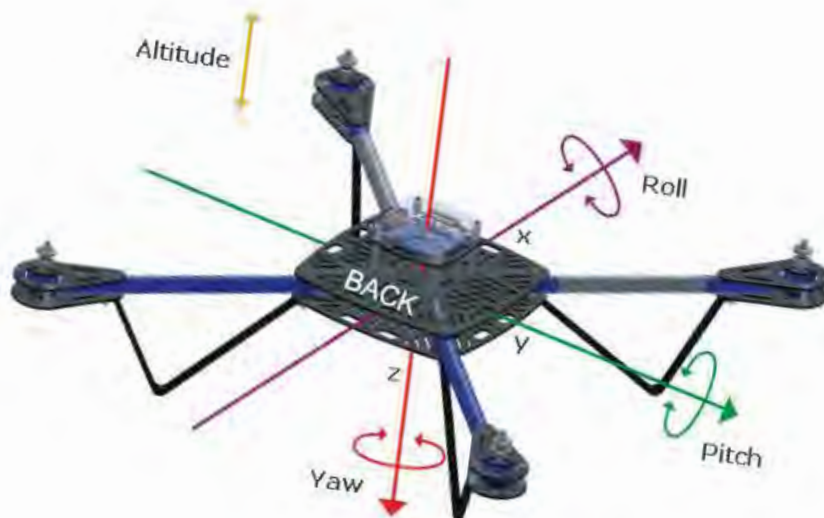


Figure 4.12: Six Degrees of Freedom of a Quadcopter [43]

An accelerometer and a gyroscope are the sensors required to measure and monitor the motion in each of these DOF. An accelerometer can measure the linear acceleration in the x, y and z axes and a gyroscope can measure angular speed about these axes [43]. For advanced motion controls, a GPS and an optical sensor can be used to further increase the accuracy and precision of the drone's movement.

A Micro-Electro-Mechanical-Systems (MEMS) gyroscope functions with the help of the Coriolis effect as shown below in Figure 4.13 [44]. When a mass is moving and rotating in a certain direction, as shown by the red and green arrow, a Coriolis force is produced as shown by the blue arrow.

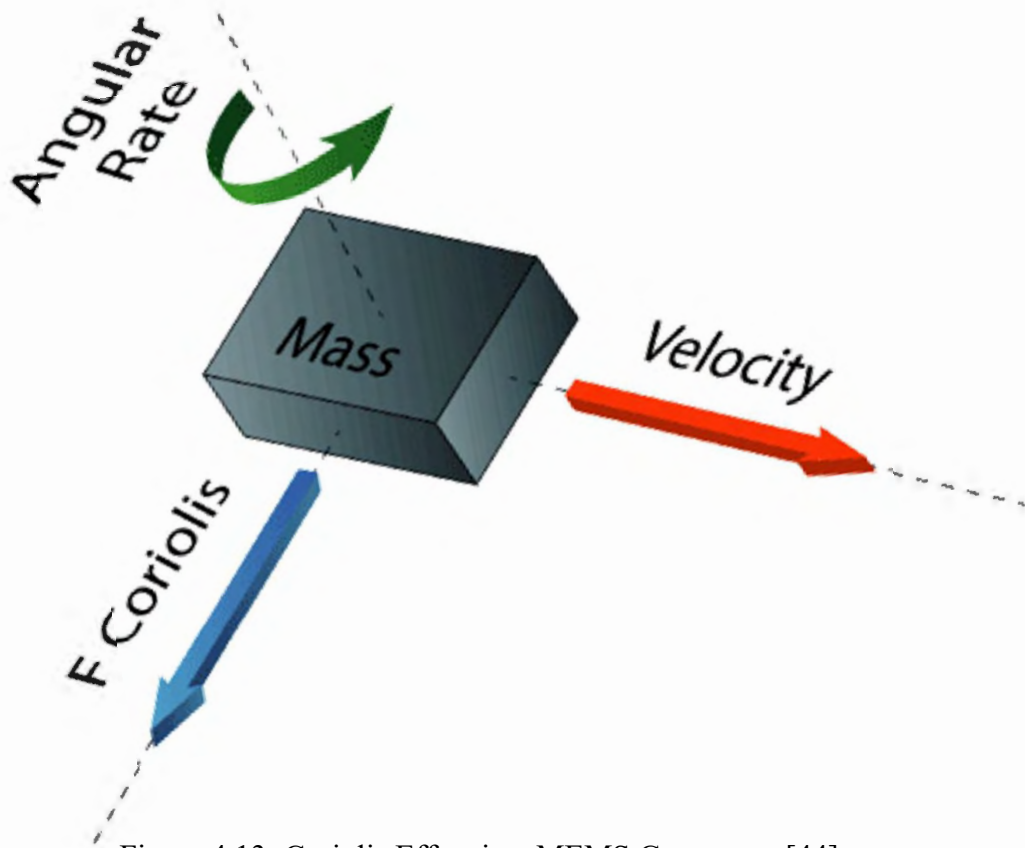


Figure 4.13: Coriolis Effect in a MEMS Gyroscope [44]

Using the concept of the Coriolis Effect, the displacement of the mass can change the capacitance within the capacitive sensing structure in the gyroscope. This change in capacitance is also proportional to angular velocity and is converted to an output voltage in analog gyroscopes or LSBs in digital gyroscopes [45]. For some MEMS gyroscopes, two of these masses are used in the form of a tuning fork configuration as shown below in Figure 4.14.

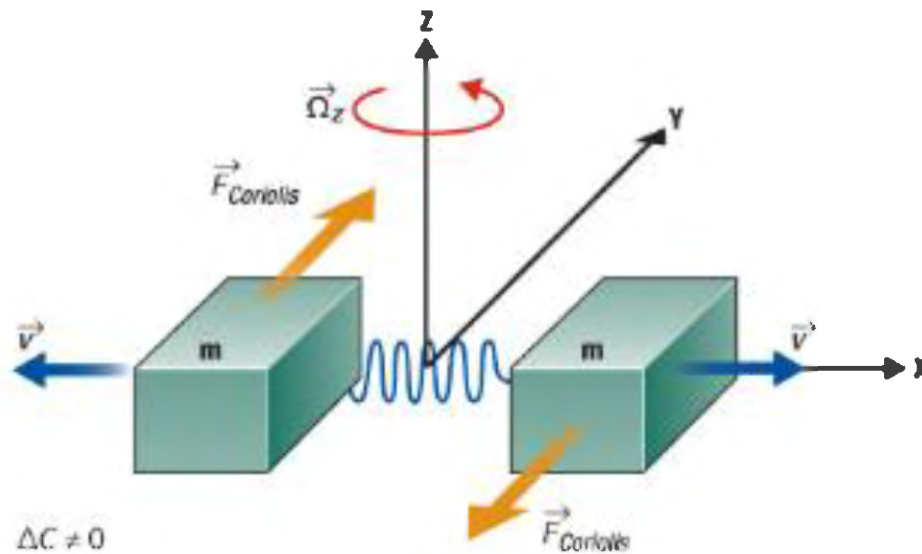


Figure 4.14: Tuning Fork Configuration in a MEMS Gyroscope [45]

4.1.4.2 Complementary Filter

An accelerometer and a gyroscope need to be used in combination with one another due to the types of errors that they independently produce. Accelerometer measurements are fairly accurate and remain at the setpoint but exhibits high frequency noise that is undesirable when implementing control. On the other hand, gyroscopes experience less noise, but their measurements, in terms of the angle, deviate over time from the setpoint [46]. Basically, the measurements from the gyroscope are only reliable when there are short-term changes. The accelerometer and gyroscope are both able to synergize with one another by summing a percentage of each device's measurements since the accelerometer and gyroscope are respectively reliable for long-term measurements and short-term changes of those measurements [46]. The accelerometer essentially allows the drone to remain stable while the gyroscope allows it to maneuver. This is known as a Complimentary Filter and is summarized by the block diagram below in Figure 4.15, where the typical split of the total angle is 98 percent from the gyroscope measurement and 2 percent from the accelerometer's measurement.

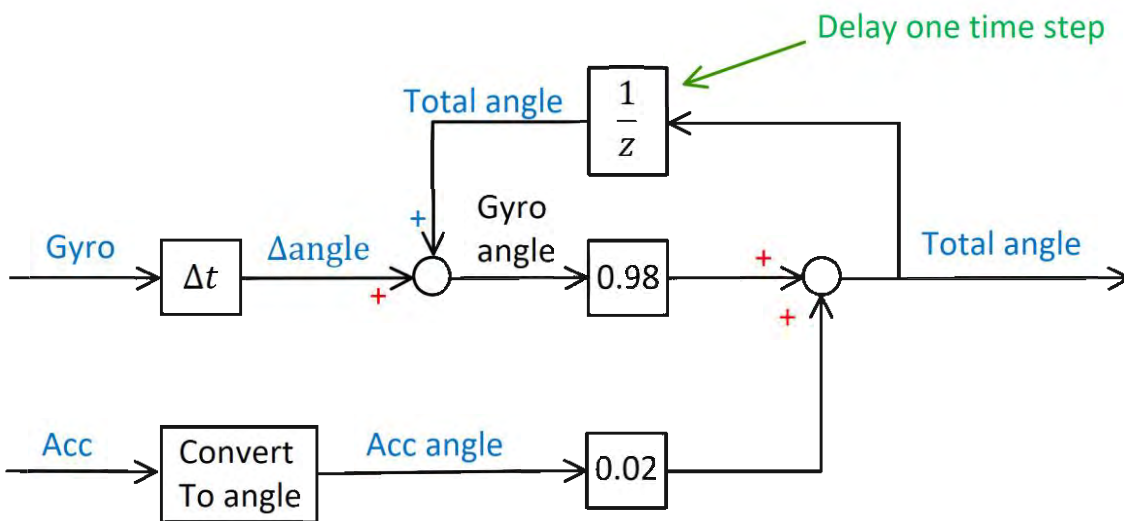


Figure 4.15: Complimentary Filter Block Diagram [46]

4.1.4.3 Drone Maneuvering: Roll, Pitch and Yaw

When each propeller from a quadcopter produce equal thrust forces, it would simply fly straight up in the z-direction as previously shown in Figure 4.12. Movement in this axis is known as throttle and can be done by increasing the power outputted by each brushless DC motor. This would only be possible if two propellers rotated clockwise and the other two rotated counter-clockwise at the same speed. Assuming the motors being used are brushless DC motors, which are typically recommended due to the high-speed requirement, two of the wires can be reversed in order to reverse the polarity of the motor [47]. This is illustrated below in Figure 4.16.

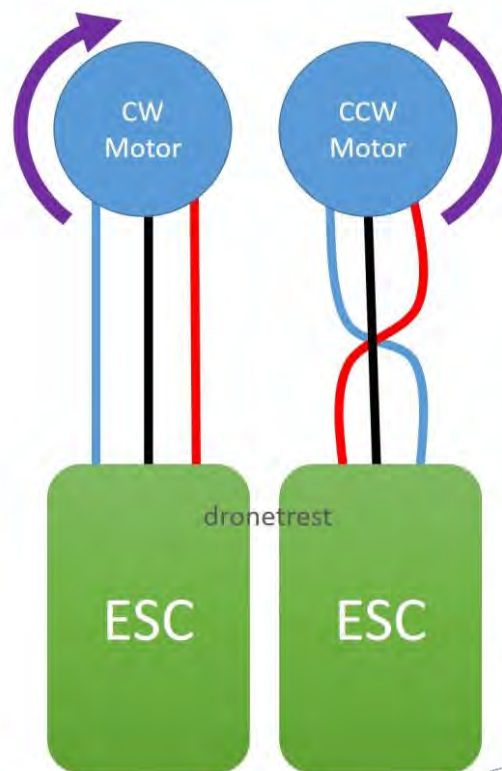


Figure 4.16: Reversing BLDC Motor Polarity [47]

However, a differential speed among the motors is required for the drone to maneuver forward, backward, sideways, and about the z axis. These are known as roll, pitch and yaw as illustrated below in Figure 4.17 and Figure 4.18. They allow the drone to both hover and maneuver. The roll, pitch and yaw are each used to describe the tilting motion of the drone towards the left or right, towards the front or back, and rotation about the z axis. These concepts are implemented in the PID controls (which is later described in further detail) that allow the drone to remain stable throughout its flight.

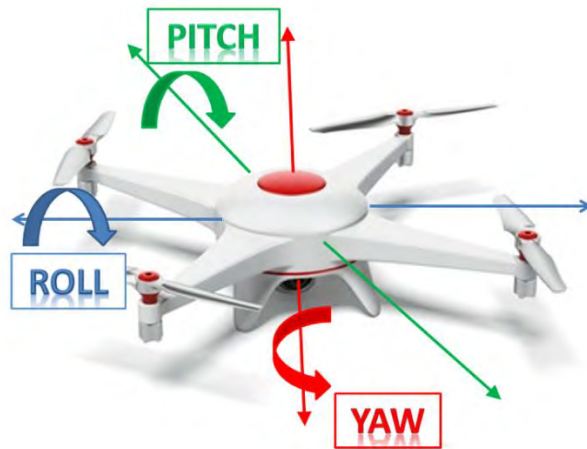


Figure 4.17: Roll, Pitch and Yaw of a Quadcopter [48]

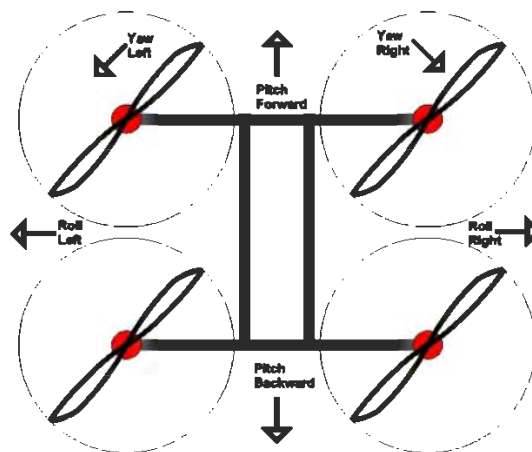


Figure 4.18: Roll, Pitch and Yaw Summary [49]

In order to properly describe how to manipulate the motor in accordance to the motion desired, Figure 4.19 below will be used to refer to motor one, two, three and four. The front of the drone is assumed to be on the side of motor one and two.



Figure 4.19: Basic Quadcopter Configuration [50]

For the drone to roll side to side, there must be a differential in motor power among the left and right motors. In this case, motor two and three would have to move slower than motor one and four to move to the right. Similarly, for the motor to pitch forward, the front motors, in this case motors one and two, would have to move slower than the back motors, motors three and four. The reverse of what was described for rolling and pitching would allow the drone to move to the left and backwards respectively. Rolling and pitching are the essential motions that allow the drone to move in a square pattern.

While rolling and pitching seems simple, yawing on the other hand was slightly more counter-intuitive and complicated to understand. The ability to yaw was due to the conservation of angular momentum. If each propeller were turning at the exact same speed, then the total angular momentum would equal to zero since there was an equal number of propellers turning clockwise and counter-clockwise. However, by slowing down the motors that are rotating in a specific direction, this would cause the drone to the same way to compensate for the loss of angular momentum in order to achieve a total of zero angular momentum. In other words, for the drone to rotate to the right, the green motors (one and three) would have to spin slower than the blue motors (two and four). In addition to rolling and pitching, yawing allows the drone to move in a circular pattern.

4.1.4.4 PID Controls and its Role

The ability for a drone to remain stable throughout its flight is provided by the PID control feedback loop implemented by a microcontroller with a desired setpoint. The drone would essentially be able to roll, pitch and/or yaw by adjusting this setpoint. PID allows the measurements of the drone's current status from the accelerometer and gyroscope to be fed back and ensures that the drone is running properly and reaching its desired setpoint. The PID controls consist of three constant terms to be set by the user: proportional (P), integral (I) and derivative (D) [51]. Each drone would have its own set of calibration as the thrust force produced by the propellers and motors varies from one another and drone to drone. Depending on how well the drone user can maneuver the drone from a controller, the PID control may not need to be accurately refined or tuned [51].

The proportional term, K_p , outputs a value that is proportional to error measurement, $e(t)$, from the sensors. Its output value, P , can be described by the following equation:

$$P = K_p e(t) \qquad \text{Equation 4.15}$$

The integral term, K_i , outputs a value that is proportional the magnitude of the error measurement over time $\int_0^t e(\tau) d\tau$. Its output value, I , can be described the following equation:

$$I = K_i \int_0^t e(\tau) d\tau \quad \text{Equation 4.16}$$

Lastly, the derivative term, K_d , outputs a value that is proportional to the rate of change of the error measurement. Its output value, D , can be described by the following equation:

$$D = K_d \frac{de(t)}{dt} \quad \text{Equation 4.17}$$

These three terms could be combined to obtain either of the following equations in a PID control feedback loop. Equation 4.19 was obtained by factoring out K_p from K_i and K_d , since it was initially a part of those terms from the very beginning. This leaves the integral time, T_i , and derivative time, T_d , in seconds or other unit of time [52].

$$u(t) = K_p e(t) + K_i \int_0^t e(\tau) d\tau + K_d \frac{de(t)}{dt} \quad \text{Equation 4.18}$$

$$u(t) = K_p \left(e(t) + \frac{1}{T_i} \int_0^t e(\tau) d\tau + T_d \frac{de(t)}{dt} \right) \quad \text{Equation 4.19}$$

A feedback control loop can be either only P, PI, PD or PID and never only I or D. Unfortunately, only having the proportional term results in having a steady state error. By adding the integral term, the steady state error can be removed by accelerating the value to move towards the setpoint [52]. However, this can also cause an overshoot if the value is set too high [52]. Lastly, adding the derivative term allows for the drone to respond quicker, thus improving settling time and stability [52]. However, it can also amplify noise in the system that may come from the environment, controller, sensors and other devices. A low pass filter may be then implemented to improve the signal but may not always work. As a result, the derivative term is not used often as it may simply worsen the signal response.

4.2. Phase 2 Theory

brushed DC motors are the most common types of motors and are mainly comprised of a stator, rotor, commutator and brushes. The circuit of a brushed DC motor is illustrated below in Figure 4.20.

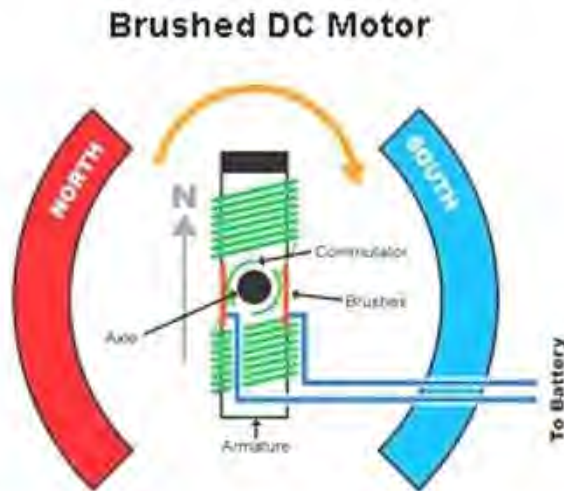


Figure 4.20: Brushed DC Motor Circuit [13]

The stator typically uses a permanent magnet or electromagnetic windings in order to create a stationary magnetic field and is depicted by the north and south magnetic poles shown in Figure 4.21. Similarly, the rotor or armature is comprised of electromagnetic windings which generate a rotating magnetic field when current runs through the wires shown in green. The attraction and repulsion of the magnetic poles from the rotor and stator produces a torque and create the rotating motion. The motor is able to continuously rotate through the help of a copper sleeve that acts as a mechanical switch known as the commutator [53]. After completing half a revolution, the current is reversed when the brushes make contact with the other opposite surface of the commutator [53].

A close-up of a commutator and brushes are illustrated in Figure 4.21 for better understanding. This reverses the magnetic poles of the rotor's electromagnetic windings after every 180 degrees, which results in the continuous rotating motion of the motor [53].

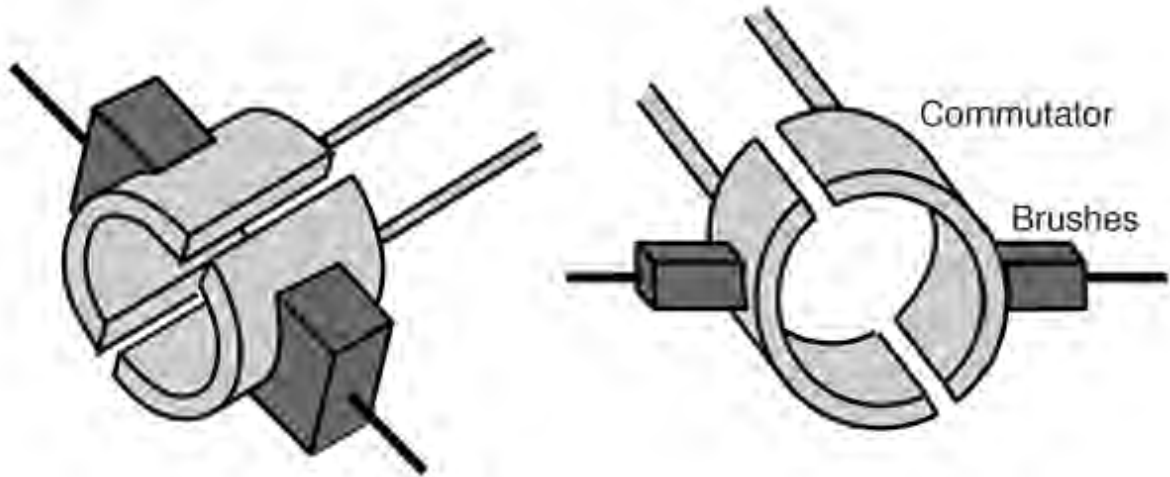


Figure 4.21: Commutator and Brushes [53]

4.2.1. Secondary Research

In this section, the secondary research conducted is described to clarify the selection process of the brushed DC motor and the motor driver.

4.2.1.1 Motor and Driver Sizing

The process of sizing the motor for Phase 2 is illustrated in Appendix C Review Package, which assumed a 3-inch wheel was being used. The analysis began by creating a trapezoidal motion profile using a desired velocity and acceleration. These were then used to determine the maximum and minimum torque required to respectively prevent slippage and allow the motor to start rotating. A brushed DC motor was then selected using the speed and torque requirements. Using the specifications of the selected motor, a motor driver was then also be selected after wards.

A motor driver is a low-level circuit used to drive a motor, typically a breakout board, and often consists an H-Bridge which allows the motor to change polarity. They can operate through a digital (in PWM) or analog signal outputted by a microcontroller [30].

4.2.2. Motor Control

Comparatively to the drone controls in Phase 1, the drive controls in Phase 2 were much less complicated. A PID control feedback loop was not required as the drone was already stable on the ground. While sensors may provide information about the position, speed and other aspects of the drone, none are necessary for the drive portion to function properly.

The drone required a minimum of two motors in order to be able to drive forward, backward and turn left and right. In order for it to remain stable on the ground, the drone required a minimum of three wheels. For the drone to move forward or backwards, both driving motors would simply have to rotate at the same speed in the same direction, either clockwise or counter-clockwise. To turn left or right on the other hand required the wheel move at different speeds. Turning left requires the left wheel to rotate at a slower speed than the right and the reverse is needed to turn right. For the drone to spin about itself, the motors would have to rotate at the same speed but opposite direction. These are all summarized below in Figure 4.22, where it is assumed that the driving motors are centered in the middle of the drone. This would also require at least one more additional wheel for the drone to remain stable while driving.

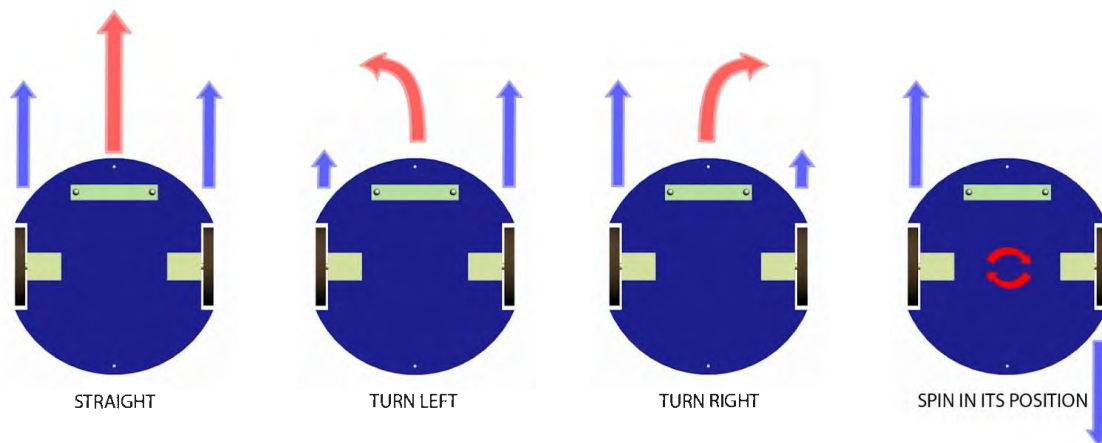


Figure 4.22: Basic Drive Configurations [54]

4.2.2.1 Reversing Motor Direction and Braking: H-Bridge

In order for the drone to reverse directions, an H-Bridge circuit is typically required to reverse the polarity of the motors. Motor drivers typically already have this circuitry integrated and it is also generally recommended to simplify the wiring and software controls. The circuit diagram of an H-Bridge can be seen below in Figure 4.23.

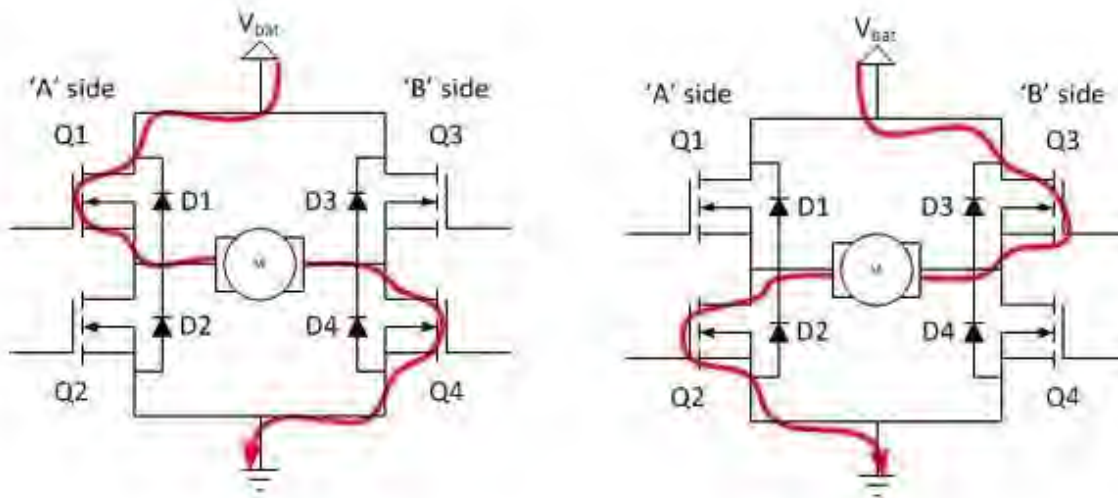


Figure 4.23: H-Bridge Circuit [55]

An H-Bridge consists of a minimum of four transistors, which are labelled as Q1, Q2, Q3 and Q4 in the figure above. These transistors are basically electrical switches that are used to control the flow of the current and allow the motor to reverse polarity, or in other words reverse the direction of rotation. As seen on the left diagram in Figure 4.23, the current can be controlled by opening transistor Q2 and Q3 and closing Q1 and Q4, or vice-versa. These configurations may already be pre-programmed and set in a motor driver by actuating only one switch, which would simplify the entire process by not having to independently control each transistor.

4.3. Stress Analysis

Due to time constraints, only a simple stress analysis was performed on the on the hybrid drone design to emulate normal flying conditions. The results from the stress analysis can be seen below in Figure 4.24..

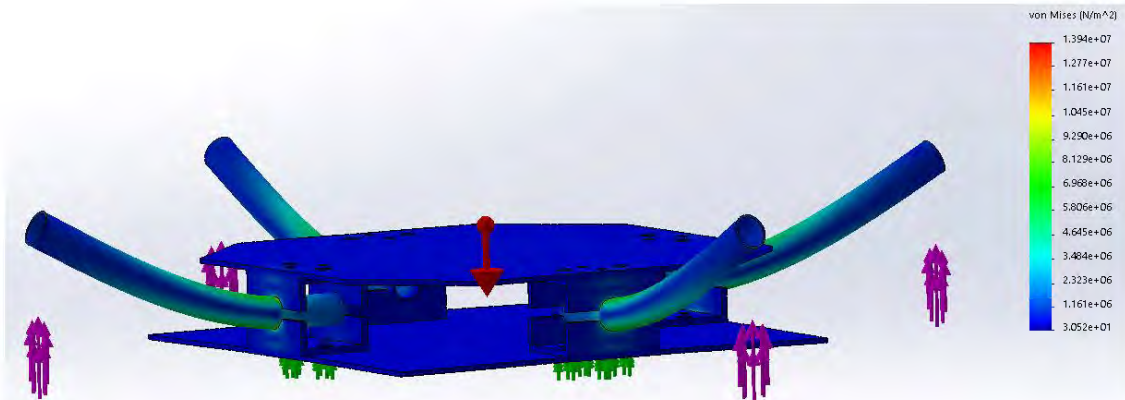


Figure 4.24. SolidWorks Stress Analysis Results

According to the SolidWorks Stress Analysis, the maximum von Mises stress would be on the carbon fibre tubes. The exact location can be seen below in Figure 4.25.. The value of the stress was only 13.94 MPa, much less than the tensile strength of carbon fibre (600 MPa) [56]. Thus, the design was considered to be safe under normal flying conditions.

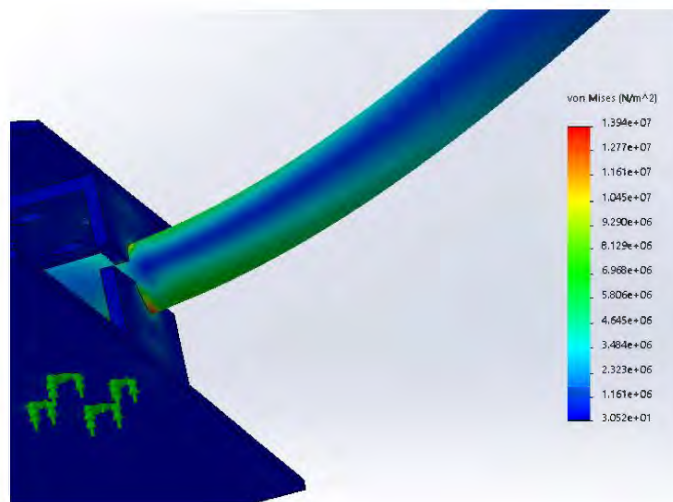


Figure 4.25. Highest Stress Location for Drone Design

5. Prototyping and Testing

After selecting the ideal concept for the hybrid drone project and theoretical research was completed, prototyping and testing began. In the following sections, the manufacturing and assembly process, along with the electrical wiring and programming processes are outlined. Finally, the testing process for this project is outlined.

As mentioned previously, this project was divided into two parts after the concept was selected. The first phase included the development of the drone's flying phase, and the second phase included the development of the drone's driving phase.

The fabrication drawings for all the hybrid drone's components can be seen in □.

5.1. Phase 1 Manufacturing

In the following section, the methods used to manufacture the components in the first phase of the project are outlined. An image of the final SolidWorks model for the project can be seen in Chapter 6.1 Final Concept and Results. An exploded, labelled view of the SolidWorks model can be seen in Chapter 5.3 Drone Assembly.

5.1.1. Top and Bottom Plates

As the drone required lightweight materials to be used, it was decided that the body should be composed of a composite material. This ensured that the drone would be lightweight as well as strong.

Through research, it was determined that a sandwich composite material should be used (personal communications, G. King, January 8th, 2019). The composite would be composed of a balsa wood core with carbon fibre and Kevlar facesheets. The carbon fibre and Kevlar would be bonded to the core with epoxy.

The following steps were taken to manufacture the sandwich composite. It is important to note that there are no images of the Kevlar in these steps as these images were taken during the fabrication of an initial version of the top and bottom plates. Later one of the carbon fibre facesheets were replaced by Kevlar (for aesthetic reasons).

1. Two sheet of a smooth plastic material were cleaned with wax to remove any contaminants.



Figure 5.1. Smooth Plastic Sheet

- Squares of carbon fibre and Kevlar were cut from their storage rolls.



Figure 5.2. Carbon Fibre Squares

- Squares of the balsa wood were cut from a larger storage piece.



Figure 5.3. Balsa Wood Stock

4. The epoxy matrix material was mixed in a container.



Figure 5.4. Mixing Epoxy Resin

5. The carbon fibre was placed onto the smooth plastic sheet and epoxy was added to it.

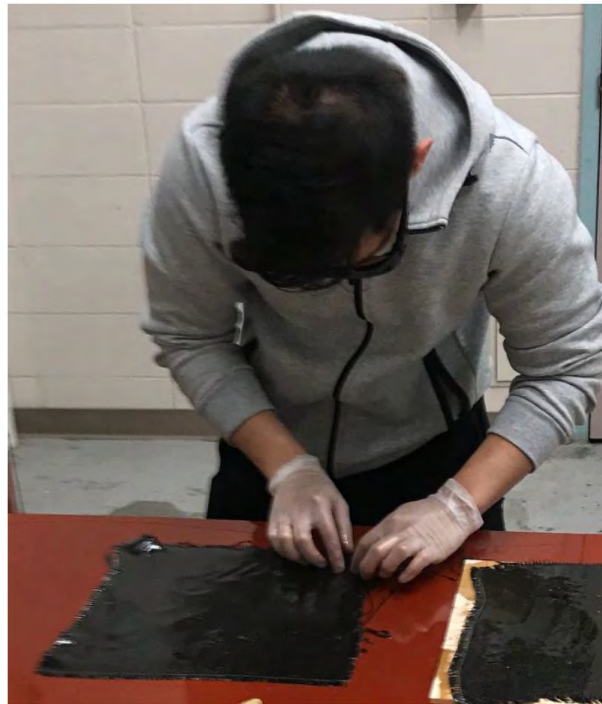


Figure 5.5. Adding Epoxy Resin to Carbon Fibre Sheet

6. The balsa wood was placed on top of the carbon fibre sheet and a layer of Kevlar and epoxy was added. In this image, there is another layer of carbon fibre instead of Kevlar.

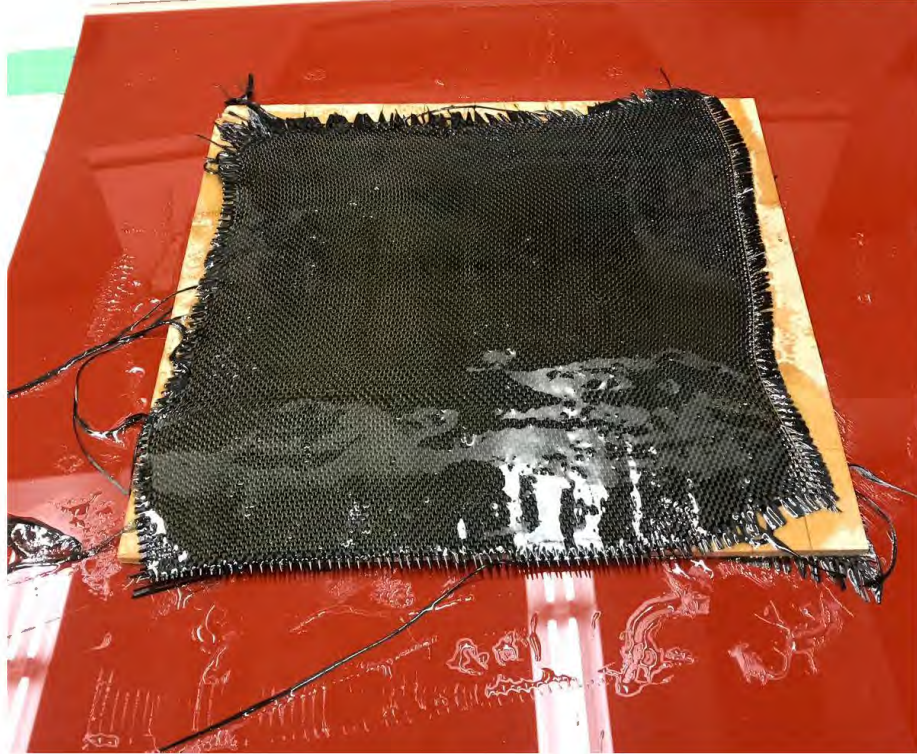


Figure 5.6. Sandwich Composite before the Epoxy Set

7. There was another plastic sheet and weights placed on top of the composite material allowing the epoxy to set properly.

After the sandwich material was finished setting overnight, the part was cut to size (9"x9") with a bandsaw. Then the corners were also cut to remove excess material (as per the fabrication drawings in □).

An image of the sandwich material can be seen below in Figure 5.7.. The holes were added to the part using a drill press.



Figure 5.7. Sandwich Composite during the Drilling Process

During any material removal processes where the carbon fibre or Kevlar was involved, extra safety equipment was used to avoid inhaling any fibres.

5.1.2. Carbon Fibre Tubes

To continue ensuring that the hybrid drone was composed of the lightest materials possible, it was determined that carbon fibre tubes should be used to connect the propeller motors to the body of the drone.

The following steps were taken to manufacture the carbon fibre tubes. A vacuum was used to ensure that no fibres were inhaled during this process.

1. The tubes were cut to the correct sizes from the stock material using a bandsaw.



Figure 5.8. Cutting of the Carbon Fibre Tubes

2. A milling machine was calibrated with an edgefinder to ensure good accuracy.



Figure 5.9. Milling Machine with Edgefinder

3. The holes were added to the carbon fibre tubes.



Figure 5.10. Adding Holes to Carbon Fibre Tubes

4. The excess fibres were removed from the holes and ends of the carbon fibre tubes.



Figure 5.11. Deburring the Carbon Fibre Tubes

An image of a finished tube can be seen below in Figure 5.12..



Figure 5.12. Completed Carbon Fibre Tube

5.1.3. Expansion Clamps

The plastic expansion clamps were used to connect the propeller motor mount to the carbon fibre tubes. They only required the addition of a hole that would be used to line up with the holes in the carbon fibre tubes. This was done using the drill press.

5.1.4. Propeller Motor Mounts

The propeller motor mounts were made with thin aluminum sheet metal. Aluminum was used because it is lighter than steel.

The following steps were taken to fabricate the part.

1. The parts' feature locations were added to the sheet metal.

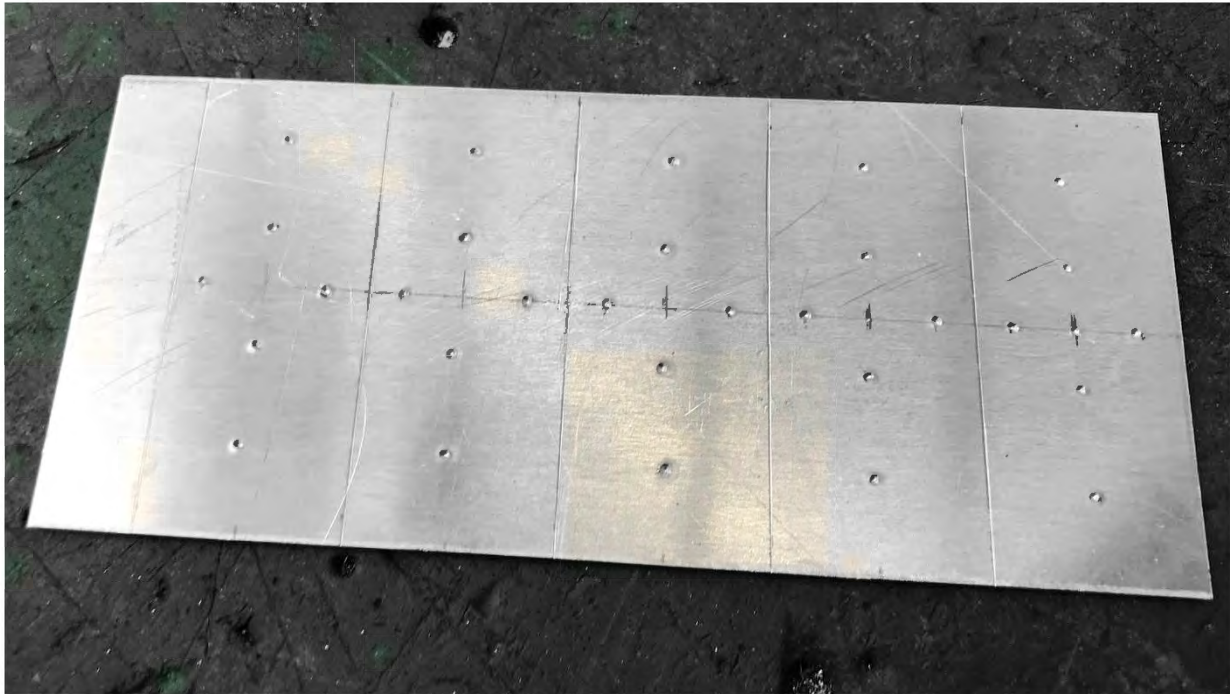


Figure 5.13. Scribed Sheet Metal for Propeller Motor Mounts

2. The holes were added to the part using a punch.



Figure 5.14. Punching Holes into the Propeller Motor Mount Parts

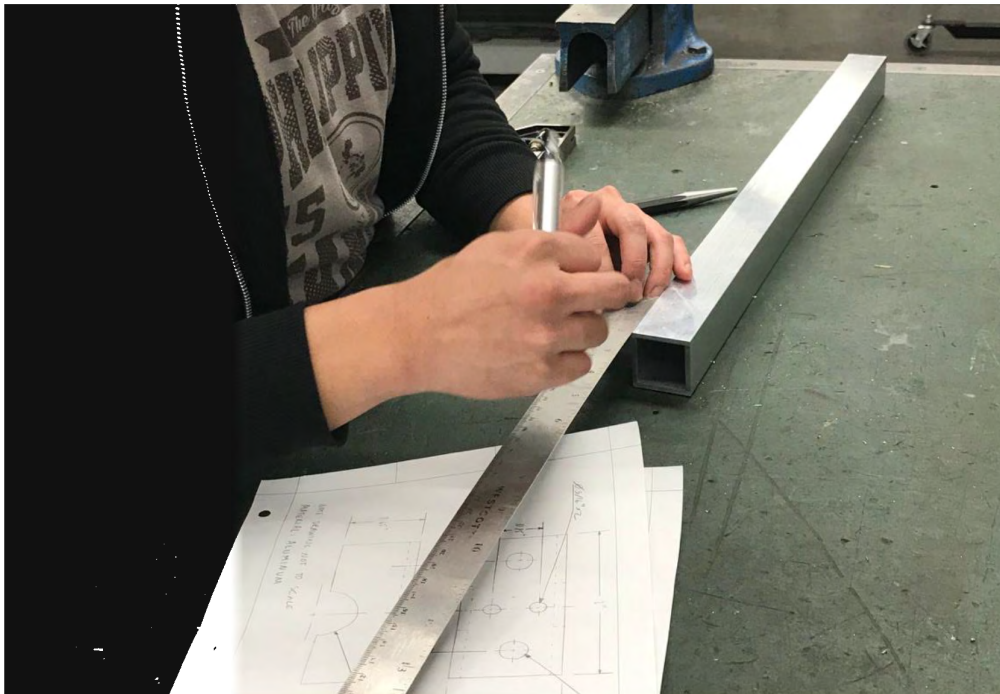
3. The individual pieces were separated using a sheet metal brake.
4. The sharp corners were removed from the parts using a sheet metal brake.

5.1.5. Tube Clamps

These parts were used to clamp the carbon fibre tubes so that they would connect to the body of the drone. They were manufactured from aluminum square tubing to ensure that they were strong and lightweight.

The following steps were taken to fabricate these parts.

1. The parts' features were located onto the square tubing.



2. A milling machine was calibrated with an edgefinder to ensure good accuracy (see Figure 5.9. for reference).

3. The holes were added to the square tubing using the milling machine.

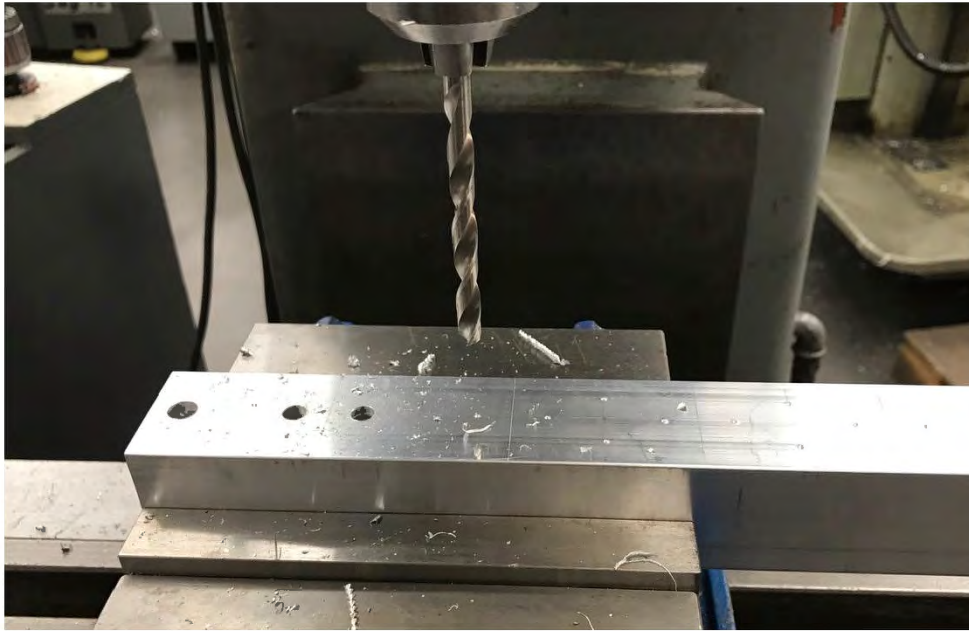


Figure 5.15. Adding Holes to the Square Tubing with the Milling Machine

4. The parts were cut from the square tubing using a bandsaw.
5. A small amount of material was removed from the parts with the milling machine. This was done to allow for enough space to clamp the tubes.



Figure 5.16. Removing Material from the Tube Clamps

An image of the tube clamps can be seen below in Figure 5.17.. The numbering was added to these parts to ensure proper alignment and the burs were removed from the parts before they were assembled.



Figure 5.17. Finished Tube Clamps

5.2. Phase 2 Manufacturing

This section involves less components because the first phase of the project included the body of the drone. The second phase only involved adding four wheels to the body of the drone.

5.2.1. Rear Motor Mounts

The rear motor mounts were made from an aluminum angle. The aluminum was chosen due to its light weight and strength. These parts were used to mount the motors used to power the drone's wheels.

The following are the steps used to fabricate the rear motor mounts.

1. The parts' feature locations were added to the stock piece of angle.
2. The parts were cut from the stock piece using a bandsaw.
3. The holes in the parts were added using a drill press.
4. Excess material from the parts were removed using a sanding machine.



Figure 5.18. Removing Excess Material Using a Sanding Machine

5.3. Drone Assembly

In this section, the assembly process for the hybrid drone is briefly outlined. A detailed view of the drone can be seen in Chapter 6.1 Final Concept and Results.

Below, in Figure 5.19. is an exploded view of the drone can be seen along with the labels for all the parts. The drawing of this image can be seen in []. There are no fasteners included in this image or drawing.

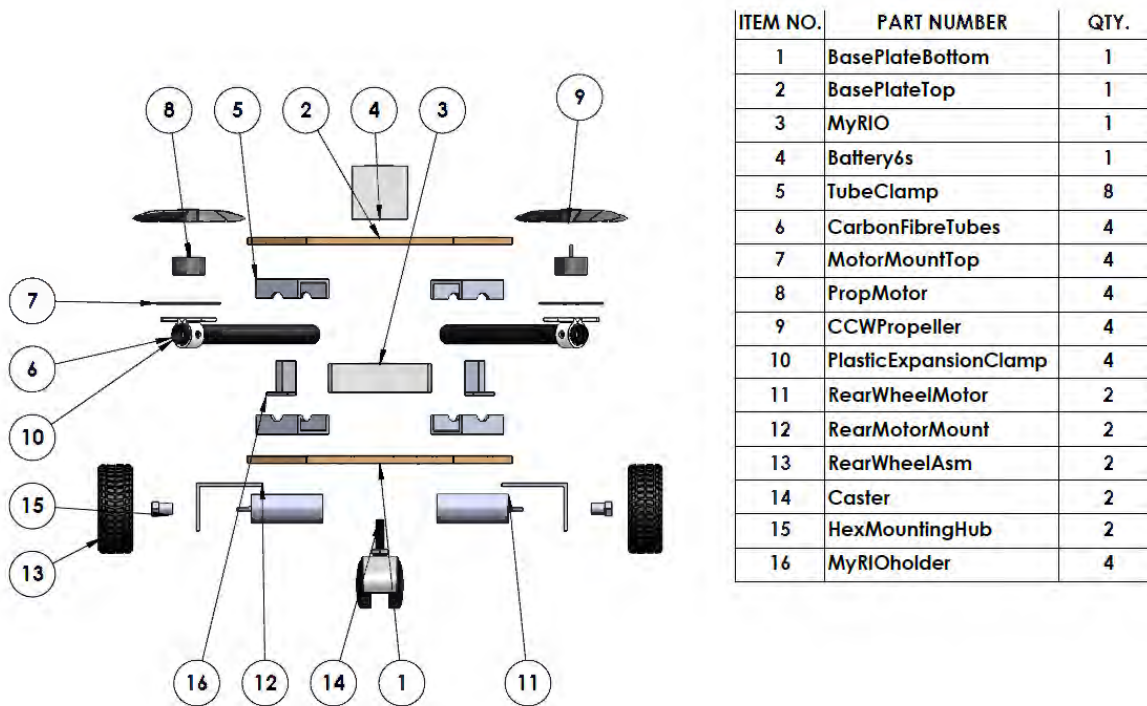


Figure 5.19. Exploded View of the Final Drone SolidWorks Model

A brief overview of the steps in the drone assembly process can be seen on the next page.

1. Fasten the rear wheel motor mounts to the bottom plate with two bolts, nyloc nut and washers each.
2. Attach the rear wheel motors to the rear motor mounts with two screws per motor.
3. Connect the hex mounting hub to the stepped shaft of the rear wheel motor with a set screw.
4. Connect the hex mounting hub to the rear wheels using a screw.
5. Place two washers into each of the caster wheel bolts to ensure alignment with the rear wheels.
6. Fasten the caster wheels to the bottom plate with a nut.
7. Feed the wires from the rear wheel motors through the slots on one side of the bottom plate.
8. Place the myRIO microcontroller into the myRIO holders and attach them to the base plate with two screws, nyloc nuts and washers each.
9. Wire the myRIO microcontroller.
10. Add the bottom half of the tube clamp assembly to the top of the bottom plate with two nylon bolts and washers each.
11. Place the propeller motors onto the propeller motor mounts using four screws and washer each.
12. Add the propeller motor mount to the expansion clamp with two nyloc nuts, bolts and four washers each. The washers are used for alignment.
13. Fasten the expansion clamps to a set of holes on the carbon fibre tubes with one nylon nut and bolt each.
14. Place the carbon fibre tubes into the bottom tube clamps.
15. Place the top tube clamps onto the long bolts used to locate the bottom tube clamps.
16. Place the top plate onto the long bolts used to locate the tube clamp assembly.
17. Add a nylon washer and nut to protruding long bolts to clamp the assembly together.
18. Add the propellers to the propeller motors with a nyloc nut and Loctite for safety.
19. Secure the 6S LiPo battery onto the top plate with Velcro.
20. Finish any last wiring required.

The next section presents the drone's wiring diagram.

5.4. Phase 1 Electrical Wiring

In this section, the hardware and the wiring diagram of the flying mode of the drone are included. The electrical components used included the following.

- Controller: NI myRIO (accelerometer imbedded)
- Battery: HRB 6S 5000mAh 22.2v 50C-100C RC Lipo Battery with XT90 Connector
- Electronic speed controller – Hobbywing XRotor G2 45A 4-in-1 ESC – BLHeli_32
- Brushless DC Motors: EMAX RSII Race Spec 2306 –1900kv Motors
- Gyroscope: NI myRIO Mechatronics Kit gyroscope (L3G4200D 3-Axis Gyroscope)

The way in which these components were connected are shown in the wiring diagram below in Figure 5.20.

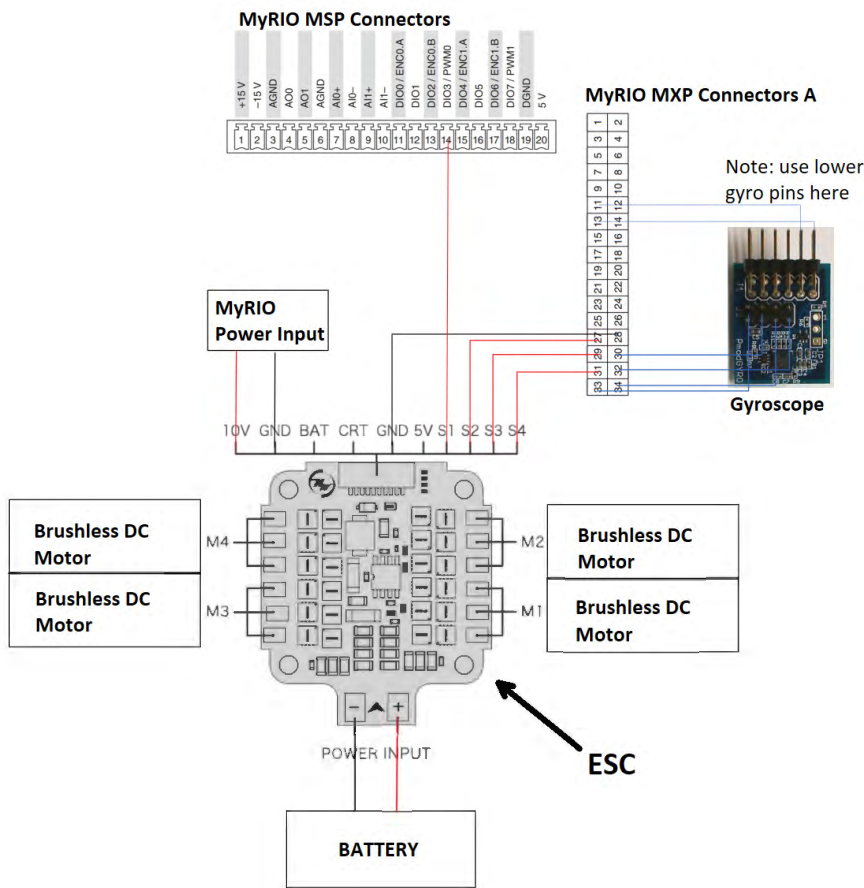


Figure 5.20: Drone Hardware Wiring Diagram

The ESC was directly powered by the battery, which in turn powers the four BLDC motors. Through the 10 V output from the ESC, the myRIO was powered and communicated with the ESC and gyroscope through PWM and I²C protocol. Details regarding the MXP Connectors are displayed in Figure 5.21.

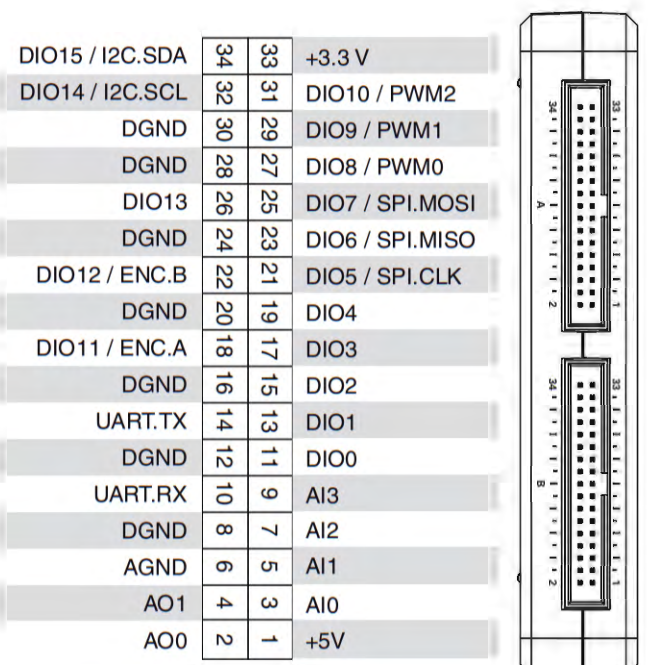


Figure 5.21: MyRIO MXP Connector Details

5.5. Phase 2 Electrical Wiring

The electrical components used in driving mode of the project include the following components.

- Controller: NI myRIO
- Battery: HRB 6S 5000mAh 22.2v 50C-100C RC Lipo Battery with XT90 Connector
- Step-Down Voltage Regulator: DROK DC-DC Buck Boost Converter (Input: 5-32V, Output: 1-30V, 10A)
- Motor Driver: Sabertooth Dual 25a 6v-24v Regenerative Motor Driver
- Brushed DC Motor: Polulu 20.4:1 Metal Gearmotor 25Dx50L mm HP 12V with 48 CPR Encoder

How these components were connected are shown in the wiring diagram below in Figure 5.22, which also includes the details of the MSP Connectors.

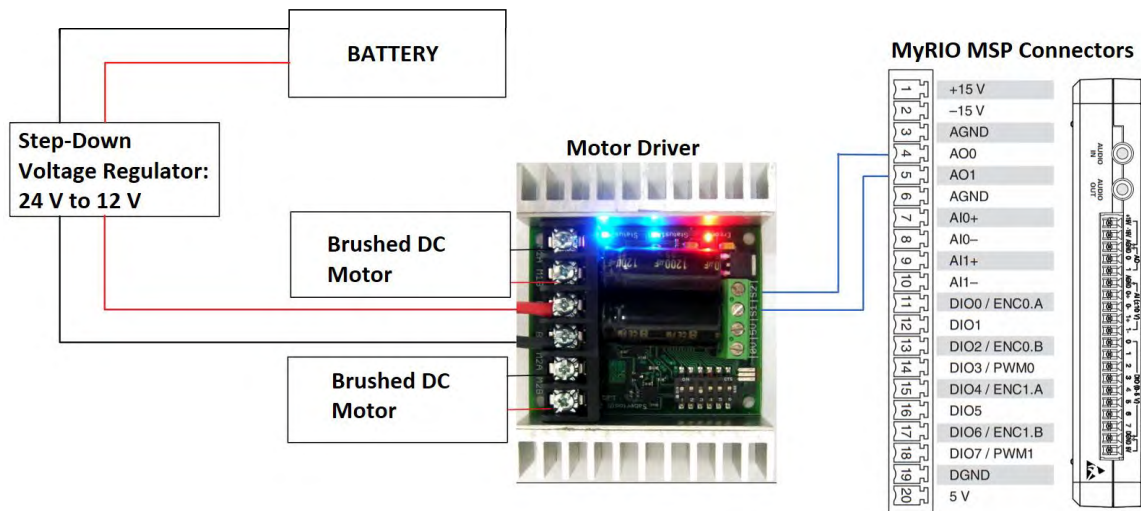


Figure 5.22: Drive Hardware Wiring Diagram

5.6. Phase 1 Programming

The programming for the hybrid drone was done using LabVIEW, which was the main software compatible with the myRIO microcontroller. It is unique as it utilizes block-based coding rather than text-based. Programming in LabVIEW involves a front panel and a virtual instrument (VI). The front panel is the user interface which allows the user to manipulate values and control the program as desired. On the other hand, the VI is where the main code resides and connects the block coding through wirings. SubVIs may also be implemented and are analogous to functions in text-based coding. They are essentially multiple blocks compressed in a single function block that serves a specific purpose. In the following subsections, the front panel and virtual instruments are shown and explained in detail regarding their function and purpose in controlling the hybrid drone.

5.6.1. LabVIEW Front Panel

The main drone controls are shown below in Figure 5.23. In this part of the front panel, the throttle is adjustable by increasing the duty cycle via the horizontal bar. Bar and numeric indicators are set to allow the user to keep track of each motor's PWM input. Controls for the pitch, roll and yaw are also included to allow the drone to maneuver. Lastly, a stop button is set to halt the program in case of emergencies.

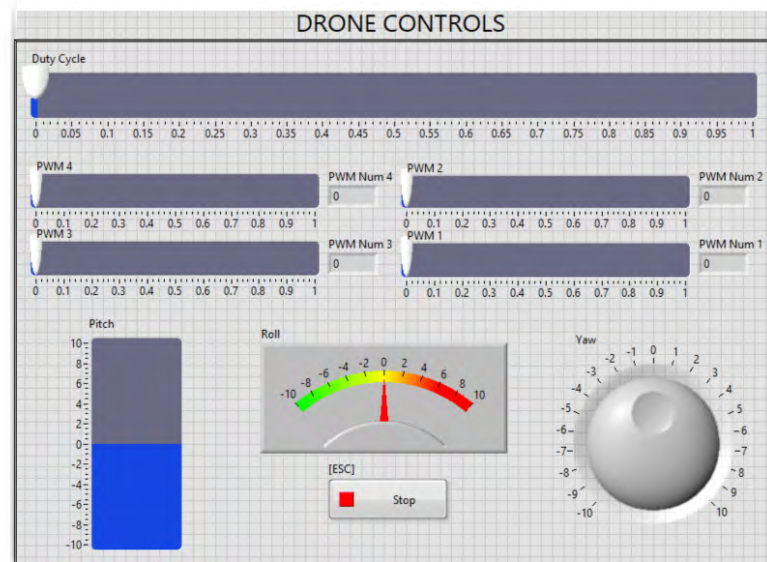


Figure 5.23: Drone Controls Front Panel

High level data about the drone is displayed in the part of the front panel shown below in Figure 5.24. To ensure the drone is flying accordingly, some graphs were included to display the feedback signal from the PID. This would be helpful as these graphs could show how the signal changes over time and would be the first graphs to investigate when troubleshooting.

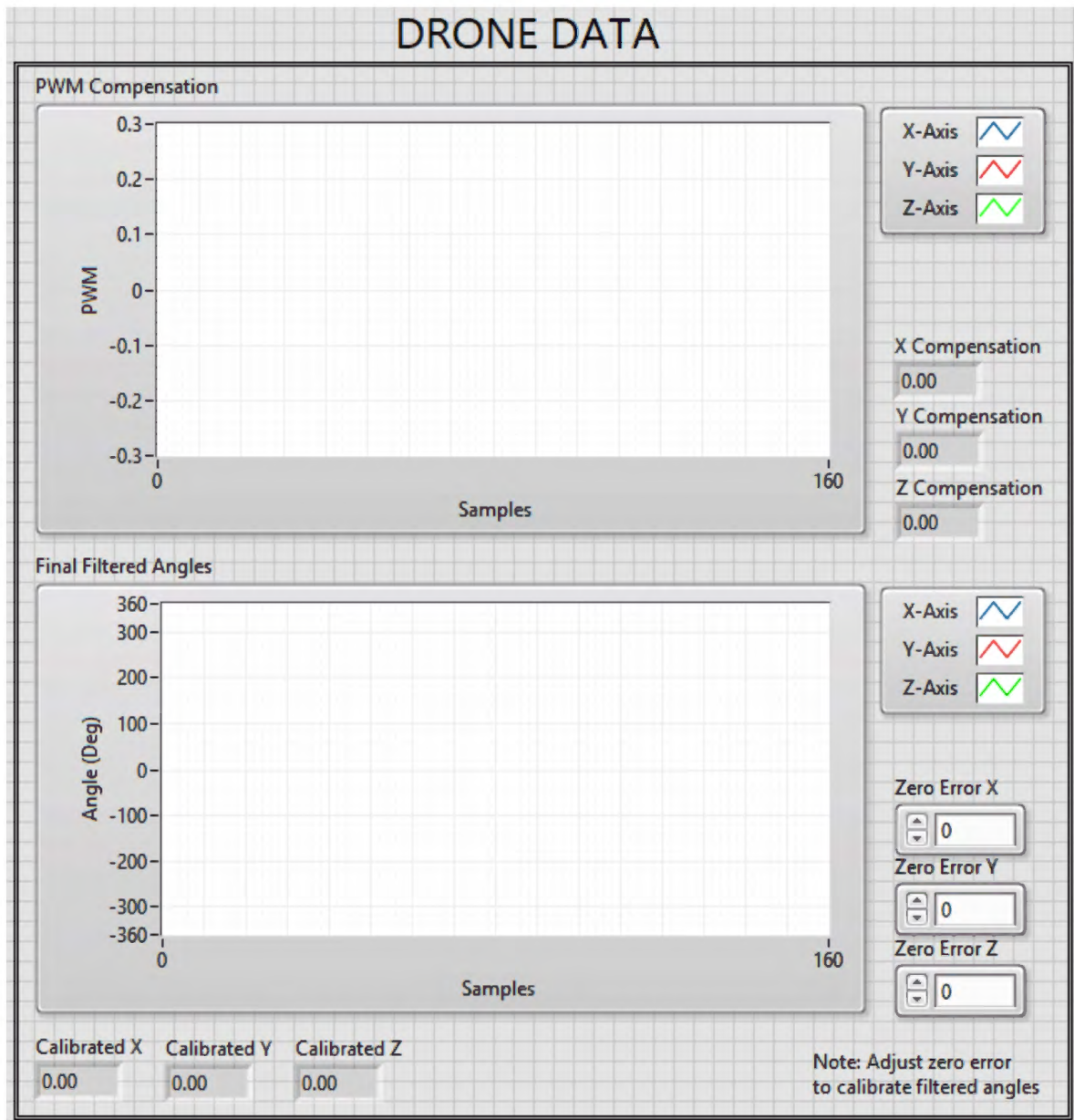


Figure 5.24: Drone Graphical Data Front Panel

The PID controls are shown below in Figure 5.25 and required three terms as previously mentioned in section 4.1.4.4 PID Controls and its Role: proportional, integral and derivative term. A PID control about each axis was required to fully stabilize the drone. These parameters were set to be adjustable in order to find the optimal value of each term.

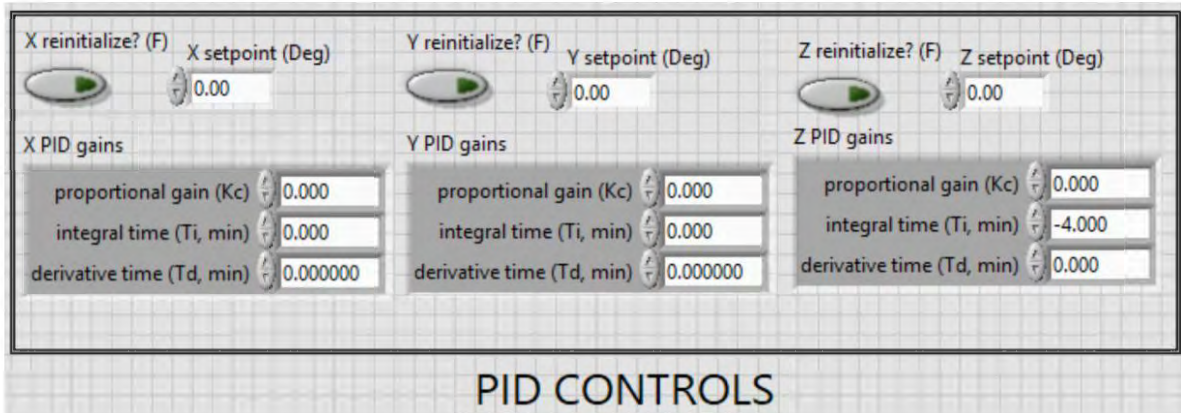


Figure 5.25: PID Controls Front Panel

The section of filter controls in the front panel is shown below in Figure 5.26. Three buttons are included which engages the filter, filter parameters and averaging. The filter parameters include the low cut-off frequency, sampling rate, filter order and number of points to average over and are adjustable to allow the user to find the optimal value when testing.

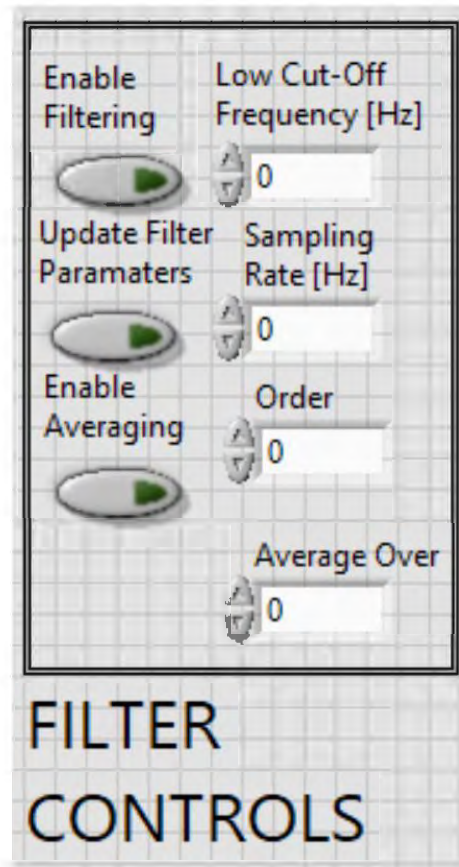


Figure 5.26: Filter Controls Front Panel

In addition to the graphical data from Figure 5.24, more graphs were provided in the front panel to display the raw data of the gyroscope and accelerometer, the converted data of the accelerometer from g-force to degrees and the unfiltered angles of the drone about each axis as seen below in Figure 5.27. This offers the user more information regarding the inner workings of the system when troubleshooting.

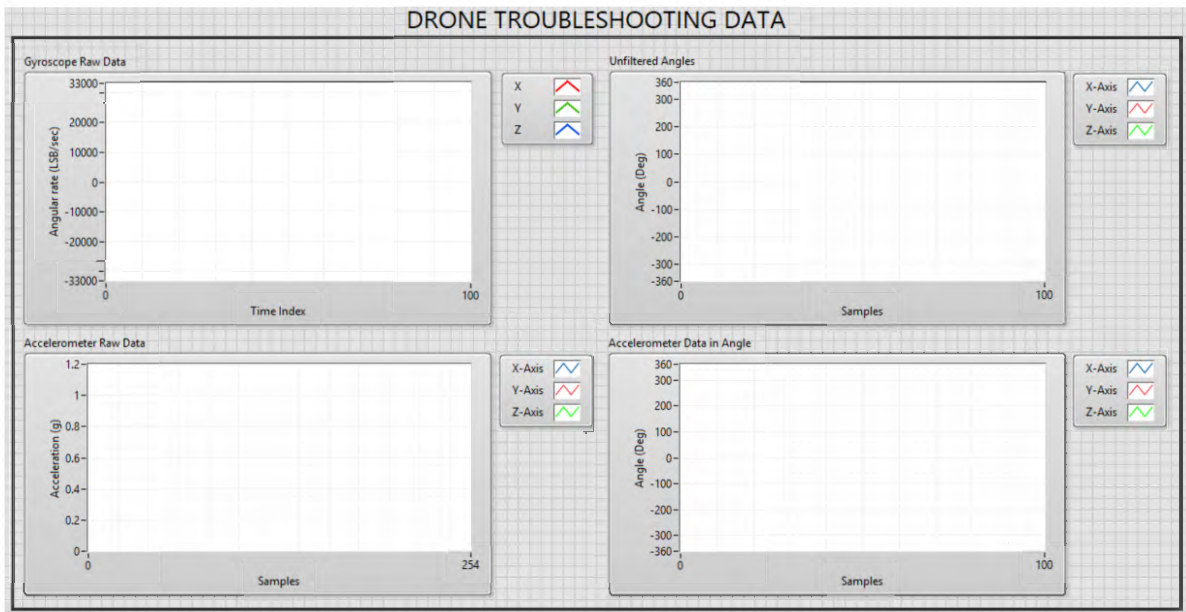


Figure 5.27: Drone Troubleshooting Graphical Data Front Panel

5.6.2. LabVIEW VI

The code created to control the flying mode of the drone utilized data gathered by the accelerometer and gyroscope. A complementary filter was implemented to combine the data in order to get a more accurate and precise measurement of the drone's angular position. The data was then averaged and filtered using a low pass filter to produce a smoother signal and remove externals and internal noise from the environment and electronic system. Through PID controls, a feedback loop was created to stabilize the drone mid-flight, to a desired setpoint. The generated signal from the PID was then used to adjust the PWM input to the drone motors, which regulated the thrust force and angular momentum of each motor. This allowed the drone to hover, roll, pitch or yaw by changing the desired setpoint. Details of the code are further explained in the following sections.

5.6.2.1 Accelerometer Code

The first step in implementing the controls was gathering the data from the accelerometer and gyroscope. The accelerometer used for this project was the FPGA myRIO onboard accelerometer and deals with three of the six degrees of freedom the drone would have during flight: the linear motion about the x, y and z axes. The program used to extract data is based on the default VI that appears when a new VI from a project file. It utilizes the accelerometer function block, as seen below in Figure 5.28, to input linear acceleration about each axis, which have a pre-programmed direction on the myRIO microcontroller.

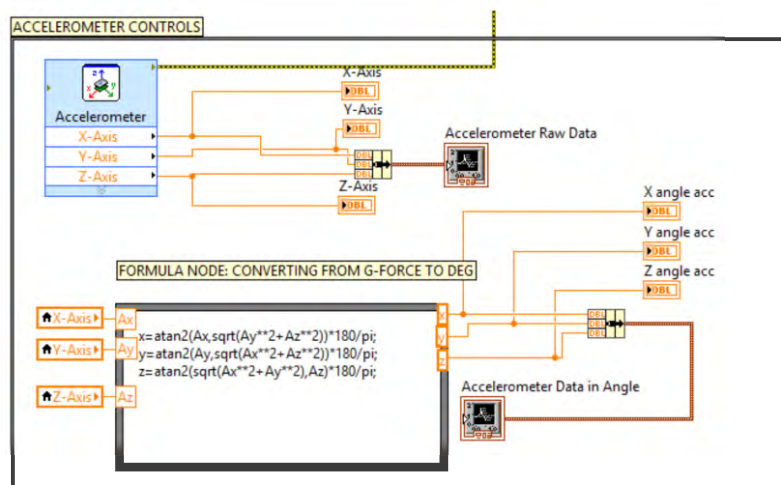


Figure 5.28: FPGA MyRIO Onboard Accelerometer VI

This extracted data, however, was in the units of g-force. The g-force unit in all three direction was converted to degrees by using trigonometry [57]. Equations 5.1, 5.2 and 5.3 were used to obtain the degree of tilt from the x-axis, θ , y-axis, ψ , and z-axis, ϕ , from the accelerations about the x-axis, A_x , y-axis, A_y , and z-axis, A_z . These angles respectively correspond to the variables “x,” “y” and “z” in the formula node (in Figure 5.28), which were also converted from radians to degrees.

$$\theta = \tan^{-1} \left(\frac{A_x}{\sqrt{A_y^2 + A_z^2}} \right) \quad \text{Equation 5.1}$$

$$\psi = \tan^{-1} \left(\frac{A_y}{\sqrt{A_x^2 + A_z^2}} \right) \quad \text{Equation 5.2}$$

$$\phi = \tan^{-1} \left(\frac{\sqrt{A_x^2 + A_y^2}}{A_z} \right) \quad \text{Equation 5.3}$$

5.6.2.2 Gyroscope Code

In addition to gathering data from the accelerometer, measurements from the gyroscope were also essential as they dealt with the last three of the six degrees of freedom: the rotational motion about the x, y and z axes. The gyroscope used was the L3G4200D three-axis gyroscope and communicated with the myRIO controller via I²C communication protocol. A program was developed using the example program for this gyroscope that came from the National Instrument (NI) myRIO mechatronic kit [58] as seen below in Figure 5.29.

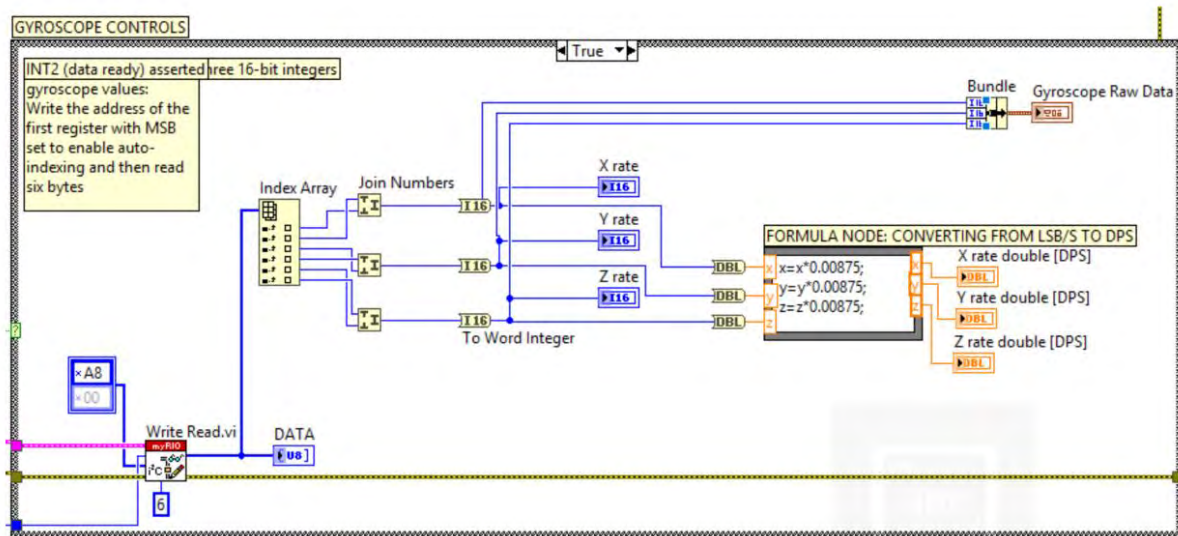


Figure 5.29: L3G4200D Three-Axis Gyroscope VI

The data extracted from the gyroscope was in the form of clustered bytes, which were indexed to separate each one and then joined together to form a word integer. The angular speed about each axes was then initially being measured in units of LSB per second and was converted to degrees per second by using the gyroscope sensitivity $8.75 \frac{mDPS}{digit}$ or $\frac{mDPS}{LSB}$ [59] as seen in the formula node in Figure 5.29. This data along with the one from the onboard accelerometer were then combined using a complementary filter to obtain a more stable and accurate data regarding the drone's roll, pitch and yaw angle.

5.6.2.3 Complementary Filter

The complementary filter served to remove the error that grows over time from the gyroscope and the high frequency noise from the accelerometer. This was done by summing a small percentage of the accelerometer data and a large percentage of the gyroscope data in order to combine the short-term benefits of the gyroscope and long-term benefits of the accelerometer. The gyroscope allowed the drone to detect short-term changes in the signal and maneuver when needed while the accelerometer ensured that the drone maintained stable in the long run, whether it was simply hovering or moving at a constant speed. All of this was done for each axis.

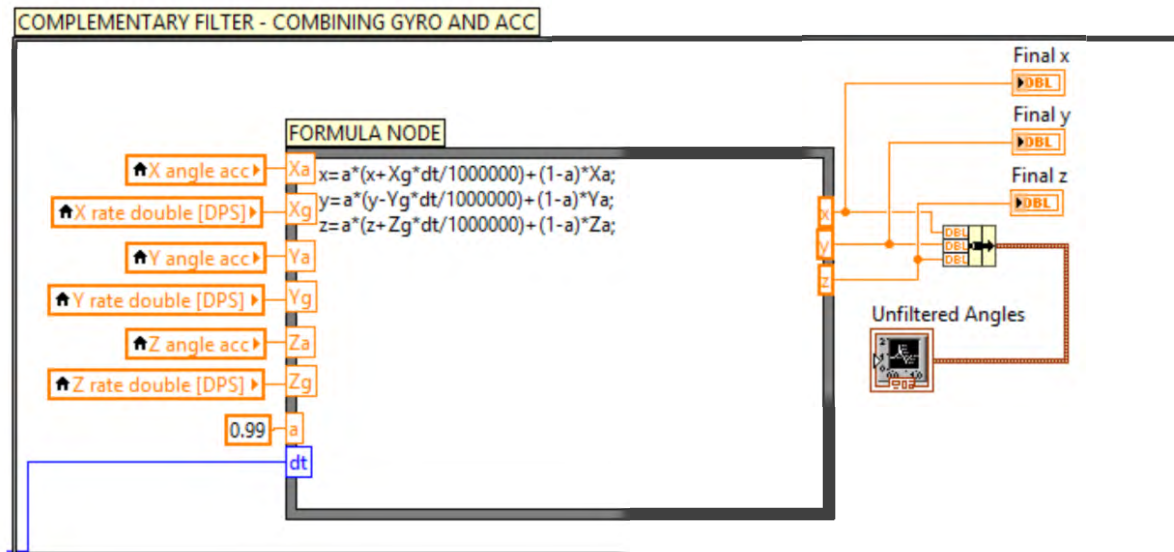


Figure 5.30: Complementary Filter VI

The equation used to implement the complementary filter is as follows, where a and $(1 - a)$ are the high and low pass constant [60].

$$angle_i = a(angle_{i-1} + angle_{Gyro} dt) + (1 - a)angle_{Acc} \quad \text{Equation 5.4}$$

For this project, 99 percent of the gyroscope data was used for the total angle while only 1 percent came from accelerometer as shown in the formula node above in Figure 5.30. The typical percentages were respectively 98 and 2 percent, but due to the large amount of noise from the accelerometer, these were changed accordingly. The total angle about each axis was then filtered and averaged to reduce any leftover errors even further and obtain a smoother response signal.

However, it was found that implementing the complementary filter on the z-axis was not useful. Its equation was included but the result was not used in the PID controls because its rotation about the z-axis (yaw angle) was not found to be the same as the degree of tilt about the z-axis, ϕ . For the accelerometer, gravity was used as a base reference to determine whether the drone was either rolling or pitching. As a result, yawing can only be detected by the gyroscope and not by the accelerometer since gravity only acts along the one axis. This also meant that while the zero error for the yawing could be calibrated in the beginning, it could never be completely removed because of the gyroscope's inherent ramping error.

5.6.2.4 Filtering and Averaging

Additional filtering and averaging are typically required to remove any unwanted disturbances and to further smoothen jagged signal after the complementary filter. The code for this step can be seen below in Figure 5.31 along with the details in Figure 5.32 and was based from a code found online aimed to filter accelerometer noise [61].

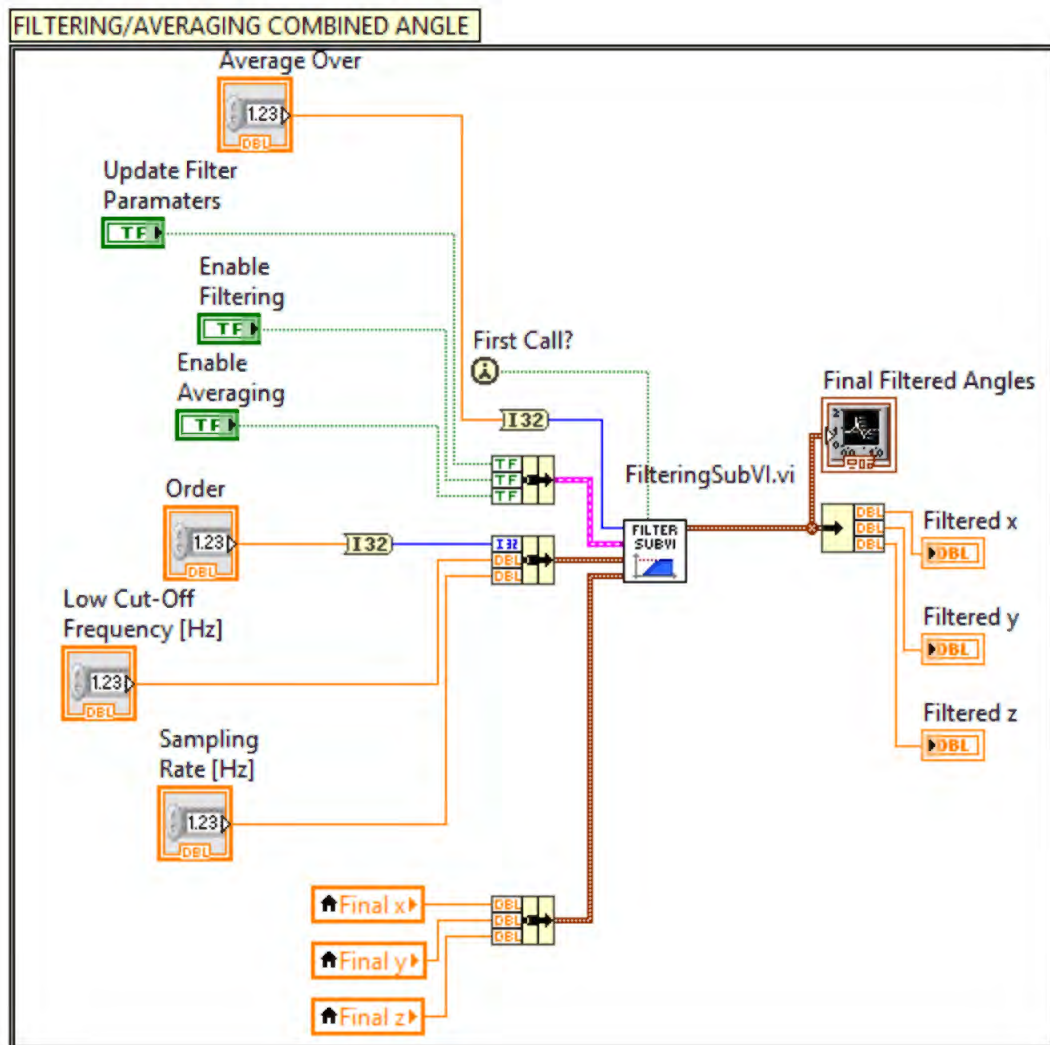


Figure 5.31: Filtering and Averaging VI

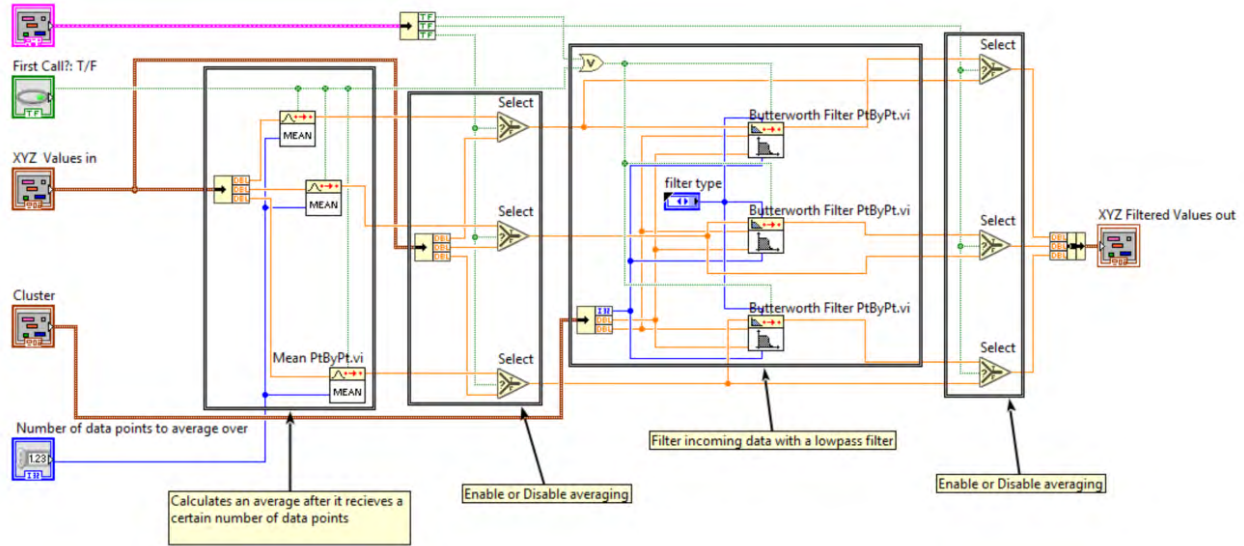


Figure 5.32: Filtering and Averaging SubVI

For this VI, the filter used was a low-pass Butterworth filter, which required three essential parameters that were needed to be set and determined by the user, including the filter low-cut off frequency, the sampling rate and the order of the filter. Additionally, the number of points to average over was another parameter that required user input. However, through experimentation, it was found that implementing the filter did not have much effect in filtering the noise from the signal. This was most likely because the vibrational noise from the motors were approximately the same or lower than the frequency signal from the accelerometer. The low cut-off frequency was also only found to be effective at a frequency near the sampling rate. As a result, implementing the filter seemed to remove both noise and the desired signal. However, averaging was found to be very useful in smoothening out the signal.

5.6.2.5 PID Controls

The PID controls introduced a feedback loop based on the data gathered from the accelerometer and gyroscope, which went through a complementary filter, low-pass filter and an average calculator, mentioned in the previous sections. This allowed the drone to maintain a specific position in the air by keeping the setpoint at zero degrees or changing it for the drone to roll, pitch or yaw as desired. The code for this part is shown below in Figure 5.33 and was created with the help of a quadcopter simulator code found online [62].

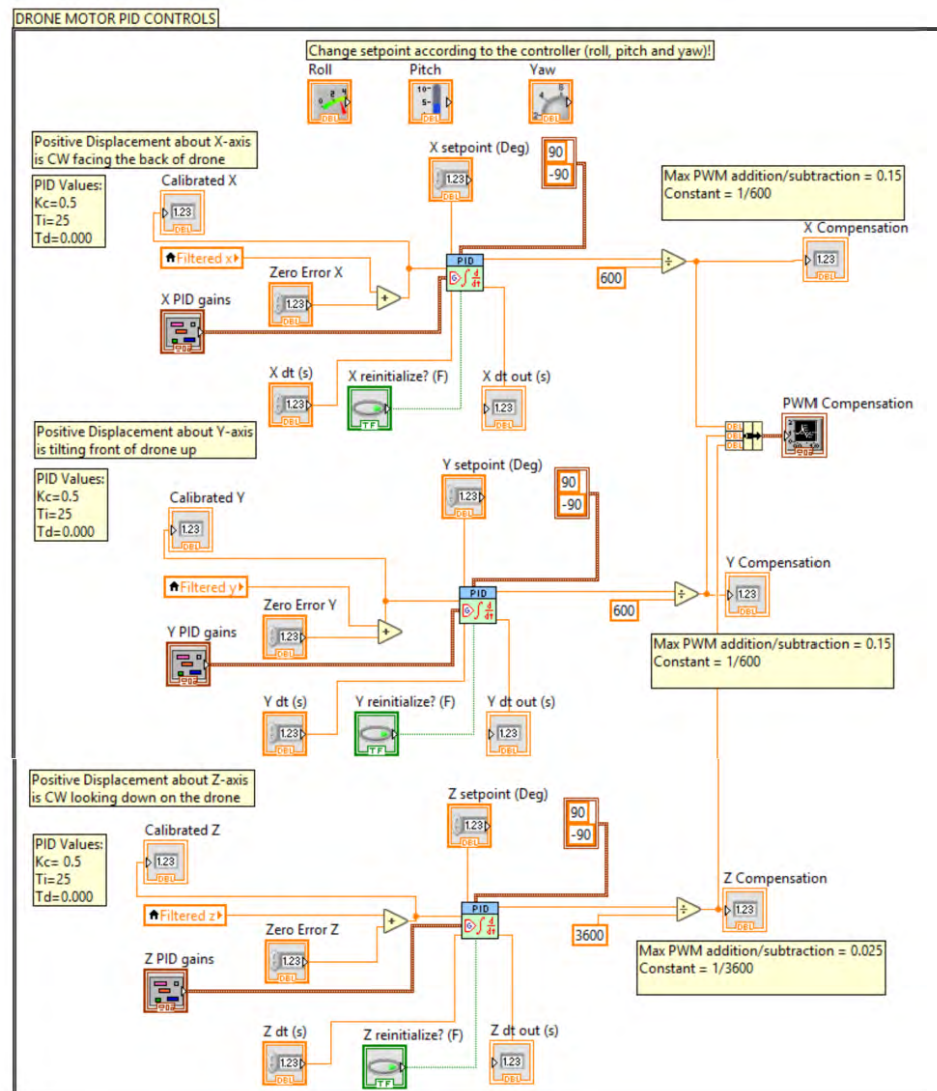


Figure 5.33: PID Controls VI

From the PID function block, limits on the output could be set, which was in terms of the rotation angle of the drone from a specified axis. The output was converted to a PWM value that was either added or subtracted from the motor control inputs to adjust the thrust force and rotational momentum produced by each propeller. Moreover, the PID terms, in this case K_p , T_i and T_d , could be numerically controlled to finely tune their values through experimentation in the testing phase of the project. Rolling, pitching and yawing would then also be possible by changing the setpoint about the x-axis, y-axis and z-axis.

5.6.2.6 PWM Motor Controls

As the flying mode of the drone used brushless DC motors, PWM was used to control their speeds. The location of the drone motors is shown below in Figure 5.34 to help explain how they would be affected when rolling, pitching and yawing.

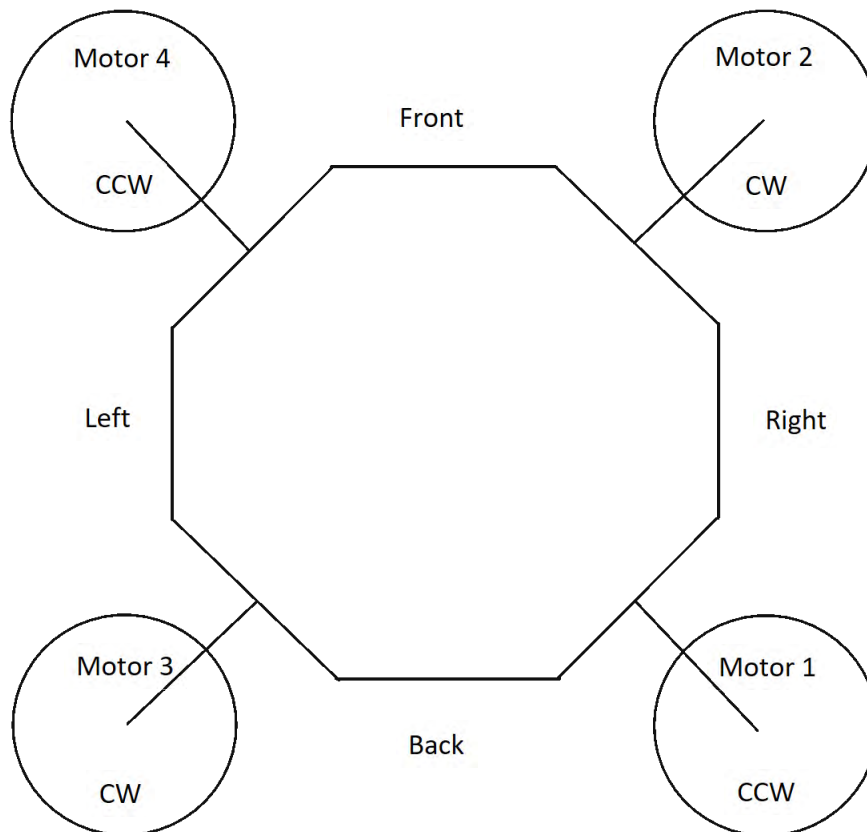


Figure 5.34: Drone Motor Configuration

When rolling, the motors on either the left or right side would need to be weaker than the other side for the drone to tilt and maneuver in that direction. This is similar for pitching, except the motors would be paired in terms of the front side and back side. Yawing would require slowing down the motors that are rotating in the direction the user wants the drone to rotate towards. In other words, to rotate to the left, the user would have to make motors 1 and 4 slower than motor 2 and 3. These concepts, which were also discussed in section 4.1.4.3 Drone Maneuvering: Roll, Pitch and Yaw, were then used to create the following code in Figure 5.35 to ensure the drone maintained the desired angle of tilt by adjusting the PWM input to each motor. Other inputs also include the zero error and frequency of the motors.

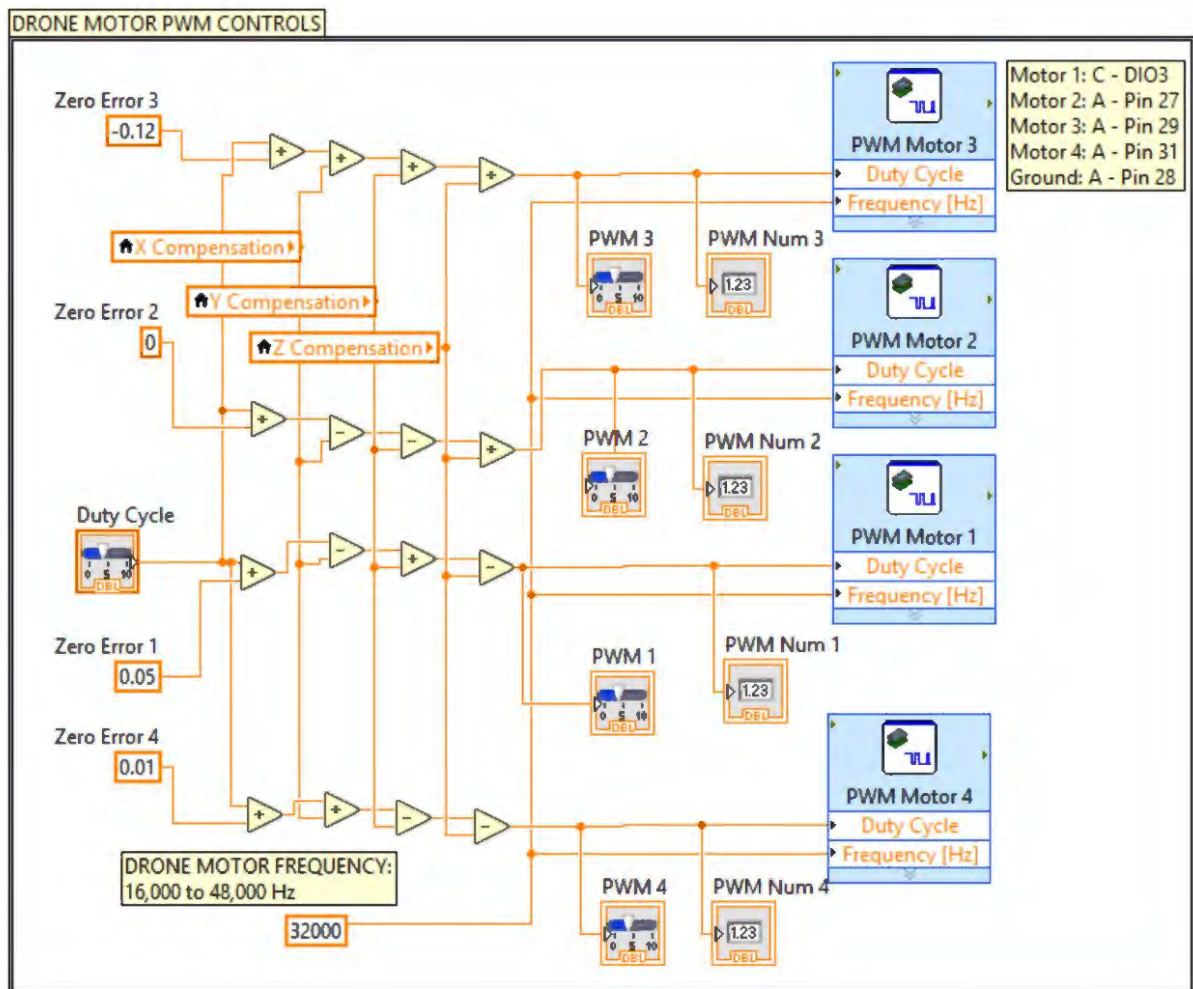


Figure 5.35: PWM Motor Controls VI

5.7. Phase 2 Programming

In addition to the flying controls implemented in Phase 1, drive controls were also applied in order for the hybrid drone to maneuver on the ground. Similarly, a user interface and code were created in the front panel and VI, which are explained in further detail in the following sections.

5.7.1. LabVIEW Front Panel

The drive controls for the hybrid drone is shown below in Figure 5.36, where the forward or backward driving and left or right turning speed are controllable via the vertical and horizontal bar control. The driving speed in each direction can also be calibrated via the zero error numeric controls in the bottom left of this panel.

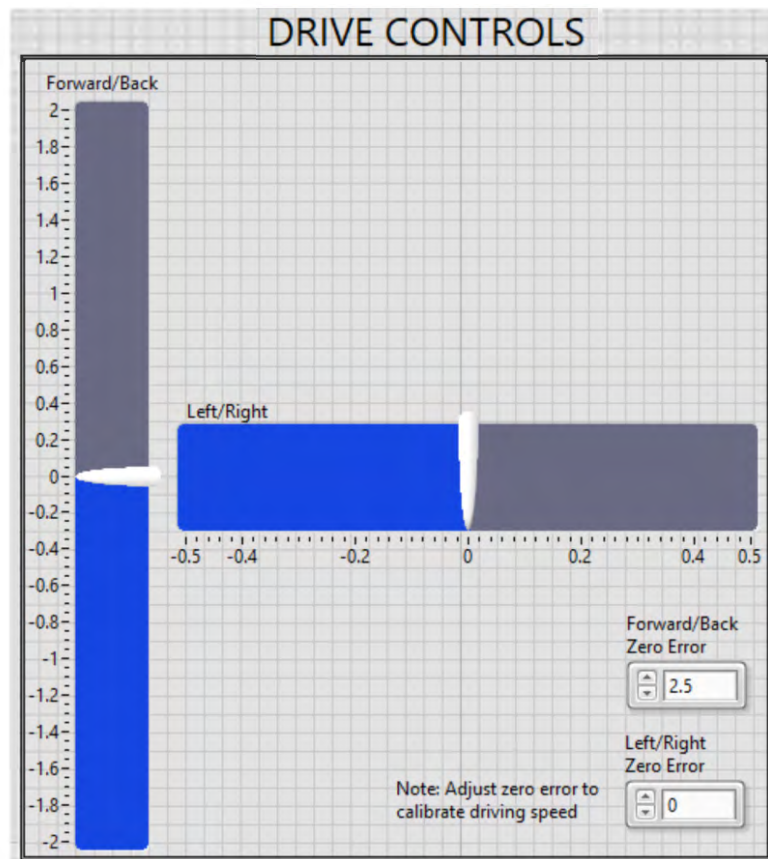


Figure 5.36: Drive Controls Front Panel

5.7.2. LabVIEW VI

In this section, the main code for the driving aspect of the project is illustrated and explained.

5.7.2.1 Drive Controls

The drive controls include for the drone utilized an analog input with a forward/back and left/right control as shown below in Figure 5.37.

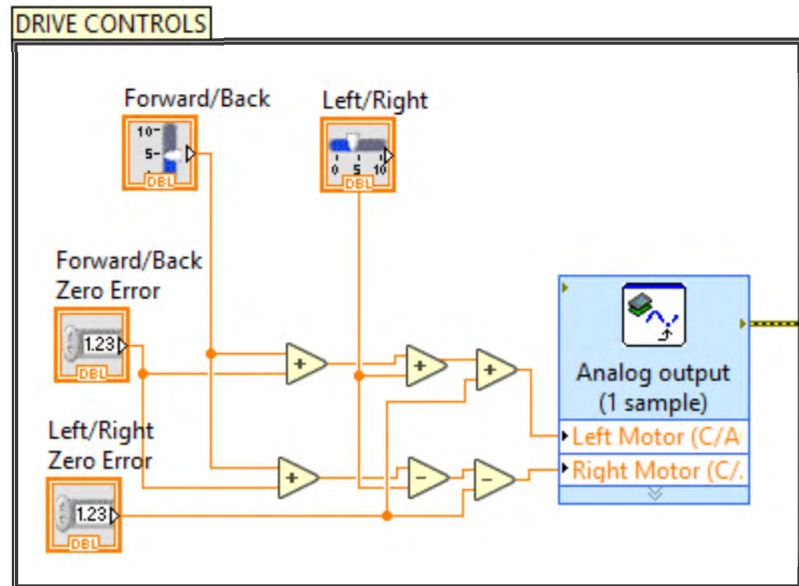


Figure 5.37: Drive Controls

The speed of the motor was implemented by adjusting the voltage input to the brushed DC motors. Moving forward or backward was associated with inputting a voltage greater or less than 2.5 V respectively. The drone was able to turn left, or right by applying a speed differential between the two motors. Turning to the right involved making the left motor spin faster than the right one.

5.8. Phase 1 Testing

The beginning of the testing for Phase 1 started with varying the speed of one brushless DC motor with its propeller. This ensured that they functioned properly. Afterwards, the gyroscope and accelerometer were individually tested. The responsiveness of the motor to these devices was then tested by creating a simple feedback loop once they were functioning properly and generating data.

The testing phase then continued by assembling the drone and testing all four motors and propellers at once. The first main goal was to get the drone to lift off the ground, which was expected to be at approximately 50 percent duty cycle. Once this was achieved, numerous tests were conducted in order to get the drone to fly off as evenly as possible. After each test, the motors were calibrated by fixing their zero errors in the LabVIEW code. This was followed by correcting the PID values, which aimed to stabilize the drone once it started flying. The tests focused on minimizing the rotational and linear speed when the drone started flying towards a certain direction as it simply hovered above the ground. Other variables that were also adjusted included ones from the complementary filter, low-pass filter and average calculator. Throughout these testing phases, personal protective equipment (PPE) were constantly worn due to the dangerous high speed required from the motor and propeller.

5.9. Phase 2 Testing

Testing of the drive mode controls were much simpler than for the drone controls as stability was less of an issue on the ground. One brushed DC motor with and without the wheel was initially test by itself. Once the subassembly was functioning properly, both motors and wheels were assembled onto the drone itself. Then, their forwards and backwards motions were tested as well as the drone's ability to turn left and right. The motors were also calibrated for their zero errors as they used an analog signal that required an input of 2.5 V to stop the motors from turning. Increasing the voltage above 2.5 V allows the motors to rotate one direction, which was reversed by decreasing it below 2.5 V.

6. Discussion of Results and Conclusion

In the following section, the final concept and results are described, including the manufacturing, electrical and programming challenges encountered throughout the prototyping and testing phases of the project. The future work also includes various refinements that could be implemented, such as improvements in weight reduction, aesthetics, software controls and electrical wiring.

6.1. Final Concept and Results

The final concept of the hybrid drone that was successfully prototyped consists four propellers and four wheels, where two of the wheels were the drive wheels and the other two were assembled for stability. An image of the final concept is shown below in Figure 6.1. The drone weighed approximately 2.5 kg. The final assembly fit within an envelope of 2 ft by 2 ft by 1 ft.



Figure 6.1: Final Hybrid Drone Concept

A front view of final concept SolidWorks model can be seen below. Followed by a side view and a top view in respectively. These images do not include fasteners.

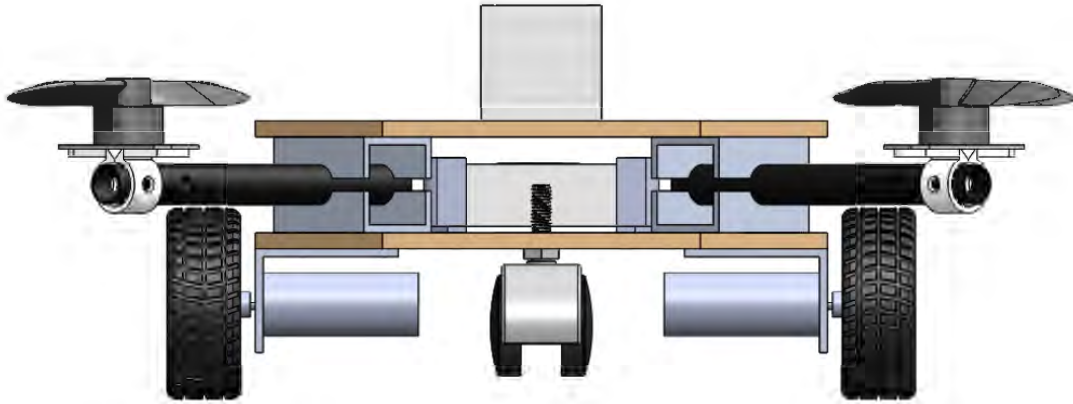


Figure 6.2. Front View of Final Drone SolidWorks Model

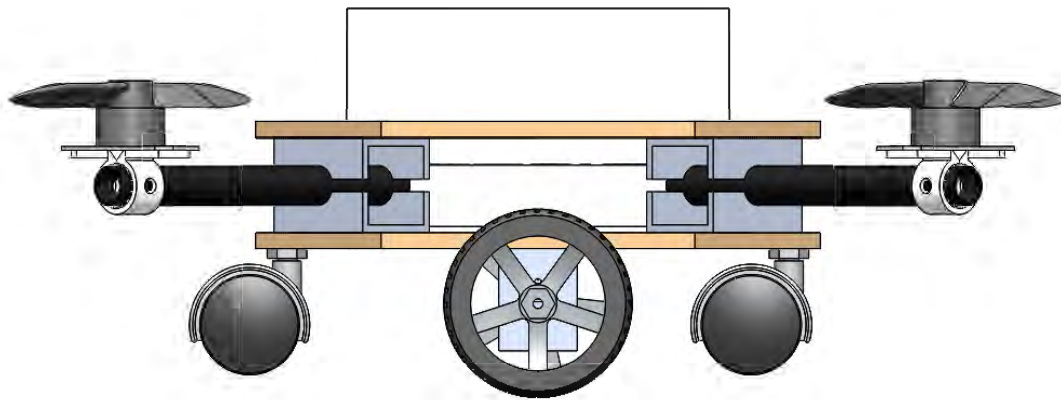


Figure 6.3. Side View of Final Drone SolidWorks Model

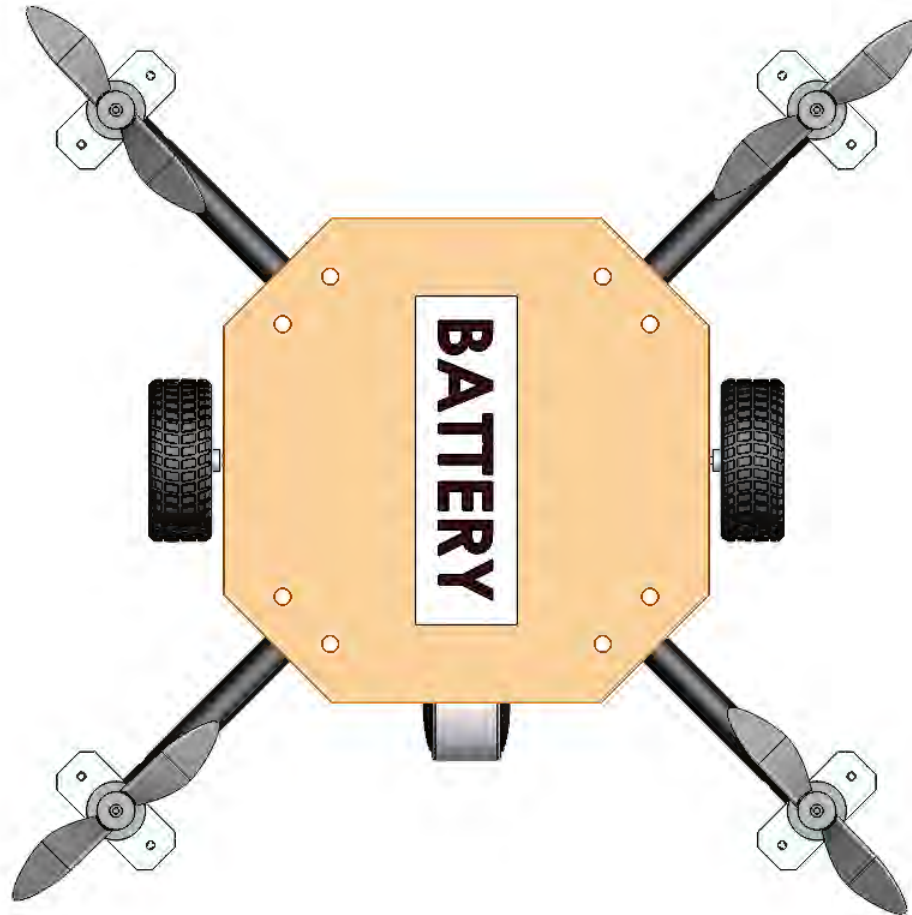


Figure 6.4. Top View of Final Drone SolidWorks Model

As the drone was not designed to perform any tricks or flips, the maximum rotation assumed for the drone was plus and minus 90 degrees about the x - and y -axis. This was linearly scaled for the drone to produce an increase or decrease in PWM input of up to 15 percent.

From the testing phase of the project, the PID controls were applied and fine-tuned to optimize the response signal. The optimal PID values, K_p , T_i and T_d were found to be approximately 0.5, 25 and 0. Implementing the derivative term was not found to be beneficial as it would simply amplify the noise in the system and produce worse results. Moreover, implementing the PID controls about the z -axis or yaw angle was not found to have much effects in simply trying to get the drone to hover. Especially, since the only feedback for this

direction came from the gyroscope and not the accelerometer, an error in the signal was unavoidable. Only the zero error could be removed in the beginning, but not the ramp error. Moreover, averaging up four samples was found to be the optimal value that provided a smoother and less noisy signal while maintaining a reasonable real-time response.

Unfortunately, despite finding the optimal values, the drone was still found to have difficulty in hovering on the spot as it would spin and eventually veer off towards a certain direction. The drone had to be stopped at that point in order to prevent the possibility of crashing. However, the drone was ultimately able to lift from the ground and drive on terrain, proving its ability to fly and drive, which was the main objective of this project.

Furthermore, it was observed that since the driving mode of the drone required lower amperages and voltages, it was able to use less battery power than the flying mode—increasing efficiency.

6.2. Conclusion

Overall, this project was completed on May 3rd, 2019 as the objectives of the projects were met as a fully functional drone prototype was built and controllable for Buzz Drone Inc. Despite having a few issues with the controls, the drone was nonetheless capable of flying and driving on the ground, which ultimately saved energy and reduces power consumption.

The hybrid drone was approximately 2.5 kg and fit within an overall size of 2.5 ft³. The hybrid drone utilized four propellers and four wheels, where two of the wheels were driven by motors. Most of the electronics were secured between the manufactured composite baseplates except for the battery and gyroscope. The drone was controlled through the myRIO microcontroller and LabVIEW software. The user interface and code were integrated in the LabVIEW front panel and virtual instrument (VI). Through the front panel, variables could be modified in order to adjust the software controls as required. Overall, the drone was unique lightweight, portable, compact, robust, easy to use and reliable as required by the customer needs.

6.3. Project Challenges

In this section, the main manufacturing, electrical and programming challenges encountered in this project are explained in the following sections.

6.3.1. Manufacturing Challenges

For this project, one of the biggest manufacturing challenges was ensuring proper alignment. With the drone's clamping mechanism used to hold its body together, it was important that the holes of the clamps, and the baseplates lined up correctly. It was also important that the propellers be as horizontal as possible to efficiently fly in the air. Thus, special care had to be taken when drilling and milling most of the components in the project.

Another manufacturing challenge was working with composites and creating the sandwich composite. This process took a few different iterations before a suitable top and bottom plate were created. This was because large air bubbles had formed in previous versions of these plates. It was found out that using less epoxy was actually better to ensure that no air bubbles formed.

6.3.2. Electrical Challenges

Some of the electrical challenges that the team faced originated from the soldering of heavy gauge wires, the voltage and current requirements for the motor drivers, and accidental drainage of the battery.

The battery selected used 10 AWG wires that were soldered to a female XT90 connector, which was used to initially power the ESC. It was required that an adaptor be created to connect the ESC to the battery, which involved using the same gauge wire and a male XT90 connector. However, it was found to be difficult to solder the wires onto the XT90 connector utilizing a typical soldering iron. Thankfully, a high-power soldering gun was acquired, which was extremely effective for this task.

Afterwards, it was found that the motor driver that was initially chosen, Digilent Motor Adapter for NI myRIO, could only output a maximum of 1.5 A. Due to time constraint, this component was replaced by an on-hand Sabertooth Dual 25A 6V-24V Regenerative Motor Driver which met the specifications requirement by the brushed DC motors.

Lastly, during the testing phase the cells in the 6S LiPo battery used to power the hybrid drone were unknowingly and significantly discharged below 3 V, killing the battery. It was later found out that this had occurred because the battery charger being used was faulty. Fortunately, a functional charger was able to be borrowed from another team, allowing this project to continue.

6.3.3. Programming Challenges

The challenges in the software side of the project includes implementing the drone controls, which included optimizing the feedback signal through using a complementary filter, average calculator and PID. Determining which variables to change was found to be challenging as there were many that could be manipulated. These include the high and low pass constant in the complimentary filter, the cut-off frequency, order and sampling rate of the low pass filter, the number of samples to be averaged, the PID limits, the motor zero errors, the range of PWM compensation and the PID terms (proportional term, K_p , integral time, T_i , and derivative term, T_d).

Another challenge was implementing the user interface to control the drone. Initially, an Xbox controller was going to be used as the drone controller. However, the code used to receive inputs from the controller was not compatible with the main code controlling the drone. As a result, the user interface for the drone was limited to the controls on the front panel provided by LabVIEW, on a labtop.

6.4. Future Work

The future work for this project consists of improvements in the mechanical, electrical and programming aspects of the drone, which include the following.

- replacing the number of metallic parts with plastic ones (screws, tube clamps, motor clamps, drive motor mount, drive motor coupling, bolts on caster wheel)
- adding protection for the propellers
- organizing and trimming wires
- using a lighter motor driver
- fine tuning the PID values
- integrating a remote controller for the user
- adding a GPS and optical sensor for better control
- reselecting new motors and propellers for better maneuverability (at the cost of a larger size)

Implementation of these improvements would increase the flight time, maneuverability and controls of the drone.

Bibliography

- [1] E. Howell, "What Is A Drone?," Space, 3 October 2018. [Online]. Available: <https://www.space.com/29544-what-is-a-drone.html>. [Accessed 10 December 2018].
- [2] Panda Mediacenter, "What is the future of drones?," Panda Security, 29 March 2018. [Online]. Available: <https://www.pandasecurity.com/mediacenter/news/what-is-the-future-of-drones/>. [Accessed 10 December 2018].
- [3] Transport Canada, "Flying your drone safely and legally (current rules)," Transport Canada, 8 January 2019. [Online]. Available: <https://www.tc.gc.ca/en/services/aviation/drone-safety/flying-drone-safely-legally-current-rules.html#flying>. [Accessed 10 December 2018].
- [4] B. Coxworth, "B-Unstoppable combines a mini tank and a drone," New Atlas, 20 May 2015. [Online]. Available: <https://newatlas.com/b-unstoppable-tank-quadcopter/37616/>. [Accessed 10 December 2018].
- [5] Just Drones, "TankCopter: The Quadcopter + Tank Hybrid Called B-Unstoppable," Just Drones, [Online]. Available: <https://justdrones.com.au/tankcopter-the-quadcopter-tank-hybrid-called-b-unstoppable/>. [Accessed 10 December 2018].
- [6] A. Sham, "Syma X9 Explorers (In-Depth Review)," The Drone Files, 17 March 2016. [Online]. Available: <https://www.thedronefiles.net/2016/03/17/syma-x9-explorers-in-depth-review/>. [Accessed 10 December 2018].
- [7] JA Deals, "FlyCar X9 RC Remote Control Quadcopter Drone Flying Car by Syma," JA Deals, [Online]. Available: <https://www.jadeals.com/product/flycar-x9-rc-remote-control-quadcopter-drone-flying-car-by-syma/>. [Accessed 10 December 2018].
- [8] PowerVision, "PowerEgg," PowerVision, [Online]. Available: <https://store.us.powervision.me/products/poweregg>. [Accessed 2018 10 December].

- [9] DJI, DJI, [Online]. Available: <https://www.dji.com/inspire-2/specs>. [Accessed 6 December 2018].
- [10] ShareGrid, "DJI Inspire 2 Drone w/ x5s 5K Gimbal/Camera + 4 Lenses," ShareGrid, [Online]. Available: <https://www.sharegrid.com/losangeles/l/17903-dji-inspire-2-drone-w-x5s-5k-gimbal-camera-4-lenses?type=rent>. [Accessed 10 December 2018].
- [11] Canadian Intellectual Property Office, "Canadian Patents Database / Patent 2787279 Summary," 22 October 2013. [Online]. Available: http://www.ic.gc.ca/opic-cipo/cpd/eng/patent/2787279/summary.html?query=aerial+and+ground+mobility&start=1&num=50&type=basic_search. [Accessed 10 December 2018].
- [12] United States Patent and Trademark Office, "Flying device with improved movement on the ground," 14 June 2011. [Online]. Available: <http://patft.uspto.gov/netahtml/PTO/index.html>. [Accessed 10 December 2018].
- [13] K. Kamel, "Diagrams of brushed and brushless DC motors," May 2016. [Online]. Available: https://www.researchgate.net/figure/Diagrams-of-brushed-and-brushless-DC-motors10_fig5_315337631. [Accessed 02 May 2019].
- [14] Nidec Corporation, "Brushless Motors," [Online]. Available: <https://www.nidec.com/en-NA/technology/capability/brushless/>. [Accessed 04 May 2019].
- [15] E. Williams, "Your Quadcopter Has Three Propellers Too Many," Hackaday, 4 May 2016. [Online]. Available: <https://hackaday.com/2016/05/04/your-quadcopter-has-three-propellers-too-many/>. [Accessed 8 December 2018].
- [16] W. Zhang, M. Mueller and R. D'Andrea, "The Monospinner: world's mechanically simplest controllable flying machine," Robohub, 3 May 2016. [Online]. Available: <https://robohub.org/the-monospinner-worlds-mechanically-simplest-controllable-flying-machine/>. [Accessed 8 December 2018].

- [17] Research Drone, "DuoCopter drone with two motors," Research Drone, [Online]. Available: <https://www.research-drone.com/en/DuoCopter.html>. [Accessed 8 December 2018].
- [18] innov8tivedesigns, "Multi-Rotor Configurations," innov8tivedesigns, [Online]. Available: <http://www.innov8tivedesigns.com/blog/multi-rotor-configurations/>. [Accessed 8 December 2018].
- [19] J. Fiest, "How many propellers does your drone need? – how to fly, the science of flight," Drone Rush, 4 March 2018. [Online]. Available: <https://www.dronerush.com/propellers-drone-need-science-of-flight-10733/>. [Accessed 10 November 2018].
- [20] F. Corrigan, "How A Quadcopter Works With Propellers And Motors Explained," DroneZon, 24 August 2018. [Online]. Available: <https://www.dronezon.com/learn-about-drones-quadcopters/how-a-quadcopter-works-with-propellers-and-motors-direction-design-explained/>. [Accessed 9 December 2018].
- [21] D. Omega, "Quadcopter Propeller Basics for Drone Pilots," [Online]. Available: <https://www.droneomega.com/quadcopter-propeller/>. [Accessed 03 May 2019].
- [22] "DJI INSPIRE 2 WITH ZENMUSE X5S, PRO PACKAGE," [Online]. Available: <https://carolinadrone.com/products/dji-inspire-2-with-zenmuse-x5s-pro>. [Accessed 03 May 2019].
- [23] Drone Trest, "How to choose the right motor for your multicopter drone," Drone Trest, 12 October 2015. [Online]. Available: <https://www.dronetrest.com/t/how-to-choose-the-right-motor-for-your-multicopter-drone/568>. [Accessed 7 November 2018].
- [24] PropWashed, "Miniquad Propeller Buyers Guide," PropWashed, 12 August 2016. [Online]. Available: <https://www.propwashed.com/miniquad-propeller-buyers-guide/>. [Accessed 8 December 2018].

- [25] KDE Direct, "Why Drone Propeller Blades Matter | Drone Upgrade Technology," KDEDirect, 9 March 2016. [Online]. Available: <https://www.kdedirect.com/blogs/news/90454595-why-drone-propeller-blades-matter-drone-upgrade-technology>. [Accessed 5 December 2018].
- [26] Pilot Friend, "Propellers," [Online]. Available: http://www.pilotfriend.com/training/flight_training/fxd_wing/props.htm. [Accessed 03 May 2019].
- [27] APC Propellers, "Performance Data," 2018. [Online]. Available: <https://www.apcprop.com/technical-information/performance-data/>. [Accessed 05 December 2018].
- [28] Learning RC, "Brushless Motor Kv Constant Explained," Learning RC, 29 July 2015. [Online]. Available: <http://learningrc.com/motor-kv/>. [Accessed 5 December 2018].
- [29] Mich Bby, "3512 6S brushless motor for multi-rotor," Mich Bby, [Online]. Available: <http://www.michobby.com/product/3512-6s-brushless-motor-for-multi-rotor/>. [Accessed 7 December 2018].
- [30] ketanco, "controllers and drivers and esc," 14 May 2017. [Online]. Available: <https://forum.arduino.cc/index.php?topic=477219.0>. [Accessed 04 May 2019].
- [31] Electronics Tutorials, "Pulse Width Modulation," [Online]. Available: <https://www.electronics-tutorials.ws/blog/pulse-width-modulation.html>. [Accessed 04 May 2019].
- [32] "Propeller Thrust," [Online]. Available: <https://www.grc.nasa.gov/www/k-12/airplane/propth.html>. [Accessed 05 December 2018].
- [33] "Static Thrust Calculation," [Online]. Available: <https://quadcopterproject.wordpress.com/static-thrust-calculation/>. [Accessed 05 December 2018].

- [34] "How to calculate thrust, given RPM, prop pitch and prop diameter?," [Online]. Available: <https://www.rcgroups.com/forums/showthread.php?288091-How-to-calculate-thrust-given-RPM-prop-pitch-and-prop-diameter>. [Accessed 05 December 2018].
- [35] "Aerodynamic Characteristics of Propellers," [Online]. Available: <https://www.mh-aerotoools.de/airfoils/propuls3.htm>. [Accessed 05 December 2018].
- [36] K. S. a. m. o. A. D.J. Auld, "Analysis of Propellers," [Online]. Available: http://www-mdp.eng.cam.ac.uk/web/library/enginfo/aerothermal_dvd_only/aero/propeller/prop1.html. [Accessed 03 02 2019].
- [37] AMME, University of Sidney, "Analysis of Propellers," [Online]. Available: http://www-mdp.eng.cam.ac.uk/web/library/enginfo/aerothermal_dvd_only/aero/propeller/prop1.html. [Accessed 03 May 2019].
- [38] D. Collins, "The Torque Equation and the Relationship with DC Motors," 09 March 2017. [Online]. Available: <https://www.motioncontroltips.com/torque-equation/>. [Accessed 05 December 2018].
- [39] D. Collins, "The relationship between voltage and DC motor output speed," 6 December 2015. [Online]. Available: <https://www.motioncontroltips.com/faq-whats-relationship-voltage-dc-motor-output-speed/>. [Accessed 03 May 2019].
- [40] "Multicopter Prop Set 5 x 4.3 Bullnose (2CW/2CCW)," APC Propellers, [Online]. Available: http://www.greathobbies.com/productinfo/?prod_id=APC050043EB4. [Accessed 03 May 2019].
- [41] "EMAX RSII 2306 1900kv Motor," EMAX, [Online]. Available: <https://www.getfpv.com/emax-rsii-2306-1900kv-motor.html>. [Accessed 03 May 2019].

- [42] "EMAX RSII 2306-1900KV: 6S Powerhouse," 21 August 2018. [Online]. Available: <https://www.youtube.com/watch?v=uY6Y6o3pTwg&t=1110s>. [Accessed 03 May 2019].
- [43] S. Etigowni, "Drone's pitch, roll, and yaw," December 2018. [Online]. Available: https://www.researchgate.net/figure/Drones-pitch-roll-and-yaw_fig2_329521700. [Accessed 01 May 2019].
- [44] D. Nedelkovski, "MEMS Accelerometer Gyroscope Magnetometer & Arduino," [Online]. Available: <https://howtomechatronics.com/how-it-works/electrical-engineering/mems-accelerometer-gyroscope-magnetometer-arduino/>. [Accessed 03 May 2019].
- [45] R. D. N. G. X. S. Jay Esfandyari, "Introduction to MEMS gyroscopes," 15 November 2010. [Online]. Available: <https://electroiq.com/2010/11/introduction-to-mems-gyroscopes/>. [Accessed 03 May 2019].
- [46] B. Douglas, "Drone Control and the Complementary Filter," 05 November 2018. [Online]. Available: <https://www.youtube.com/watch?v=whSw42XddsU&t=201s>. [Accessed 02 May 2019].
- [47] Sam, "ESC to motor connection guide - how to reverse your motor direction the easy way," 29 September 2015. [Online]. Available: <https://www.dronetrest.com/t/esc-to-motor-connection-guide-how-to-reverse-your-motor-direction-the-easy-way/1297>. [Accessed 02 May 2019].
- [48] Janson, "DroneBuilds - WE are FPV," 06 July 2017. [Online]. Available: <https://forum.wearefpv.fr/topic/1841-pitch-roll-yaw-throttle-param%C3%A8tres/>. [Accessed 01 May 2019].
- [49] UAV Coach, "How To Fly A Drone: A Beginner's Guide to Multicopter Systems & Flight Proficiency," [Online]. Available: <https://uavcoach.com/how-to-fly-a-quadcopter-guide/#guide-2>. [Accessed 01 May 2019].

- [50] F. Corrigan, "How A Quadcopter Works With Propellers And Motors Explained," 24 August 2018. [Online]. Available: <https://www.dronezon.com/learn-about-drones-quadcopters/how-a-quadcopter-works-with-propellers-and-motors-direction-design-explained/>. [Accessed 01 May 2019].
- [51] T. Agarwal, "The Working Principle of a PID Controller for Beginners," [Online]. Available: <https://www.elprocus.com/the-working-of-a-pid-controller/>. [Accessed 01 May 2019].
- [52] P. Vance Vandoren, "Understanding PID control and loop tuning fundamentals," 26 July 2016. [Online]. Available: <https://www.controleng.com/articles/understanding-pid-control-and-loop-tuning-fundamentals/>. [Accessed 03 May 2019].
- [53] R. Nave, "Commutator and Brushes on DC Motor," [Online]. Available: <http://hyperphysics.phy-astr.gsu.edu/hbase/magnetic/comtat.html>. [Accessed 04 May 2019].
- [54] Technology Robotix Society, IIT Kharagpur, "Differential Drive," 2018. [Online]. Available: <https://2019.robotix.in/tutorial/mechanical/drivemechtut/>. [Accessed 02 May 2019].
- [55] A. Yong, "What is the working of a H-bridge circuit?," 10 May 2017. [Online]. Available: <https://www.quora.com/What-is-the-working-of-a-H-bridge-circuit>. [Accessed 02 May 2019].
- [56] Performance Composites, "Mechanical Properties of Carbon Fibre Composite Materials, Fibre / Epoxy resin (120C Cure)," [Online]. Available: http://www.performance-composites.com/carbonfibre/mechanicalproperties_2.asp. [Accessed 10 December 2018].

- [57] C. J. Fisher, "Using An Accelerometer for Inclination Sensing," 06 May 2011. [Online]. Available: <https://www.digikey.ca/en/articles/techzone/2011/may/using-an-accelerometer-for-inclination-sensing>. [Accessed 02 May 2019].
- [58] Dr. Ed Doering , "Gyroscope," Rose-Hulman Institute of Technology, [Online]. Available: <https://learn.ni.com/teach/resources/57/gyroscope>. [Accessed 02 May 2019].
- [59] STMicroelectronics, "L3G4200D MEMS motion sensor: ultra-stable three-axis digital output gyroscope Preliminary data," 2010. [Online]. Available: <https://www.pololu.com/file/0J491/L3G4200D.pdf>. [Accessed 02 May 2019].
- [60] B. Baker, "Apply Sensor Fusion to Accelerometers and Gyroscopes," DigiKey, 30 June 2018. [Online]. Available: <https://www.digikey.ca/en/articles/techzone/2018/jan/apply-sensor-fusion-to-accelerometers-and-gyroscopes>. [Accessed 02 May 2019].
- [61] dacook13, "Filtering Accelerometer Noise in LabVIEW," Instructables by Autodesk, [Online]. Available: <https://www.instructables.com/id/Filtering-Accelerometer-Noise-In-labVIEW/>. [Accessed 02 May 2019].
- [62] Joel_G, "Quadcopter Simulations," National Instruments, 30 May 2012. [Online]. Available: <https://forums.ni.com/t5/Example-Program-Drafts/Quadcopter-Simulations/ta-p/3495303?profile.language=en>. [Accessed 02 May 2019].

Appendix A. Request for Proposal

Company Background

Buzz Drone Inc. was started in 2012 by a group of highly motivated individuals. They shared a vision of the future, where drones would be used everywhere and by everyone. From military purposes to package delivery, drones are uniquely capable of many different applications due to their portability, affordability, and modularity. The company is based in Langley, British Columbia, near the popular Honeybee Centre (hence the company's name).

The focus of Buzz Drone Inc. has been the manufacturing and selling of a variety of drone concepts. Recently, they have had major success through the mass production and commercialization of the popular "Banana Drone".

As such, Buzz Drone Inc. is requesting a proposal from a variety of strong organizations, for a compact, foldable drone design to be manufactured and sold by the company – which will garner the same success as the "Banana Drone". The requirements, objectives, and overview of the project can be seen below along with other important details.

Project Overview

In an ever-changing, fast-paced world, new concepts and ideas are needed to continue competing with modern technology. One of the projects being developed at Buzz Drone Inc. is a new compact, foldable drone, that can fly and travel on land. In other words, a drone with a combination of propellers and/or wheels. The purpose of the project is to investigate a new and interesting drone concept that has not yet been popularized.

Buzz Drone Inc. has worked on this project in the past, where they completed an unfinished prototype. While the concept was interesting, its validity was not confirmed. Their past work is still documented and may be reviewed to serve as a baseline or as a reference for gathering ideas.

Project Goals and Target Audience

The compact, foldable drone design will be used to help Buzz Drone Inc. target a new audience and gain success in a different drone sector. Previously, the “Banana Drone” appealed to an audience of zoologists who study monkeys. With this new design, they are hoping to target a broader, more inclusive audience. Specifically, they hope to target drone enthusiasts/hobbyists, videographers, and miners. Buzz Drone Inc. is hoping that the originality and versatility of the compact, foldable design will appeal to these customers, leading to a monetary profit. This drone concept is planned to be mass produced and sold in the future; thus, a functional prototype of the design should be completed as validation of its manufacturability and functional feasibility.

Project Requirements

For this project, the deliverables should include a SOLIDWORKS model of the drone, fabrication drawings, and a manufactured and tested physical prototype. A stress analysis should also be conducted to validate the drone’s design.

The drone should use either a BeagleBone or Raspberry Pi microcontroller to maneuver the drone. The microcontroller should also be programmed using MATLAB Simulink software. Ideally, the drone will be autonomous (GPS controlled), but may also be controlled using a remote controller (computer, iPad, iPhone, Xbox controller, etc.).

The scope of work for this project includes the manufacturing, purchasing and integration of the physical components, the electrical wiring, and the controls programming. The drone should be desktop-sized (1-2 ft³), and should also be stiff/strong enough to handle its own weight on land and survive slight impacts. Furthermore, the drone should be lightweight enough to fly in the air. The propellers must be made of a material with a high stiffness-to-weight ratio to address these issues and to be efficient. The drone must be stable on land and in the air.

Proposal Selection Criteria

To select the best organization for this project, Buzz Drone Inc. will consider the feasibility of the final compact foldable drone concept, its estimated cost (of the prototype), and the originality of the final concept. As enthusiasts are typically willing to pay more money for original, interesting designs, the cost will not be as important. However, the feasibility of mass-producing the design is extremely important, more so than originality. This is because, if the drone cannot be manufactured, then it cannot be sold to generate a profit. Only proposals, which meet the format outlined in the next section, will be considered.

Proposal Submission Criteria

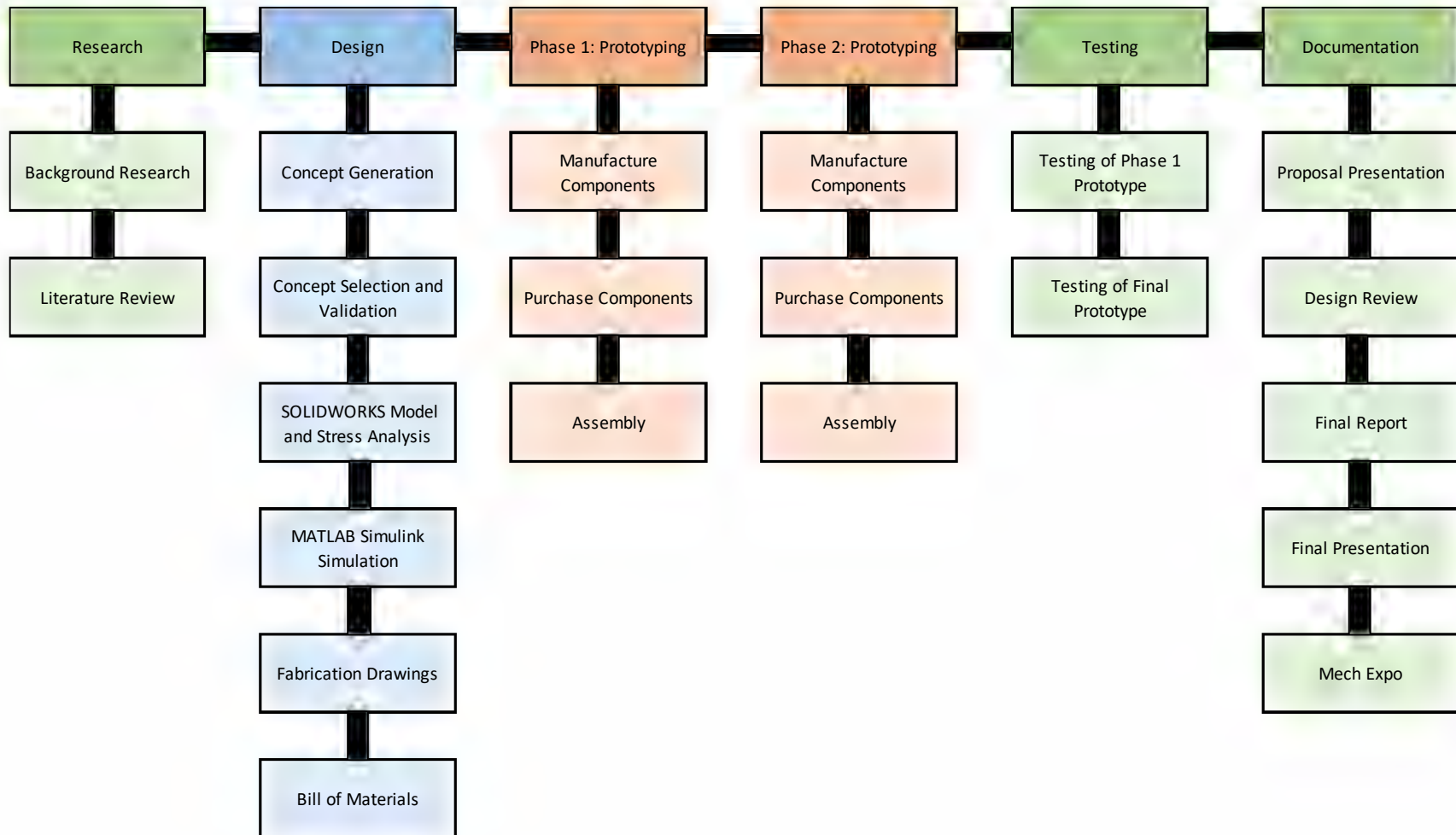
Please submit your project proposal by 8:30 am on Tuesday, October 30th, 2018. Any proposals submitted later will be excluded from consideration. The project proposals should be submitted as a PDF email attachment to the address, *buzzdroneinc@buzz.com*.

The proposal should include, at a minimum, an introduction of your organization and team, your proposed drone concept with justifications, the estimated budget, a task list, and the project's schedule (including major milestones). Please include other pertinent information, and sections per your judgement.

Appendix B. Buzz Drone Inc. thanks you for your time. Only the selected organization will be contacted, moving forward.

Appendix B. Project Management Items

B.1. Work Breakdown Structure

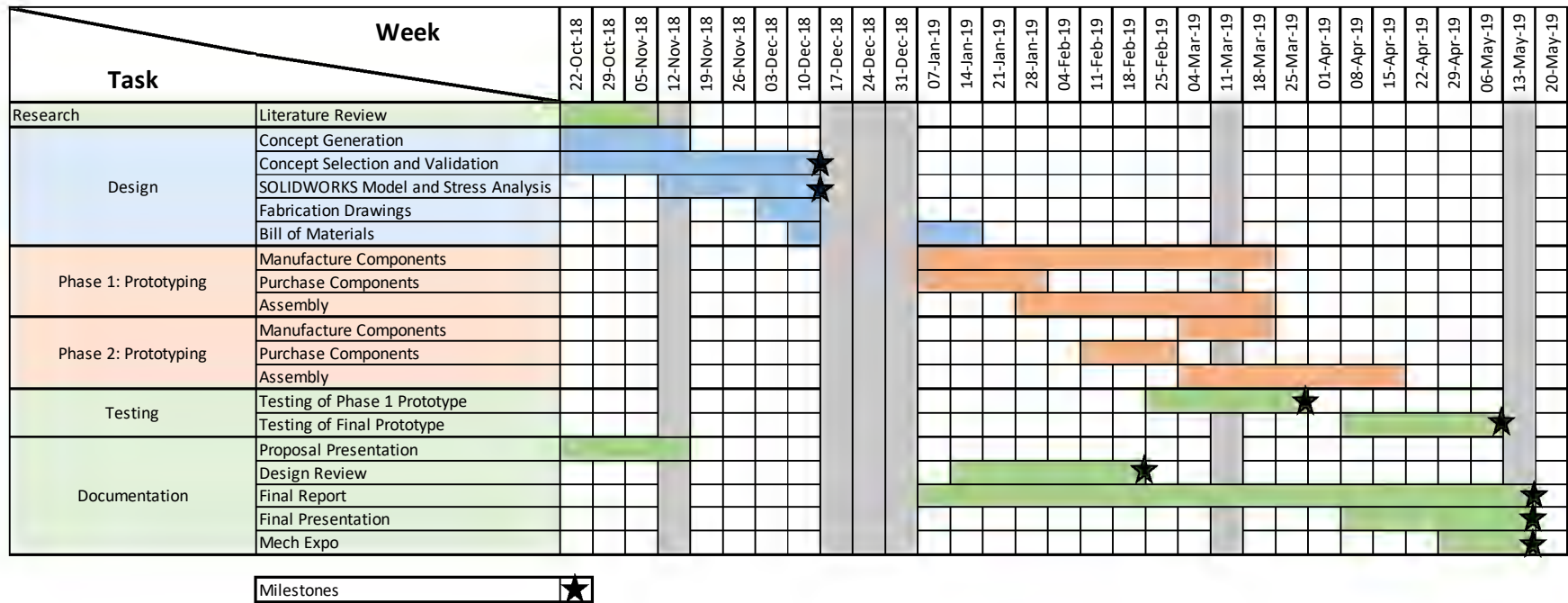


B.2. Simplified Responsibility Assignment Matrix

| | | Falcon Drone Inc. | | Stakeholder |
|----------------------|--------------------------------------|-------------------|----------------|------------------|
| | | Eleazar Pestano | Reeghan Osmond | Dr. Cyrus Raoufi |
| Research | Literature Review | R | A | I |
| Design | Concept Generation | R | A | I |
| | Concept Selection and Validation | A | R | C |
| | SOLIDWORKS Model and Stress Analysis | R | A | C |
| | MATLAB Simulink Simulation | A | R | C |
| | Fabrication Drawings | R | A | I |
| | Bill of Materials | A | R | C |
| Phase 1: Prototyping | Manufacture Components | R | A | I |
| | Purchase Components | A | R | C |
| | Assembly | A | R | I |
| Phase 2: Prototyping | Manufacture Components | R | A | I |
| | Purchase Components | A | R | C |
| | Assembly | A | R | I |
| Testing | Testing of Phase 1 Prototype | R | A | C |
| | Testing of Final Prototype | A | R | C |
| Documentation | Proposal Presentation | A | R | I |
| | Design Review | R | A | C |
| | Final Report | R | A | C |
| | Final Presentation | A | R | I |
| | Mech Expo | A | R | I |

R: Responsible, A: Accountable, C: Consultant, I: Inform

B.3. Simplified Gantt Chart



B.4. Milestone Chart

| <div style="text-align: right;">Week</div> <div style="text-align: left;">Milestones</div> | 22-Oct-18 | 29-Oct-18 | 05-Nov-18 | 12-Nov-18 | 19-Nov-18 | 26-Nov-18 | 03-Dec-18 | 10-Dec-18 | 17-Dec-18 | 24-Dec-18 | 31-Dec-18 | 07-Jan-19 | 14-Jan-19 | 21-Jan-19 | 28-Jan-19 | 04-Feb-19 | 11-Feb-19 | 18-Feb-19 | 25-Feb-19 | 04-Mar-19 | 11-Mar-19 | 18-Mar-19 | 25-Mar-19 | 01-Apr-19 | 08-Apr-19 | 15-Apr-19 | 22-Apr-19 | 29-Apr-19 | 06-May-19 | 13-May-19 | 20-May-19 | | | | |
|--|-----------|-----------|-----------|-----------|-----------|-----------|-----------|-----------|-----------|-----------|-----------|-----------|-----------|-----------|-----------|-----------|-----------|-----------|-----------|-----------|-----------|-----------|-----------|-----------|-----------|-----------|-----------|-----------|-----------|-----------|-----------|--|--|--|--|
| Concept Selected | | | | | | | | | | | | | | | | | | | | | | | | | | | | | | | | | | | |
| Stress Analysis Completed | | | | | | | | | | | | | | | | | | | | | | | | | | | | | | | | | | | |
| Design Review | | | | | | | | | | | | | | | | | | | | | | | | | | | | | | | | | | | |
| Functional Phase 1 Prototype | | | | | | | | | | | | | | | | | | | | | | | | | | | | | | | | | | | |
| Functional Final Prototype | | | | | | | | | | | | | | | | | | | | | | | | | | | | | | | | | | | |
| Submission of Deliverables | | | | | | | | | | | | | | | | | | | | | | | | | | | | | | | | | | | |

Appendix C. Design Review Package

HYBRID DRONE DESIGN AND DEVELOPMENT

Design Review Package

Prepared for:

Cyrus Raoufi, PEng, PhD
Johan Fourie, PEng, PhD

Prepared by:

Reeghan Osmond
Eleazar Pestano



FEBRUARY 13, 2019
FALCON DRONE INC.

Introduction

This document will include the necessary information required to complete a Preliminary Design Review for the second phase of the project, as its design is nearing completion. A description of the two phases of the project is outlined in the next section.

Current Product Development Specifications

The objective of this project was to design a lightweight, compact drone which has the ability to drive on land. This will allow the battery power to be conserved as driving on land does not require continuous power. The drone can rest on land and move more easily instead of landing and taking off. Furthermore, this can allow the drone to maneuver in different locations, including ones where flying is not ideal.

This project has been divided into two phases. The first phase represents the flying aspect of the design, and the second phase represents that driving aspect.

The technical requirements can be seen below in Table C.1.

| Technical Requirements | |
|------------------------------------|--------------------------------|
| Transport Canada Drone Regulations | Flight below 90 m above ground |
| | Weigh less than 35 kg |
| Max Overall Size | 2.5 ft ³ |
| Max Weight | 8 lbs |
| Max Air Speed | 8 – 15 m/s |
| Max Land Speed | 1 – 3 m/s |
| Cost of Components | \$500 |
| Materials | Mostly composites and plastic |
| Controller | MyRIO |

Table C.1: Technical Requirements

There are a few limits and exclusions associated with this project which are relevant to this design review:

- the design should use mostly off-the-shelf components,
- there will be no power efficiency calculations,
- and the drone will be restricted to simply motion.

Calculations

The following calculations were completed to specify an appropriate motor for the rear wheels of the design. Any comments or suggestions regarding these calculations are welcome.

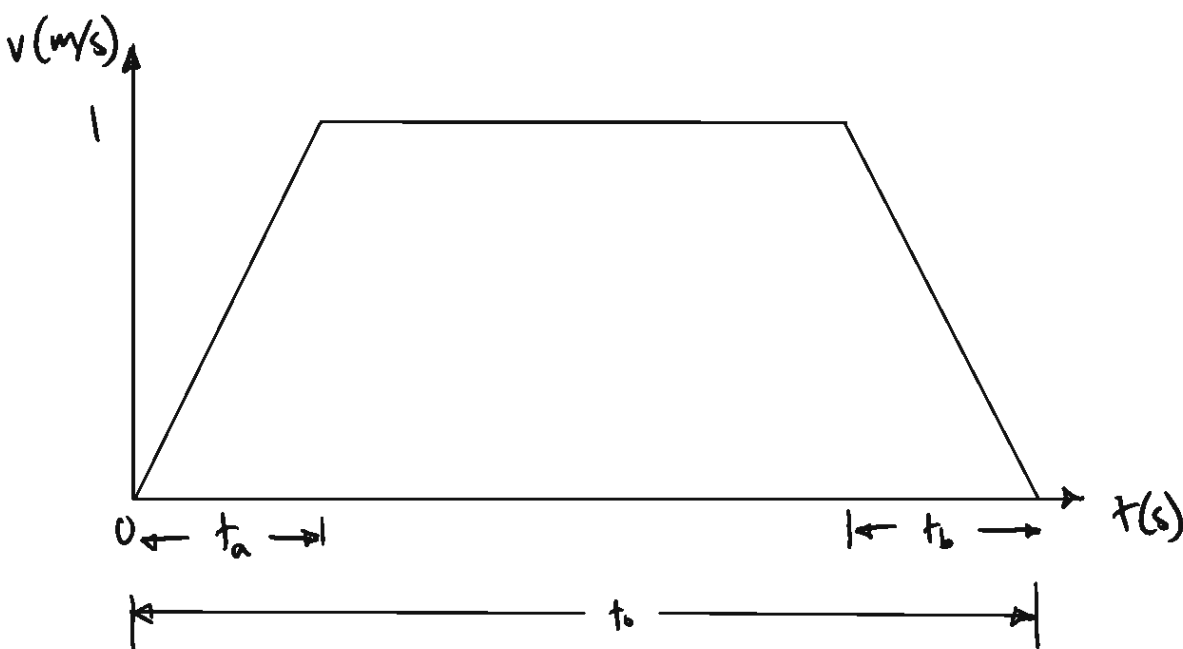


Figure C.1: Desired Motion Profile of the Rear Motors

As represented in Figure C.1, the motor should be able to drive with a minimum speed of 1 m/s (v). This should be accomplished within 1 s (t_a). For these calculations, the assumed wheel radius was 1.5 inches or 0.0381 m (r). A gearbox ratio (N) of 5 was also assumed.

Calculating Angular Speed Requirement

$$\omega = \frac{v}{r} = \frac{1}{0.0381} = 26.25 \frac{\text{rad}}{\text{s}} \left(\frac{\text{rev}}{2\pi \text{ rad}} \right) \left(\frac{60 \text{ s}}{\text{min}} \right) = \mathbf{251 \text{ rpm}}$$

Calculating Total Moment of Inertia

$$\text{Linear acceleration: } a_o = \frac{v}{t_a} = \frac{1}{2} = 0.5 \frac{\text{m}}{\text{s}^2}$$

$$\text{Angular acceleration: } \alpha = \frac{a_o}{r} = \frac{0.5}{0.0381} = 13.123 \frac{\text{rad}}{\text{s}^2}$$

$$\text{Total moment of inertia required to overcome: } J_{total} = \frac{J_{wheel}}{\epsilon N^2} + J_{motor}$$

$$\rightarrow J_{wheel} = \frac{1}{2} m r^2$$

$$\rightarrow J_{total} = \frac{\frac{1}{2} m r^2}{\epsilon N^2} + J_{motor}$$

$$\text{But, } J_{motor} \text{ not known yet } \therefore J_{total} = \frac{\frac{1}{2} m r^2}{\epsilon N^2}$$

Assuming efficiency, $\epsilon = 100\%$,

$$\rightarrow J_{total} = \frac{\frac{1}{2} (0.034)(0.0381)^2}{5^2} = 9.8705E - 7 \text{ kgm}^2$$

Calculating Total Minimum Torque Required

$$T_{total} = J_{total} \alpha + T_{friction}$$

$$J_{total} \alpha = (9.8705E - 7)(13.123) = 1.2951 E - 5 \text{ Nm}$$

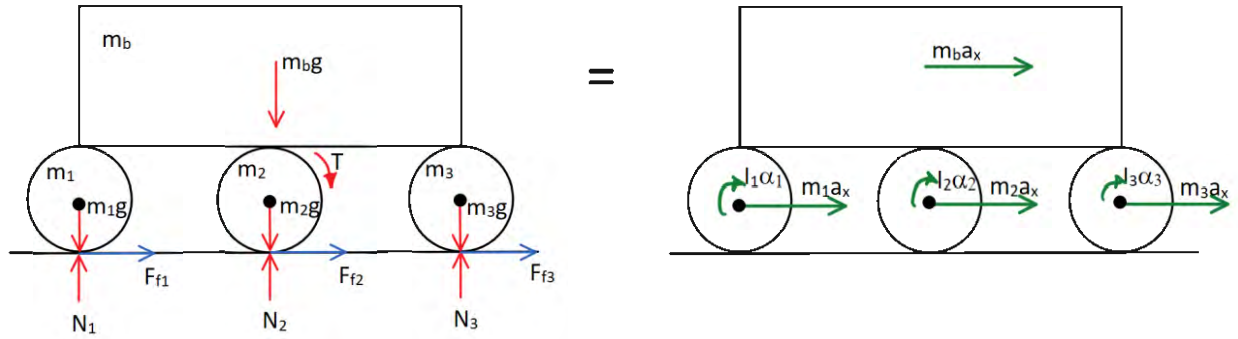


Figure C.2: Free Body Diagram of Drone Assembly

Note: there is an additional wheel behind the middle wheel with a mass of m_4 .

To simplify calculations, it will be assumed that the masses of all the wheels are the same ($m = m_1 = m_2 = m_3 = m_4$). Therefore, the normal force and friction force acting on each wheel will be assumed to be the same as well ($N = N_1 = N_2 = N_3 = N_4$ and $F_f = F_{f1} = F_{f2} = F_{f3} = F_{f4}$). As well, the total mass, M , will be equal to 2 kg and the mass of the body, m_b , will be equal to 1.5 kg.

The following system of equations can be found from the Free Body Diagram in Figure C.2:

$$\sum M_o = 2T - 4F_f r = 4I\alpha + m_b a_o, \text{ where } I = J_{total} \text{ a}$$

$$\sum F_x = 4F_f = M a_o$$

$$\sum F_y = N - W = 0$$

$$\sum F_y = N - W = 0$$

$$\text{From } \sum F_x \rightarrow 4F_f = M a_o = (2 \text{ kg}) \left(0.5 \frac{\text{m}}{\text{s}^2} \right)$$

$$F_f = \frac{(2 \text{ kg}) \left(0.5 \frac{\text{m}}{\text{s}^2} \right)}{4} = 0.25 \text{ N}$$

$$\text{From } \sum M_o \rightarrow T = 4I\alpha + m_b a_o d + 4F_f r$$

$$\rightarrow T = \frac{4(3.8861 E - 5 Nm) + (1.5 kg) \left(0.5 \frac{m}{s^2}\right) (0.127 m) + 4(0.25 N)(0.0381 m)}{2}$$

$$T_{min} = 0.06683 Nm$$

To ensure no slippage, F_f was compared to the static friction force (F_{fs}). A static friction coefficient (μ_s) of 0.05 was assumed.

$$F_{fs} = \mu_s N$$

$$F_{fs} = 0.5 \left(\frac{2}{3} kg\right) \left(9.81 \frac{m}{s^2}\right)$$

$$F_{fs} = 3.27 N > F_f$$

Since F_{fs} was greater than F_f , the wheels will not slip when T_{min} is applied.

Calculating the Maximum Torque Limit

$$\text{Similarly to } T_{min} \rightarrow T_{max} = 4I\alpha + m_b a_o d + 4F_f r$$

$$T_{max} = 4(3.8861 E - 5 Nm) + (1.5 kg) \left(0.5 \frac{m}{s^2}\right) (0.127 m) + 4(3.27 N)(0.0381 m)$$

$$T_{max} = 0.59375 Nm$$

Therefore, the desired motor torque is between $0.06683 Nm < T < 0.59375 Nm Nm$.

Once the final motor is specified, the calculations will be redone to include J_{motor} .

LabVIEW Code

Below in Figure C.3 and Figure C.4 are the two basic codes that will be used to control the DC and Servo motors in the driving aspect of the design. To simulate an analog signal, PWM will be used as the input to these motors to control the speed for the DC motor and position for the Servo motor.

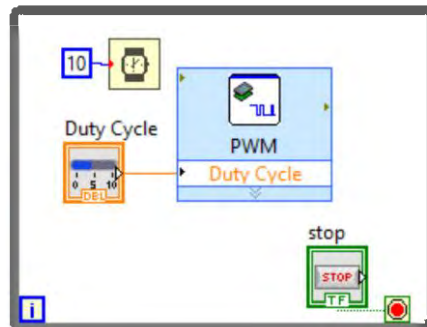


Figure C.3: DC Motor Control Code with LabVIEW

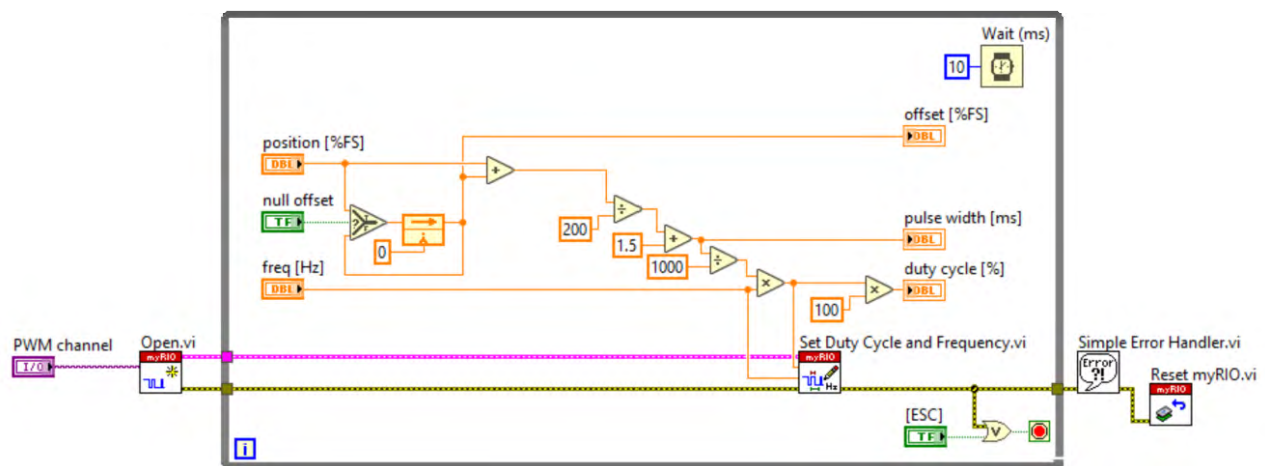


Figure C.4: Servo Motor Control Code with LabVIEW

SolidWorks Model and Areas of Concern

As this Preliminary Design Review is focusing on the second phase of the project (the driving aspect), the focus of this section will be in this area. Therefore, suggestions and feedbacks about the following topics are welcomed:

- An alternative design to the front wheel assembly
- A way to move the back wheels farther to the back
- How to implement suspension/shock absorption into the design

Other parts of the design that also require suggestions and feedback are stated below:

- Method of securing battery
- Adding a cover to prevent damage to the propellers

An isometric view of the overall drone design can be seen below in Figure C.5.

Different views of the rear and front wheel assemblies can be seen on the next few pages.

Please note that any suggestions should ideally require minimal changes to the first phase of the project (including the body) as it is already being manufactured.

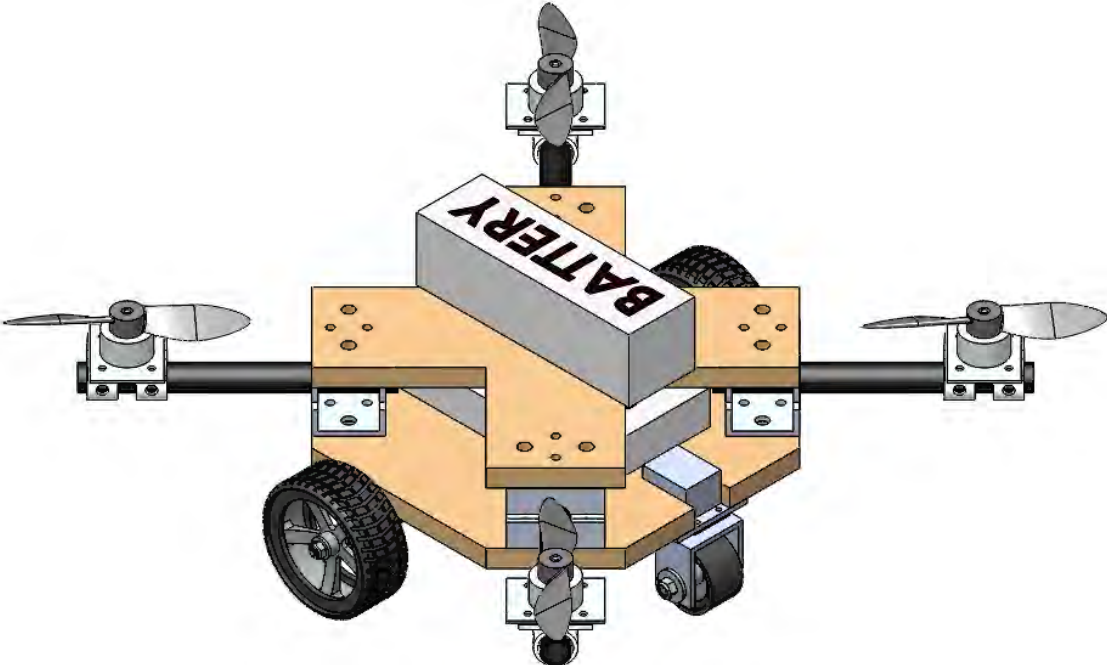


Figure C.5: Model of Overall Drone Design

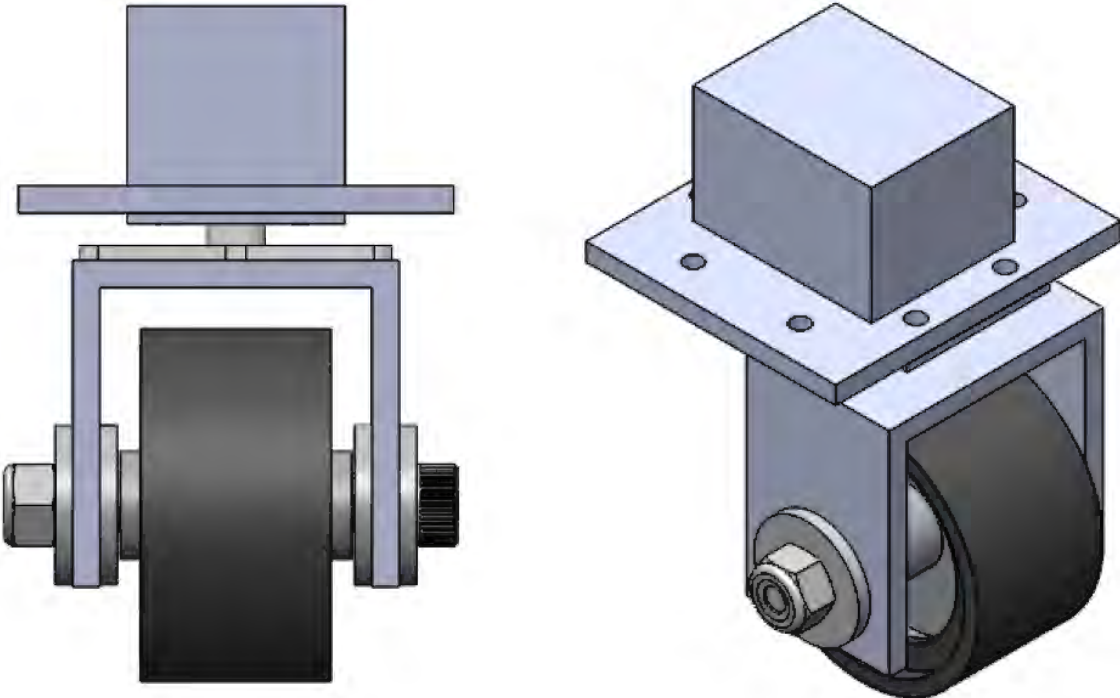


Figure C.6: Model of Front Wheel Assembly

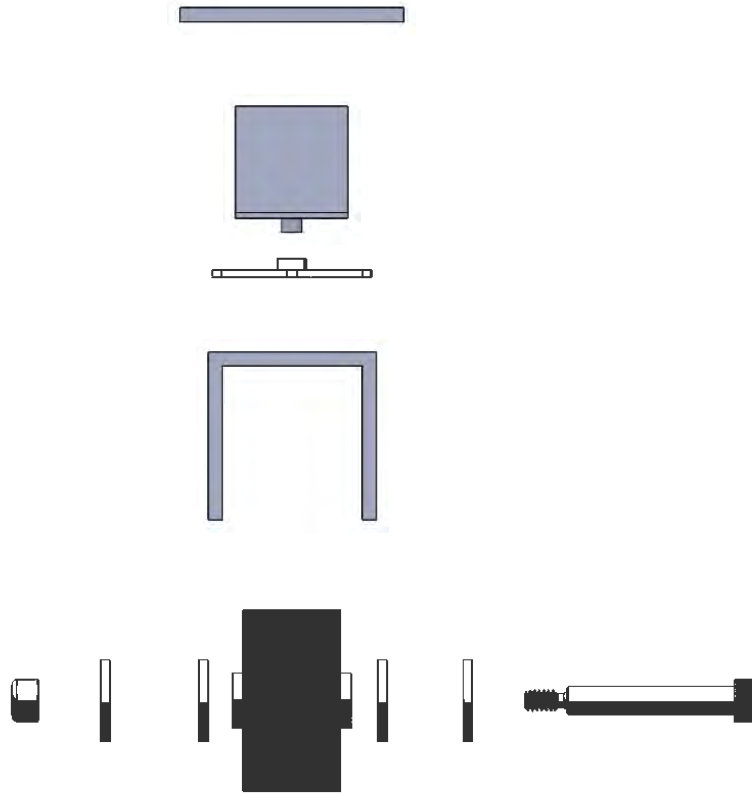


Figure C.7: Exploded View of the Front Wheel Assembly

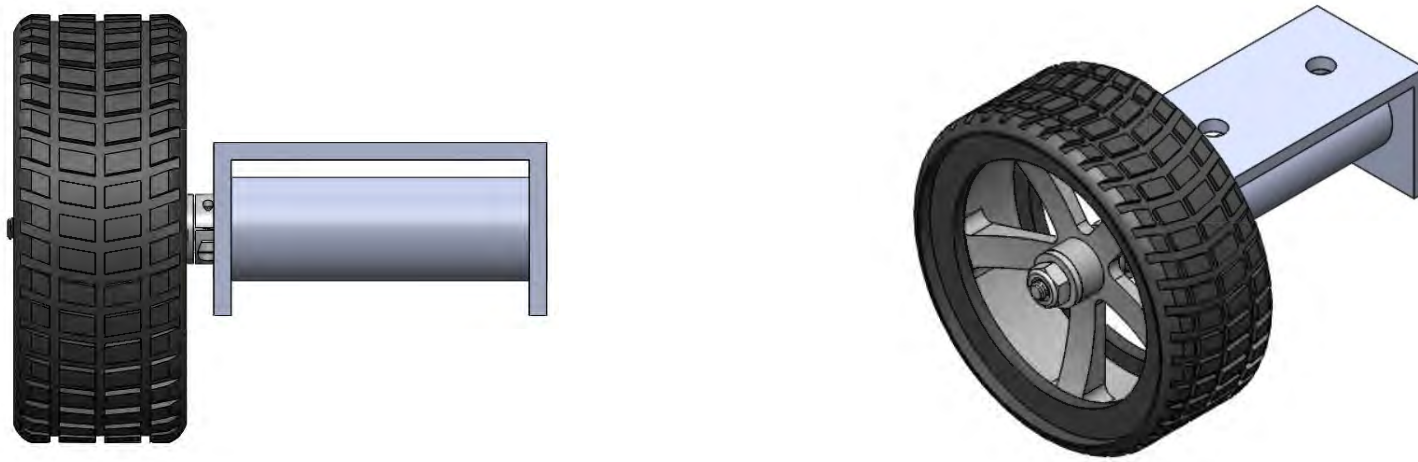


Figure C.8: Model of Rear Wheel Assembly

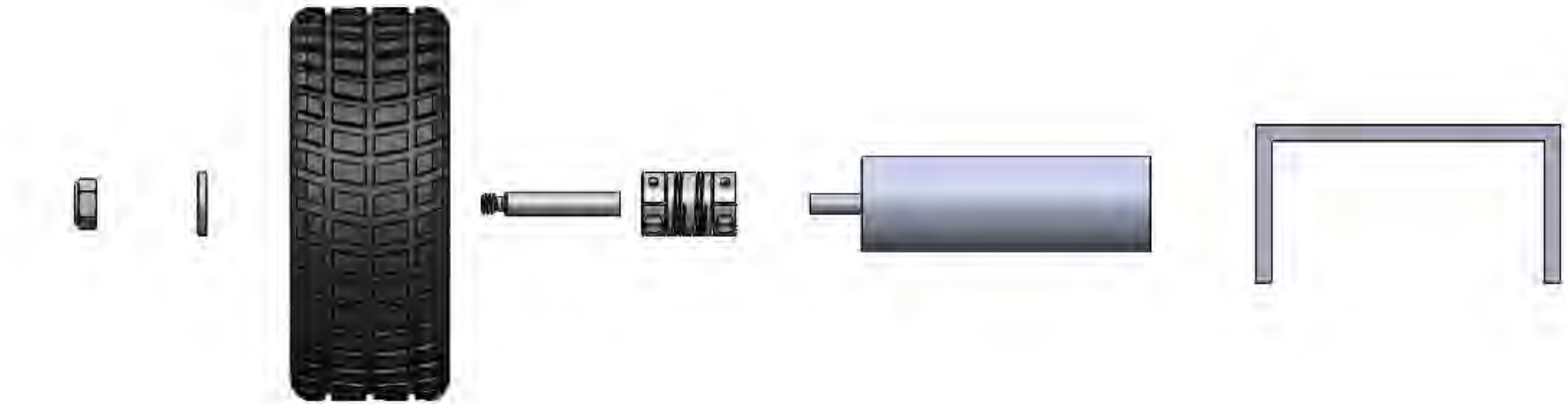


Figure C.9: Exploded View of the Rear Wheel Assembly

Gantt Chart

The schedule for this project is shown in Figure C.10 where the milestones are illustrated in black stars. The team is on schedule with all the tasks needed to be achieved and are currently also working in the phase 2 of the project.

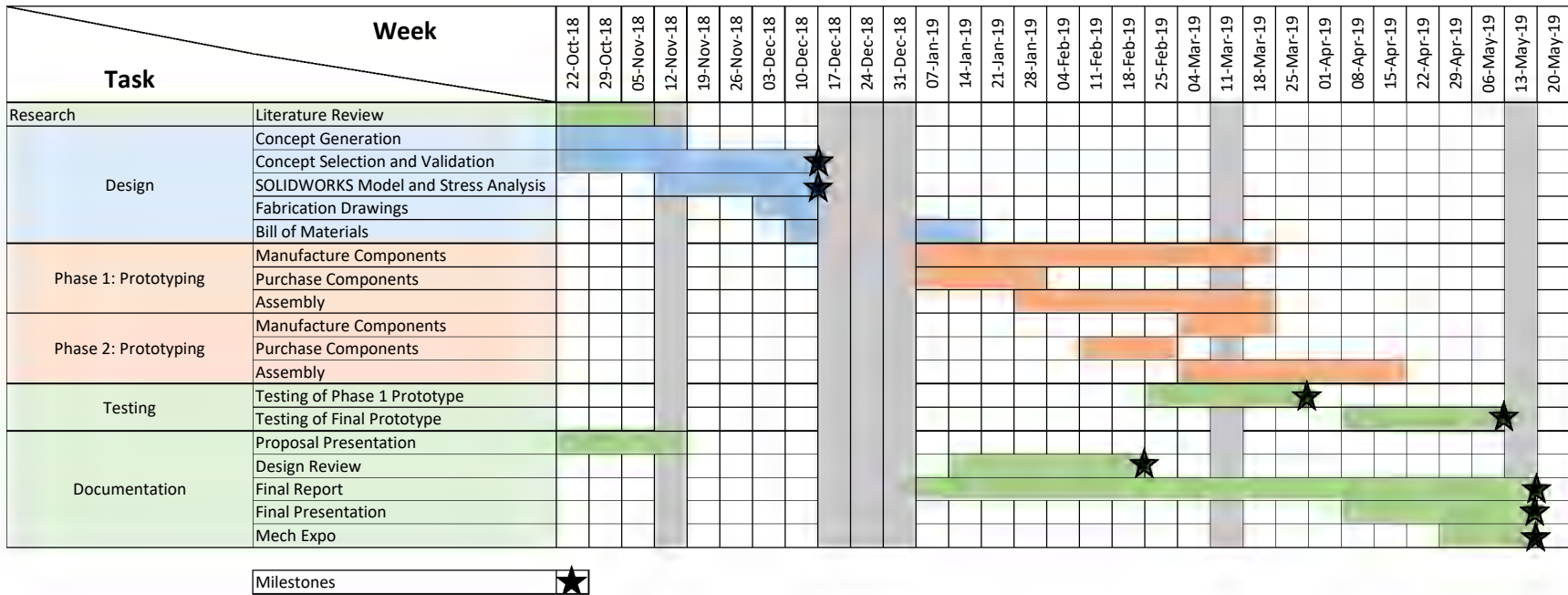


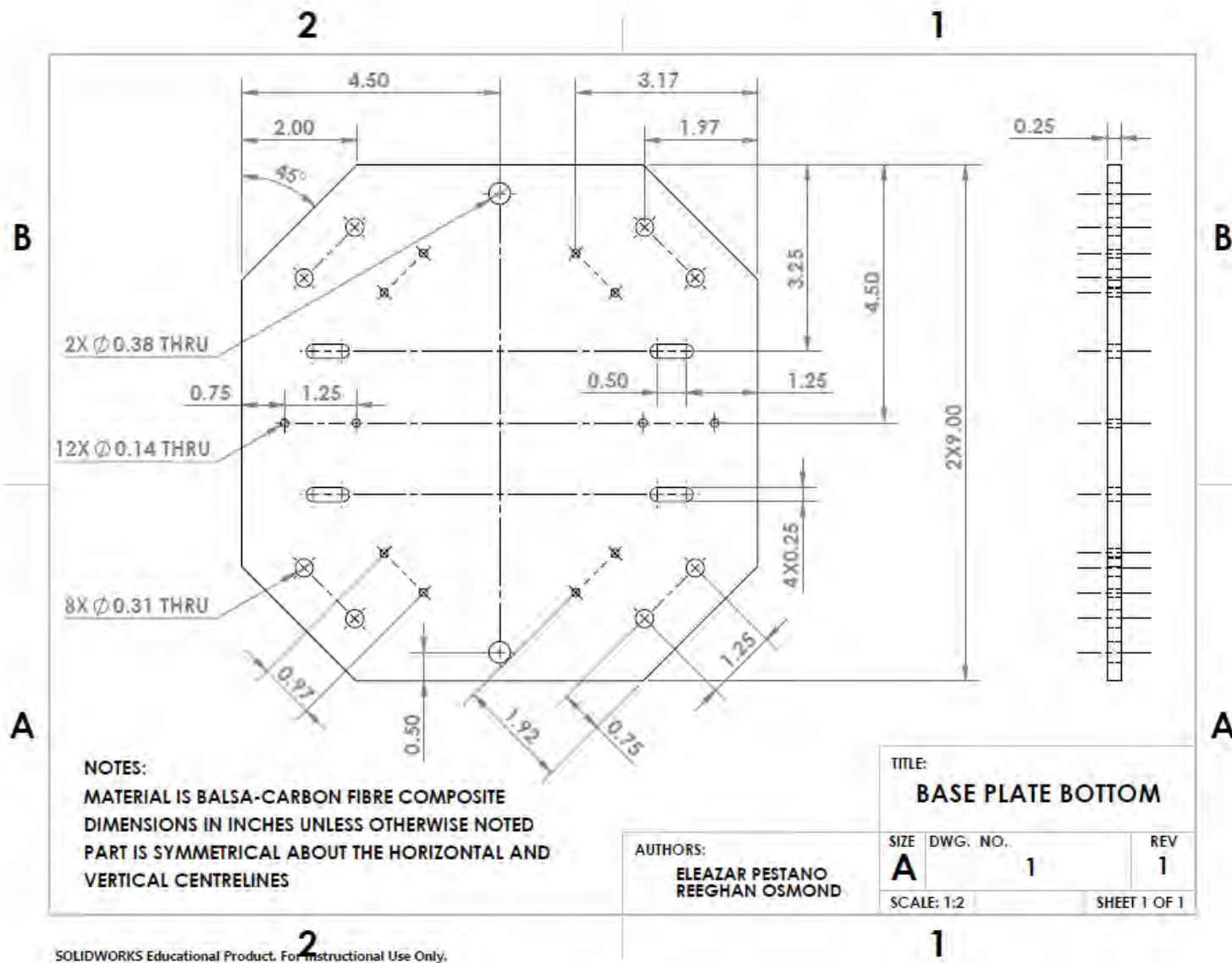
Figure C.10: Gantt and Milestone Chart

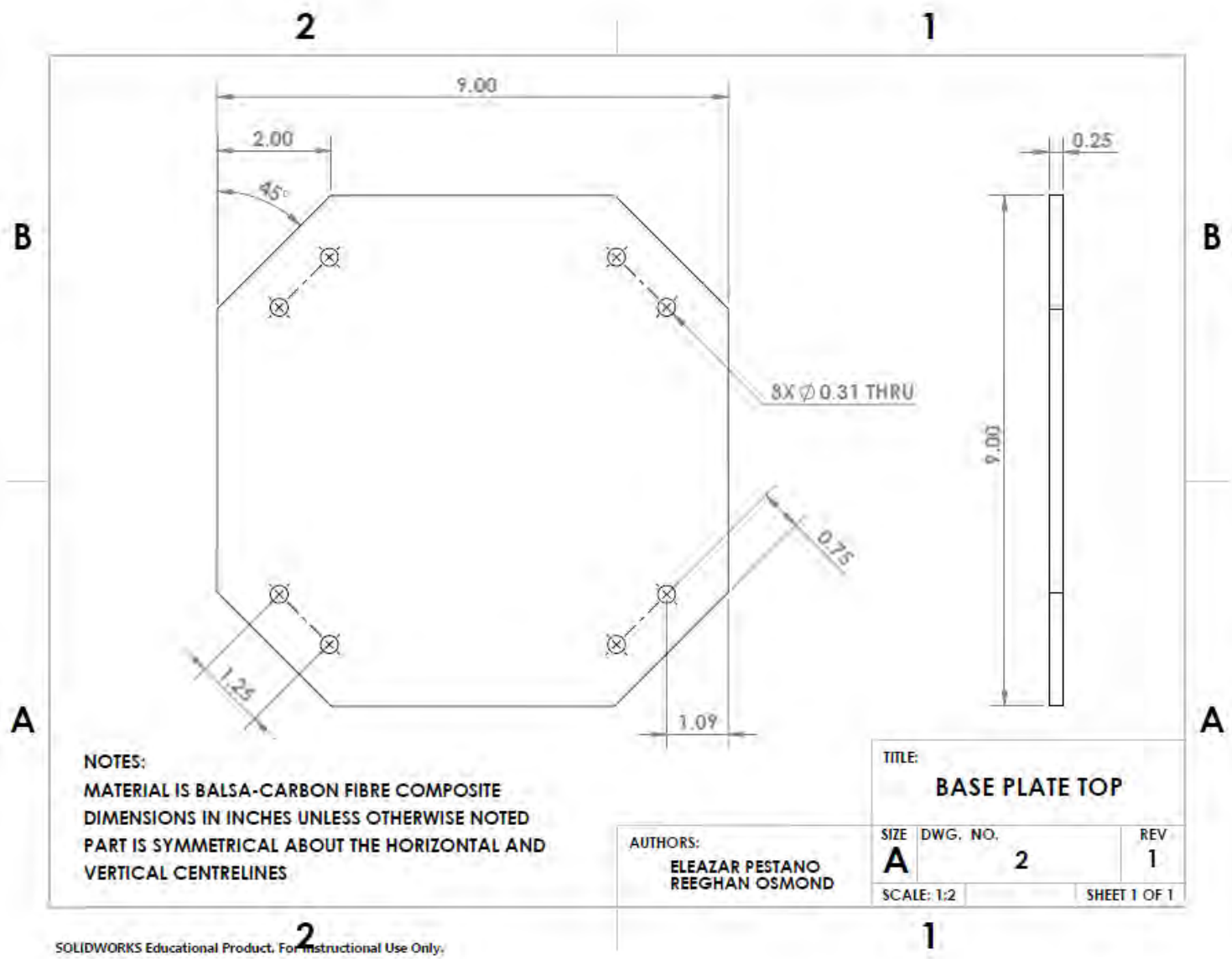
Project Risk Analysis

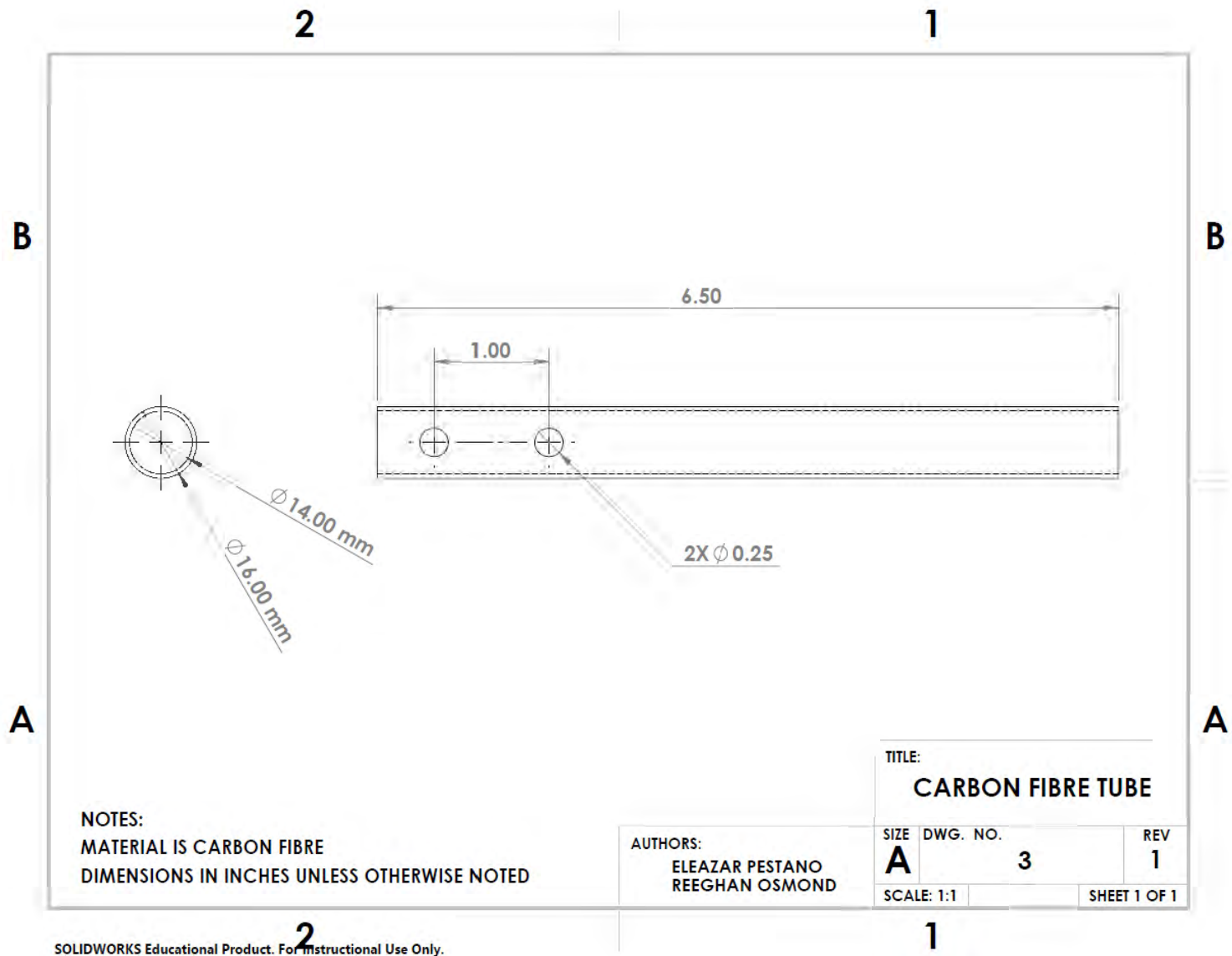
The following is a list of potential risks and mitigations for the second phase of the project:

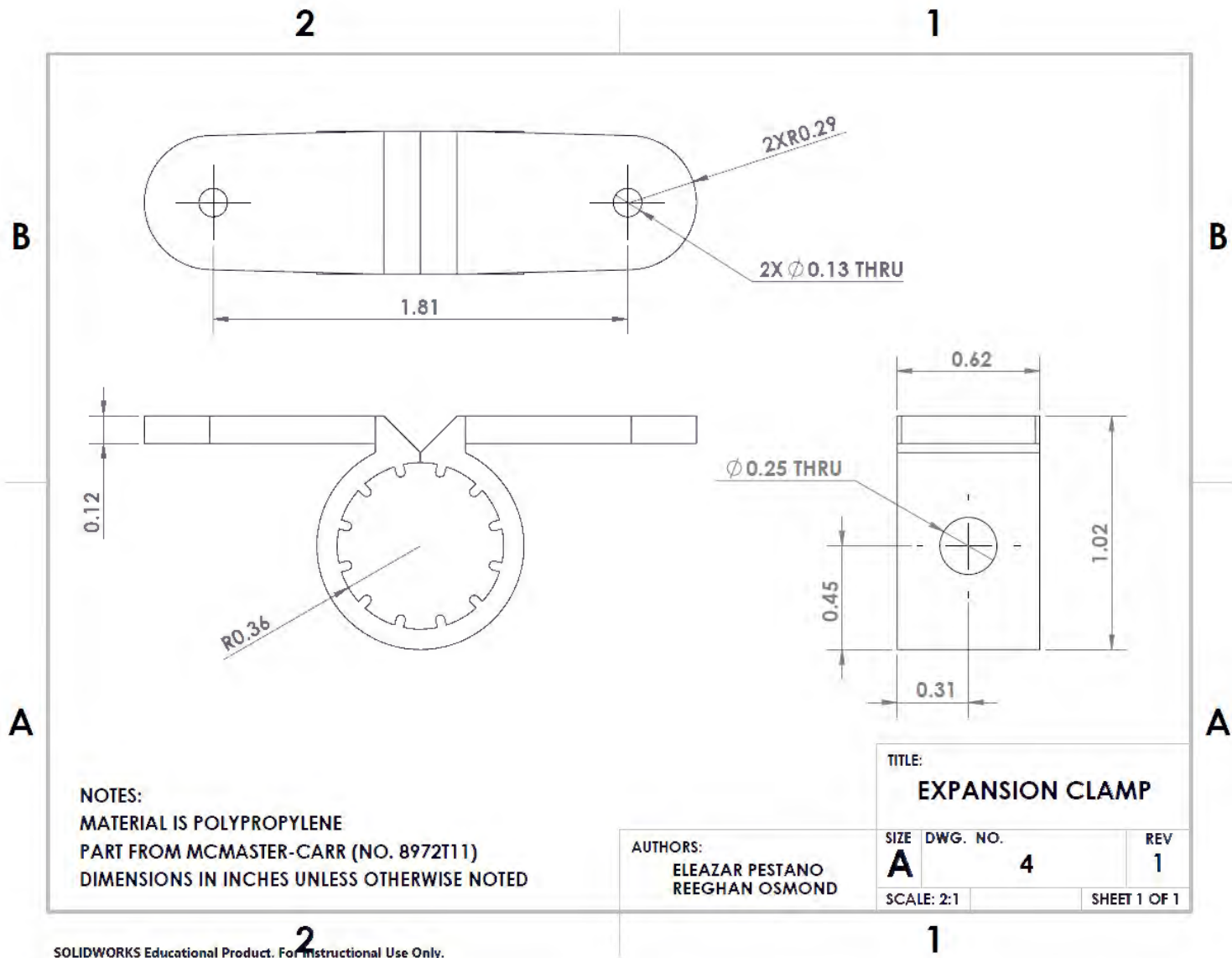
1. Accidentally destroying parts during the testing phase
 - Doing incremental testing to ensure that we are aware of how the drone will behave
2. Integrating controls from both phases of the project
 - If the controls cannot be integrated, two microcontrollers may have to be used
3. Precision of manufacturing processes
 - Minimizing the requirement for precise manufacturing
 - Using mostly off-the-shelf components
 - Using simple geometry
4. Lead time of the phase two components
 - Ordering components within one week after the design review
5. Phase two components of the project being too heavy
 - Prioritizing component weight over other aspects

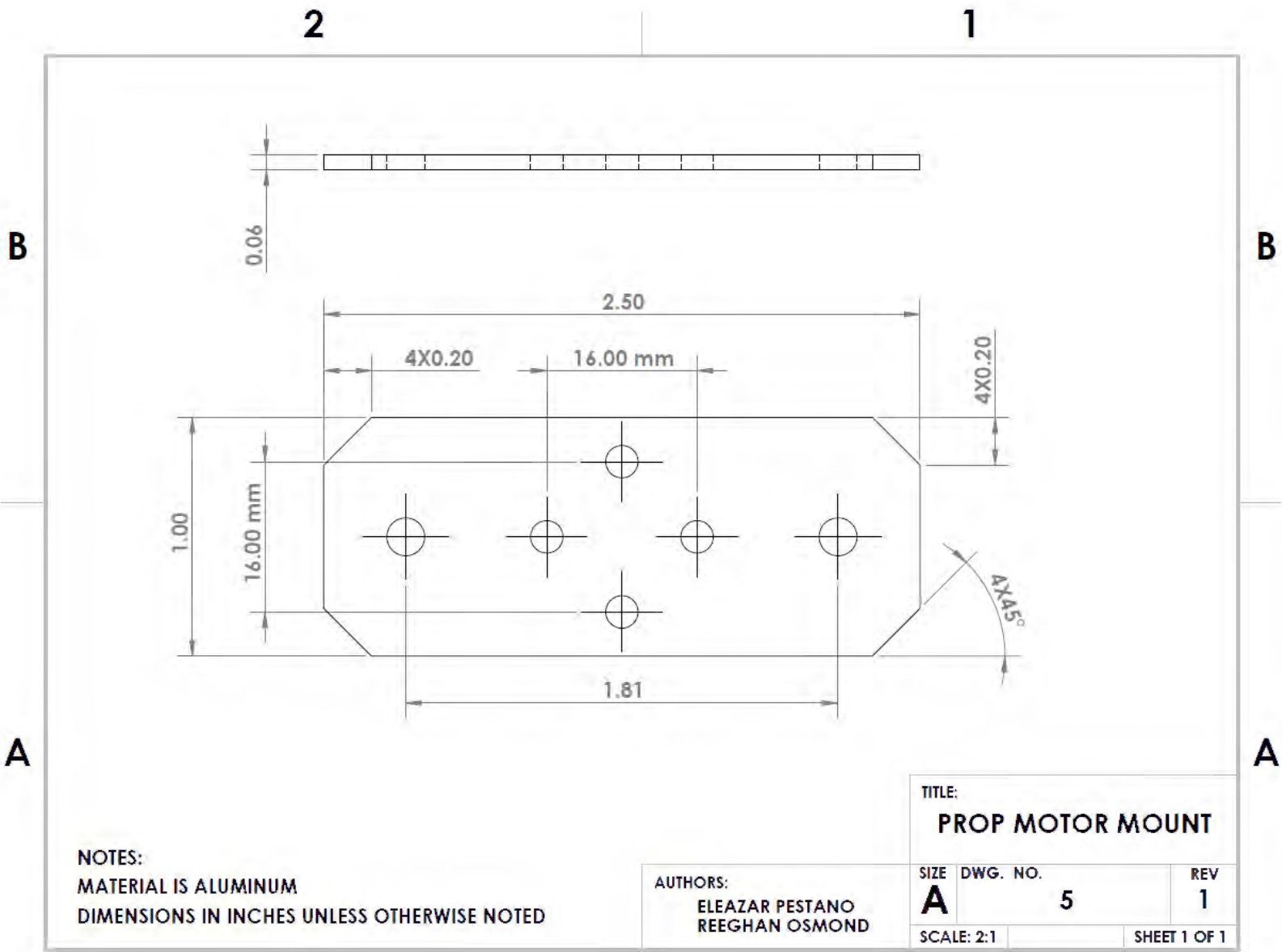
Appendix D. Manufacturing Drawings

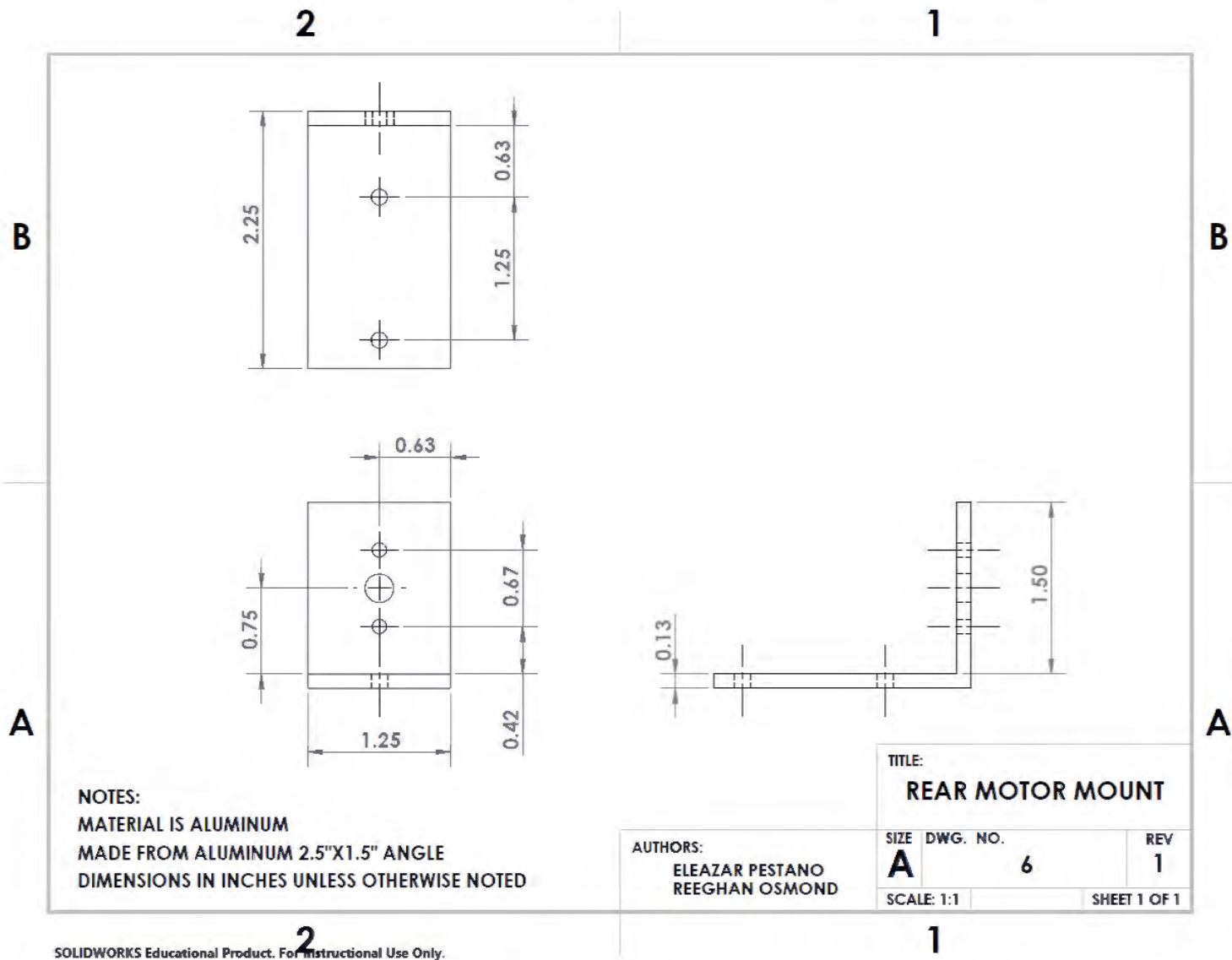


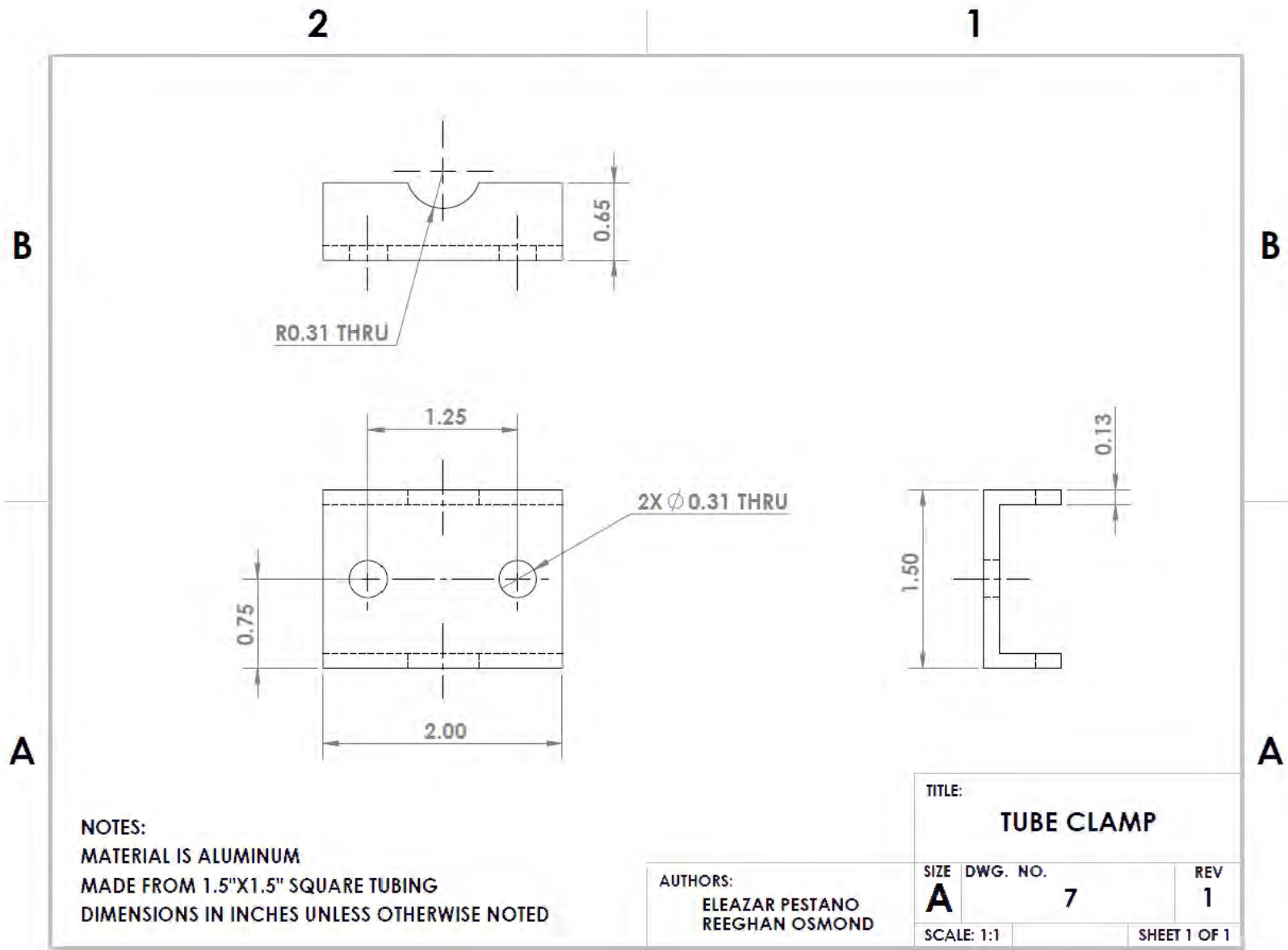


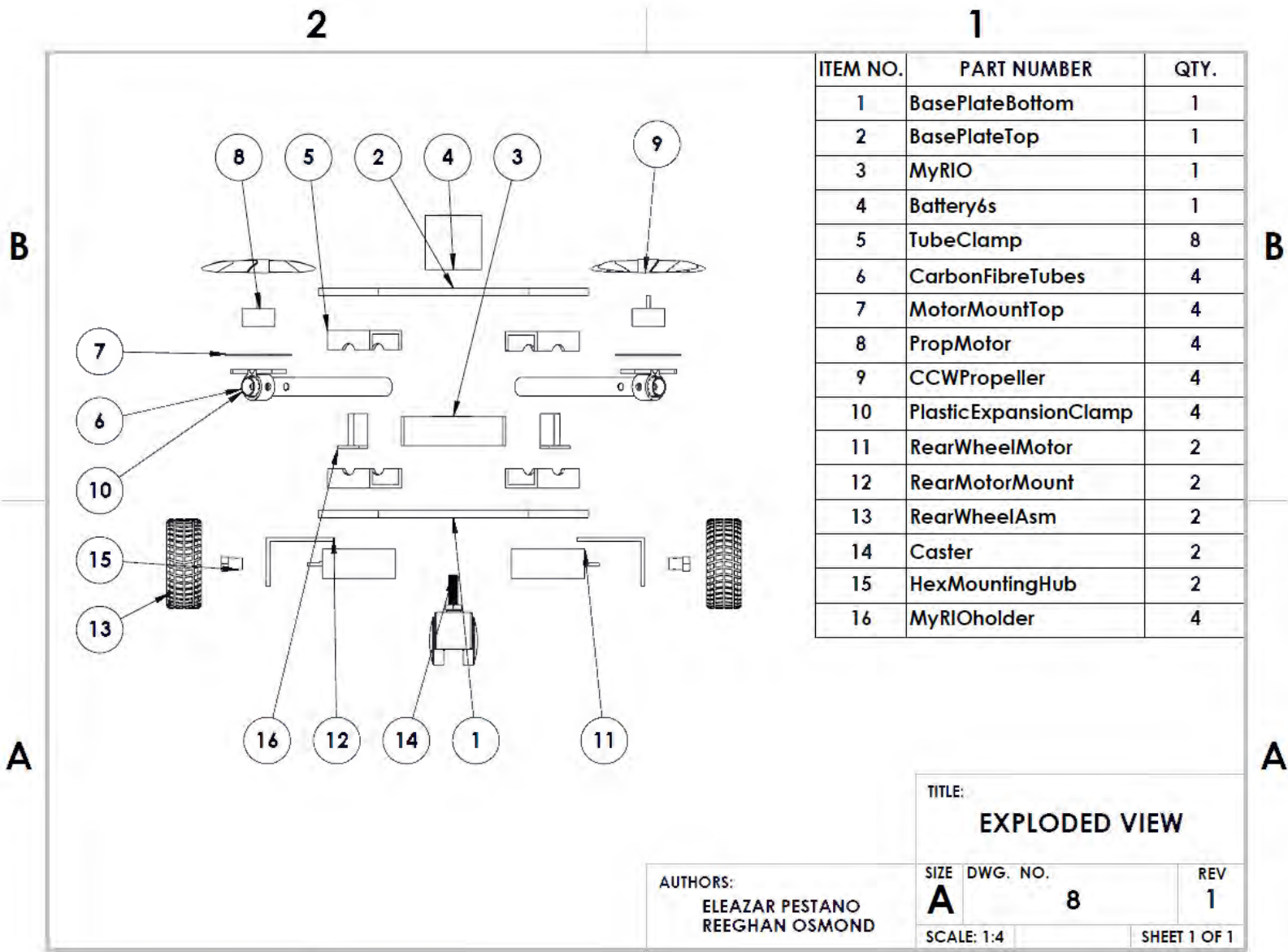












| ITEM NO. | PART NUMBER | QTY. |
|----------|-----------------------|------|
| 1 | BasePlateBottom | 1 |
| 2 | BasePlateTop | 1 |
| 3 | MyRIO | 1 |
| 4 | Battery6s | 1 |
| 5 | TubeClamp | 8 |
| 6 | CarbonFibreTubes | 4 |
| 7 | MotorMountTop | 4 |
| 8 | PropMotor | 4 |
| 9 | CCWPropeller | 4 |
| 10 | PlasticExpansionClamp | 4 |
| 11 | RearWheelMotor | 2 |
| 12 | RearMotorMount | 2 |
| 13 | RearWheelAsm | 2 |
| 14 | Caster | 2 |
| 15 | HexMountingHub | 2 |
| 16 | MyRIOholder | 4 |

TITLE:
EXPLODED VIEW

SIZE DWG. NO. REV
A 8 1

SCALE: 1:4 SHEET 1 OF 1

AUTHORS:
ELEAZAR PESTANO
REEGHAN OSMOND